THE UNIVERSITY *of* EDINBURGH

Dynamic control of Nanog expression in embryonic stem cells

Violetta Anna Karwacki-Neisius

Thesis presented for the degree of Doctor of Philosophy

University of Edinburgh

2011

I declare that the work described in this thesis is my own, except where otherwise stated

Violetta Anna Karwacki-Neisius

Acknowledgements

A special thank you goes to my supervisor Professor Ian Chambers for the opportunity to undertake my PhD in his lab and for his constant support and guidance in the last three years. I also would like to thank Dr. Simon Tomlinson and Florian Halbritter for their great work regarding the Solexa raw data analysis and my secondary supervisors Dr. Sally Lowell and Dr. Joe Mee for providing useful advice. A big thanks goes as well to the members of the Chambers lab "Team Nanog" for creating a good atmosphere and to Dr. Nick Mullin for looking after our lab. Especially I would like to thank Dougie Colby for his great support during my extensive experiments in TC.

Furthermore, I am very grateful for the financial support provided by BBSRC and Stem Cell Sciences.

I would like to dedicate this thesis to three special people without whom this work would not be possible. At first to my mum (Edyta Karwacka) for being the best mum and person I can imagine, for her endless love and for all the sacrifices she made for me. Secondary, I would like to dedicate this thesis as well to my dad (Stanislaw Karwacki) for his love and support and to my husband (Ulf Neisius), for being always there for me when I needed him and for his love and understanding, even when I spent literally night and day in the lab.

Abstract

Embryonic stem cells are defined by two key characteristics; apparently symmetrical self-renewing cell division and the ability to differentiate into cells of all three germ layers. Self-renewal depends on several extrinsic and intrinsic cues including a gene regulatory network centered around Oct4, Sox2 and Nanog that has been hypothesized to be reinforced by positive reciprocal interactions. Studies measuring Nanog expression by fluorescent reporters and immunoflourescence have shown that some undifferentiated Oct4 positive cells do not express Nanog (Chambers et al., 2007). However, the mechanisms responsible for generating this heterogeneity in Nanog expression are unknown.

Here I show that Oct4 heterozygote ES cells lack Nanog-negative cells. Consistent with a model in which ES cell differentiation proceeds effectively through Nanog-negative cells, these Oct4 heterozygotes are retarded in their differentiation kinetics. Importantly, restoring Oct4 levels towards wild type reestablished both heterogenous Nanog expression and rapid differentiation.

Analysis of ES cells carrying a mutation in the Oct4 binding site in the proximal Nanog promoter showed that Oct4 acts as a positive activator on the endogenous Nanog.

Finally, comparison of gene expression in Nanog expressing and Nanog non-expressing ES cells has identified candidate genes that may be responsible for the switch in Nanog expression.

Abbreviations

Ab	antibody
AP	alkaline phosphatase
β-gal	β-galactosidase
β-geo	β-galactosidase/neomycin fusion
BIO	biotin tag
bp	base pair
BSA	Bovine serum albumin
BSD	Blasticidin
cDNA	complimentary DNA
ChIP	chromatin immunoprecipitation
CMV	cytomegalovirus
DAPI	4',6-diamidino-2-phenylindole
dCTP	Cytidine triphosphate
DEPC	Diethylpyrocarbonate
DMSO	Dimethyl sulfoxide
DNA	deoxyribonucleic acid
dNTP	Deoxynucleoside triphosphate
Dox	Doxycycline
EC	embryonal carcinoma
EDTA	ethylenediamine tetraacetic acid
EG	embryonic germ
eGFP	enhanced green fluorescent protein
EMSA	electromobility shift assay
ERK	extracellular receptor kinase
ES	embryonic stem
FCS	Foetal calf serum
FRV	fast red violet
g	gravitational force
GCNF	germ cell nuclear factor
GFP	green flourescent protein
h	hour
HDAC	Histone deacetylases
HPLC	high-performance liquid chromatography
ICM	inner cell mass
IgG	Immunoglobulin G
IgM	Immunoglobulin M
IL-6	interleukin 6
IRES	internal ribosome entry site
Jak	Janus kinase
kb	kilobase
kDa	kilodalton
KV	kilovolts
*lac*Z	β-galactosidase
LB	Luria broth
LIF	leukaemia inhibitory factor
LIF-R	LIF receptor
mA	Milliampere
MAPK	mitogen activated protein kinase
min	Minutes
MOPS	3-N-morpholino propanesulfonic acid
mRNA	messenger RNA
neo	Neomycin
NLS	nuclear localisation signal
NO	nitric oxide
P	puromycine
pac	puromycin acetyl transferase
PAGE	polyacrylamide gel electrophoresis
PBS	phosphate buffered saline
PCR	polymerase chain reaction
PE	Phycoerythrin
PFA	Paraformaldehyde
PGC	primordial germ cell
pgk	phosphoglycerate kinase
PI	propidium iodide
polyA	polyadenylic acid
Q-PCR	quantitative PCR
RNA	ribonucleic acid
rpm	revolutions per minute
RT	room temperature
R	Resistance
sec	Second
SDS	sodium dodecyl sulphate
soc	super optimal broth with catabolite repression
SSC	saline-sodium citrate
TAE	Tris-acetate-EDTA
Taq	Thermus aquaticus
TBE	Tris-borate-EDTA
TBS	Tris buffered saline
TBS-T	TBS-Tween
Tc	Tetracycline
TE	Tris-EDTA
Tm	melting temperature
u	Unit
UHP	ultra high purity
µF	microfarads
UTR	Untranslated Region
UV	Ultraviolet
V	Volt
wt	wild type
zeo	Zeocin

Table of Contents

List of Figures:

List of Tables:

Chapter 1

Introduction

1.1 Early mouse development

The earliest stages of mouse development that follow fertilisation are characterised by multiple cleavage divisions that lead to the 8–cell embryo (Figure 1.1). At this stage an increase in the adhesive properties of the cells causes the embryo to adopt a spherical structure in a process termed compaction. Subsequently, at approximately day 3.5 a cavity appears on one side of the embryo (now called a blastocyst) that separates tissues of the inner cell mass (ICM) from the majority of exterior trophectoderm cells (Beddington, 1999). Later on in embryogenesis the trophectoderm develops into the placental tissues and the ICM develops into the embryo proper (Gardner, 1983). The blastocoel cavity then enlarges to occupy most of the expanded blastocyst. At day 4.5 primitive endoderm, an extraembryonic tissue that later generates the parietal and visceral endoderm, occurs on the blastocoelic suface of the ICM (Tam, 1997). The rest of the ICM tissue is the epiblast, the source of the embryo proper. At about day 5.0 the blastocyst implants into the uterus and the epiblast proliferates. The process referred to as gastrulation begins approximately at day 6.5. This term describes a complex movement of epiblast cells resulting in the appearance of mesoderm that starts from the proximal end of the epiblast and proceeds to the distal tip of the epiblast. In this way the embryonic anterior-posterior axis including the proximal tip of the primitive streak appears. During this developmental process there is a change in the development

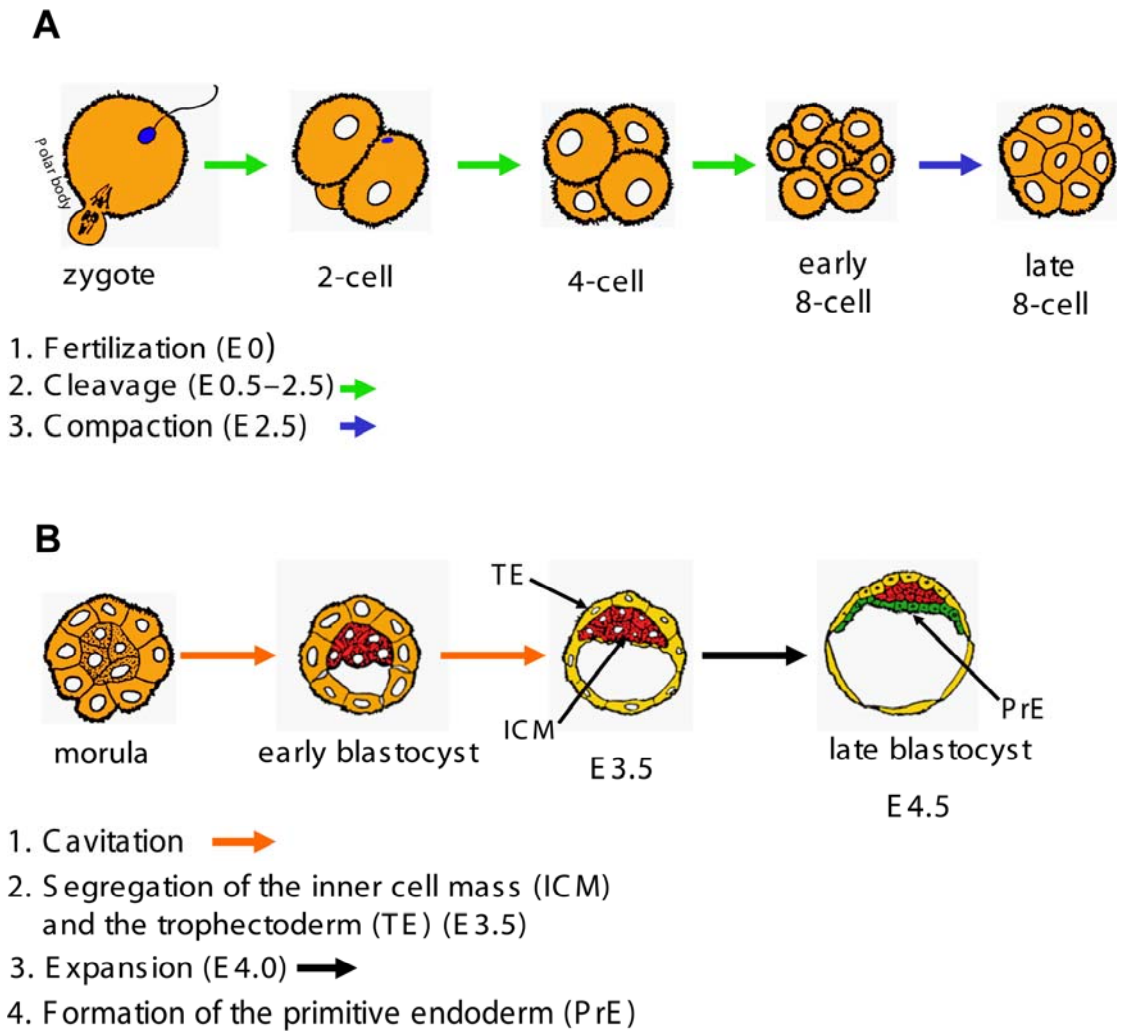

Figure 1.1 Pre-implantation embryo

A: Embryo development until the late 8 cell stage. The particular developmental stages are indicated with arrows.
B: Development from the morula stage until the late blastocyst. Days and particular stages are indicated.
Pictures were kindly provided by Dr.Tilo Kunath.

.

potential, or potency of the cells. Early blastomeres of the embryo are totipotent (Tarkowski and Wroblewska, 1967). Totipotency describes the competency of cells to produce all cells of the organism including extraembryonic tissues. Loss of totipotency is associated with the fifth cleavage division as only some single blastomeres of 16- and 32-cell mouse embryos are still capable to develop into foetuses and mice (Suwinska et al., 2008).

The inner cell mass, the origin of ES cells is pluripotent. Pluripotent cells have the ability to generate tissues of all three germ layers (endoderm, mesoderm and ectoderm) but they lack the competency to contribute to extraembryonic tissue. Pluripotency persists in the postimplantation epiblast until around the time of gastrulation.

1.2 From teratocarcinoma to embryonic stem cells

Research on pluripotency originated in 1954 when Stevens and Little reported that the mouse strain 129 spontanously generated testicular teratomas at a frequency of 1% (Stevens, 1954) reviewed by (Andrews, 2002; Chambers and Smith, 2004; Morange, 2006; Solter, 2006). Teratocarcinomas differ from other neoplasms as they contain many distinct differentiated cells and even tissue types such as muscle, teeth, bones, hair, nerve and skin cells. The terms teratoma and teratocarcinoma were initialy used interchangeably (Damjanov and Andrews, 2007) but this later changed as it was understood that teratomas are benign tumors consisting of differentiated cells whereas teratocarcinomas also contain undifferentiated embryonal carcinoma (EC) cells. Leroy Stevens and Barry Pierce contributed greatly to our knowledge of the biology of teratocarcinomas (Andrews, 2002; Chambers and Smith, 2004; Morange, 2006; Solter,

2006). Stevens was able to induce teratocarcinoma in strain 129 mice by explanting genital ridges of fetuses between 11 and 13.5 days of development to ectopic sites (Stevens, 1967a; Stevens, 1970b). Teratocarcinomas could also be induced by transfer of 1-7.5 day old inbred mouse embryos to extra-uterine sites in syngenic mice (Solter et al., 1970; Stevens, 1970a). Interestingly, those carcinomas could not be distinguished from those previously described. Considering that teratocarcinomas were only induced by embryos prior to gastrulation and by isolated epiblast grafts, it was suspected that EC cells originate probably from the latter (Diwan and Stevens, 1976). Knowing this, Stevens followed the first events of teratocarcinogenesis and suggested that a small nest of undifferentiated EC cells was the origin of teratomas or teratocarcinomas (Andrews, 2002; Chambers and Smith, 2004; Morange, 2006; Solter, 2006). Kleinsmith & Pierce were able to show that a single EC cell when transplanted could give rise to complex teratomas (Kleinsmith and Pierce, 1964). This proved a stem cell origin for teratocarcinomas. From these studies Stevens suggested that oncogenesis mimics normal mouse development (Stevens, 1967b). Independent of the number of in vivo passages, embryonal carcinoma cells remained mostly in their pluripotent state able to grow into derivatives of the three germ layers (Stevens, 1958).

Embryonal carcinoma cells were showed to be amenable to culture *in vitro* and to give rise to stable EC cell lines (Finch, 1967). Consequently, research on the topic accelerated and the morphological and biochemical analogy between the blastocystic cells in the inner mass and EC cells became more and more evident (Jacob, 1977; Martin et al., 1978) reviewed by (Andrews, 2002; Morange, 2006; Solter, 2006). These

experiments led to the transfer of EC cells into blastocysts (Brinster, 1974; Mintz and Illmensee, 1975; Papaioannou et al., 1975). When these blastocysts were reimplanted into the uterus of surrogate mothers, mosaic animals grew indicating that in the appropriate environment the chaotic differentiation of EC cells could be corrected. Yet EC cells were unable to transmit their genome through the germ line (Moragne, 2006).

In 1981 permanent pluripotent embryonic stem cells (ES) lines were first established by direct explantation of ICMs (Evans and Kaufman, 1981; Martin, 1981). The authors assigned their success to three critical factors, the exact stage of cell development, the explantation of a sufficient number of cells from each embryo and optimised tissue culture conditions, especially the use of feeder layers, which were supportive for multiplication rather then differentiation of these cells. ES cells were able to grow indefinitely in culture without losing their ability to differentiate both *in vitro* and in teratocarcinomas. In contrast to EC cells, ES cells are stably diploid (Martin, 1981) and importantly, following chimera formation are able to transmit their genome through the germline to create a complete mouse in which all cells carry the ES cell genome (Bradley et al., 1984).

1.3 The derivation of human EC and ES cells

Research on human EC cells was, with exclusion of an attempt to study them following xenotransplantation into the hamster cheek pouch, for a long time non existent (Pierce et al., 1957) reviewed by (Andrews, 2002; Chambers and Smith, 2004; Morange, 2006; Solter, 2006). Development of human EC cells was achieved *in vitro* during the 1970s

(Hogan et al., 1977). Despite a limited capacity for differentiation, these cells allowed the identification of several features characteristic of human EC cells (Andrews, 2002; Solter, 2006). In the following years human EC cell lines with the ability to differentiate could be established (Andrews et al., 1984; Damjanov and Andrews, 1983; Pera et al., 1989). From the start it was evident that despite some common characteristics, human and mouse EC cells differ highly. Similarities include for example the growth in clusters, as well as expression of high levels of alkaline phosphatase (Berstine et al., 1973) reviewed by (Andrews, 2002). Differences however exist in the tendency for human EC cells to differentiate into trophectoderm and in the expression of cell surface antigens, (Andrews et al., 1980; Andrews et al., 1982; Damjanov and Andrews, 1983), including stage-specific embryonic antigen 1 (SSEA1) (Solter and Knowles, 1978), SSEA3 (Andrews et al., 1982; Shevinsky et al., 1982) and SSEA4 (Kannagi et al., 1983). The murine EC cells characteristics persist in murine ES cells, consistent with the idea that both resemble cells of the ICM. In the absence of human ES cell lines and direct information about human embryos, these interspecies variations rendered the relationship of human EC cells to the early human embryo uncertain (Andrews, 2002). When human ES cell lines were established by Thomson et al., the resemblance to human EC cells became obvious and the interspecies difference appeared also to apply to human ES cells (Thomson et al., 1998). Furthermore, the maintenance of pluripotency in both species requires different signaling pathways. Mouse ES cells depend on leukaemia inhibitory factor (LIF) and bone morphogenetic protein (BMP), whereas human ES cells rely on signaling from activin/nodal and fibroblast grow factor (FGF).

1.4 Other pluripotent cells

Another type of pluripotent stem cells are embryonic germ cells (EG) established from primordial germ cells (PGCs) which were isolated either during migration or shortly after arriving in the gonads (Matsui et al., 1992; Resnick et al., 1992). Although EG and ES cell lines share similar phenotypic and molecular characteristics, EG cells can not be considered as completely equal to ES cells as they have undergone global erasure of imprints at the latter stage of PGC development and therefore have a decreased developmental capacity (Tada et al., 1998). The counterpart for mouse embryonic germ cells was as well established from human primordial germ cells. However, in contrast to the situation in the mouse, human EG cells vary from human ES and EC cells due to differences in surface antigens (Shamblott et al., 1998).

Despite the fact that the post implantation embryo was shown to contain pluripotent cells (Stevens, 1970a), attempts to establish pluripotent cell lines from post implantation embryos were unsuccessful. However, in 2007 pluripotent epiblast stem cells (EpiSCs) were isolated from the late epiblast layer of post-implantation mouse and rat embryos using chemically defined, activin containing culture medium (Brons et al., 2007; Tesar et al., 2007). These EpiSCs share similarities with human ES cells although their nature still needs a careful investigation.

Induced pluripotent stem cells (iPSC) were first isolated in 2006 (Takahashi and Yamanaka, 2006) from mouse cells and in 2007 (Takahashi et al., 2007; Yu et al., 2007) from human cells. These iPSC cells were produced by transfecting non-pluripotent cells

such as fibroblast with a limited number of particular transcription factors expressed in pluripotent cells and culturing transfectants in ES cells medium.

1.5 Significance of pluripotent cells for basic research and regenerative medicine

Embryonic stem cells allow production of genetically modified organisms, facilitate exploration of facets of developments difficult to investigate in vivo and hold potential for regenerative medicine (Smith, 2001). Genetic modifications in ES cells allow analysis of gene function by deletion through homologous recombination (Thomas and Capecchi, 1987). ES cells thereby provide a means to transmit an altered genome through the germline allowing analysis of gene function during development and in adulthood (Thompson et al., 1989). As ES cells share many features with pluripotent cells of the early embryo their study allows investigation of early mammalian development. However, it remains uncertain if ES cells are an equivalent of embryonic cells or if they display a culture artefact (Smith, 2001). Nevertheless, ES cells are useful to investigate differentiation pathways in vitro and to create a homogenous source of tissue specific stem cells (Conti et al., 2005; Smith, 2001). The ability of mouse ES cells to differentiate into many tissues in *in vitro* aggregation cultures (Doetschman et al., 1985; Martin, 1981) and in vivo (Beddington and Robertson, 1989) implies that ES cells have great potential for medicine. iPS cells may overcome the ethical dilemma of using human embryos as an ES cell source for therapy while at the same time avoiding the problems of immune rejection (Yamanaka, 2007).

1.6 Exogenous signals required for ES cell self-renewal

1.6.1 LIF/STAT3 signalling

Early cultivation attempts of mouse ES cells depended on feeder layers necessary for their proliferation (Evans and Kaufman, 1981; Martin, 1981). Subsequent studies indicated that ES cells could be maintained in the absence of co-culture provided conditioned medium from Buffalo Rat Liver cells was added to the culture (Smith and Hooper, 1987). Fractionation of conditioned medium defined LIF as the major component important for ES cell self-renewal (Smith et al., 1988) reviewed by (Chambers, 2004b). LIF is a cytokine of the IL-6 family of cytokines that signal to cells via a cell surface receptor glycoprotein of 130 kD, called gp130 (Yoshida et al., 1996). In this context LIF becomes obsolete if IL6 together with a soluble form of the IL6 receptor, which can induce homodomerisation of gp130, is added to culture (Yoshida et al., 1994) reviewed by (Chambers, 2004b; Niwa, 2001). LIF binds to the LIF-specific receptor and subsequently this complex binds gp130 (Yoshida et al., 1996). Dimerisation of the homologous intracellular domains of gp130 and LIFR activates receptor associated Janus kinases (JAKs) which phosphorylate tyrosine residues on the cytoplasmatic domain of gp130 and LIFR (Niwa et al., 1998). These phosphorylated tyrosine residues act as docking sites for signal transducing molecules including STAT3 (Signal Transducer and Activator of Transcription number 3). Phosphorylation of STAT3 by JAKs allows STAT3 dimerisation through reciprocal interaction of a SH2 domain and a phosphotyrosine residue (Niwa et al., 1998). This triggers translocation of STAT3 to the nucleus and subsequent activation of target genes (Niwa et al., 1998; Zhang et al., 1997). c-Myc for example is a candidate target of STAT3 (Cartwright et

al., 2005). LIF also stimulates ras-MAKP signaling. This is of interest, as this pathway is known to suppress ES cell self-renewal (Burdon et al., 1999).

The significance of STAT3 for ES cell self-renewal was shown in two studies. In the first, overexpression of a dominant-negative form of STAT3 in ES cells led to differentiation although LIF was added to the culture (Niwa et al., 1998) reviewed by (Chambers, 2004b; Niwa, 2001). Interestingly the morphological changes resulting from the overexpression of the dominant-negative form of STAT3 were similar to changes arising from the withdrawal of LIF in culture (Niwa et al., 1998). Also, when cells were cultured at high density and grown in serum-supplemented medium, activation of STAT3 lead to maintenance of self-renewal in the absence of LIF (Matsuda et al., 1999). Despite this, knockout mice for LIF (Stewart et al., 1992), LIFR (Li et al., 1995), gp130 (Yoshida et al., 1996) and STAT3 (Takeda et al., 1997) all expanded beyond the egg cylinder stage (Chambers, 2004b; Niwa, 2001). Further, Dani et al. reported an unknown factor secreted by ES cells, which they termed the ES selfrenewal factor (ESRF) (Chambers, 2004b; Niwa, 2001). ESRF supported ES cell self-renewal even when both endogenous LIF alleles were disrupted (Dani et al., 1998). It was shown that ESRF does not activate Stat3 (Dani et al., 1998). These findings in summary suggest the existence of unknown intracellular pathways (Dani et al., 1998) reviewed by (Chambers, 2004b; Niwa, 2001). The biological significance of LIF signaling for the blastocyst was subsequently shown to be during delayed implantation where lack of gp130 reduced embryonic survival during this diapause (Nichols et al., 2001).

1.6.2 BMP signalling

In addition to LIF it has been demonstrated that serum contributes to self-renewal and that this requirement can be replaced by bone morphogenic proteins (BMPs) (Ying et al., 2003). BMPs stimulate the transcriptional activation of the Id genes through the activation of Smads (Nakashima et al., 2001; Ruzinova and Benezra, 2003). In ES cells it is the expression of the Ids which is of importance for the self-renewal capacity of BMP (Ying et al., 2003). Cells constitutively expressing a loxP-flanked Id1 transgene or Cre-treated derivatives, were plated at clonal density in N2B27 with LIF or LIF plus BMP. Whereas loxP-flanked Id1 cells formed ES cell colonies in LIF only and were ably to bypass the BMP requirement, the Cre-treated derivatives were not able to produce ES cell colonies in the absence of BMP (Ying et al., 2003). However BMP alone is not sufficient to keep ES cells in an undifferentiated state. The BMP function is dependent on co-stimulation with LIF, which can be seen by the fact that in the presence of BMP alone, the cells are driven into non-neural differentiation (Ying et al., 2003). In LIF without serum or BMP, neural differentiation occurs. Taken together, BMP treatment suppresses neural differentiation and in combination with LIF is sufficient to sustain ES cell self-renewal without feeders or serum factors (Ying et al., 2003).

1.6.3 Wnt signaling

The Wnt signaling pathway has been implicated to have a role in self-renewal of both mouse and human ES cells (Sato et al., 2004). Activation of the Wnt pathway by 6-bromoindirubin-3`-oxime (BIO), a pharmacological inhibitor of glycogen synthase kinase-3 (GSK3), was reported to maintain the undifferentiated phenotype of mouse and

human ES cells and to sustain the expression of Oct4, Rex-1 and Nanog, which are important for the pluripotent cell state (Sato et al., 2004). In support of this data more recent studies showed that GSK-3a and GSK-3b null ESCs display differentiation defects and sustain high expression of Nanog in EBs (embryonic bodies) at day 12 of differentiation (Doble et al., 2007).

Importantly, both GSK3 isoforms (GSK-3a and GSK-3b) are equally capable of maintaining low levels of β-catenin (Doble et al., 2007). In addition, it has been reported that LIF increases the level of nuclear beta-catenin, a component of the Wnt signaling pathway, and that this up-regulates Nanog in an Oct4-dependent manner (Takao et al., 2007). Yet an importance for Nanog expression needs still further exploration.

1.6.4 Are extrinsic stimuli indispensable for ES cell self-renewal?

Recently, Ying et al. have questioned the importance of LIF and BMP for ES cell self-renewal (Ying et al., 2008). By adding different small-molecule inhibitors of the fibroblast growth factor (PD184352), mitogen-activated protein kinase (SU5402) pathway and glycogen synthase kinase-3 pathways (CHIR99021), the authors were able to maintain ES cell self-renewal without LIF and BMP. This led to the suggestion that LIF and BMP do not regulate self-renewal but act downstream of phospho-Erk to block ES cell commitment. The authors have further hypothesised that ES cells are in a basal cell state, that is intrinsically self-maintaining, provided the cells are shielded from inductive differentiation stimuli including FGF4. Despite these interesting conjectures, the mechanisms of action of these inhibitors is incompletely understood.

1.7 Intrinsic factors required for efficient ES cell self-renewal

Oct4, Nanog and Sox2 are transcriptional factors that play key roles in specification and maintenance of the epiblast during peri-implantation development and in the self-renewal of pluripotent ES cells.

1.7.1 Oct4

Mouse Oct4 was initially identified as an octamer (ATGCTAAT) binding transcription factor expressed in embryonal carcinoma (EC) cells (Rosner et al., 1990; Scholer et al., 1990). Oct4 is a member of the POU (Pit, Oct, Unc) family of transcriptional factors that share a homologous bipartite DNA binding domain known as the POU binding region that contains two domains, a specific domain (POU_S) and a homeodomain (POU_{HD}), that each bind in the major groove to 4 bp elements of the octamer consensus sequence (Chambers and Tomlinson, 2009; Williams et al., 2004) (Figure 1.2). During development, expression of Oct4 occurs in the unfertilised egg and at the 4- to 8-cell stage becomes restricted to the inner cell mass (ICM) cells at the early blastocyst stage. At the late blastocyst stage Oct4 is readily detected in the ICM and also in the primitive endoderm of the blastocyst (Palmieri et al., 1994). Postimplantation Oct4 is restricted to the epiblast before becoming limited to the migratory primordial germ cells where its expression continues through the formation of the genital ridges in both sexes (Chambers 2004). The importance of Oct4 in mouse development was emphasized by Nichols et al., 1998 (Nichols et al., 1998; Niwa, 2001). By gene deletion studies the authors demonstrated that embryos lacking Oct4 expression failed to produce the pluripotent cell compartment and the result of this was redirection of ICM cells into the

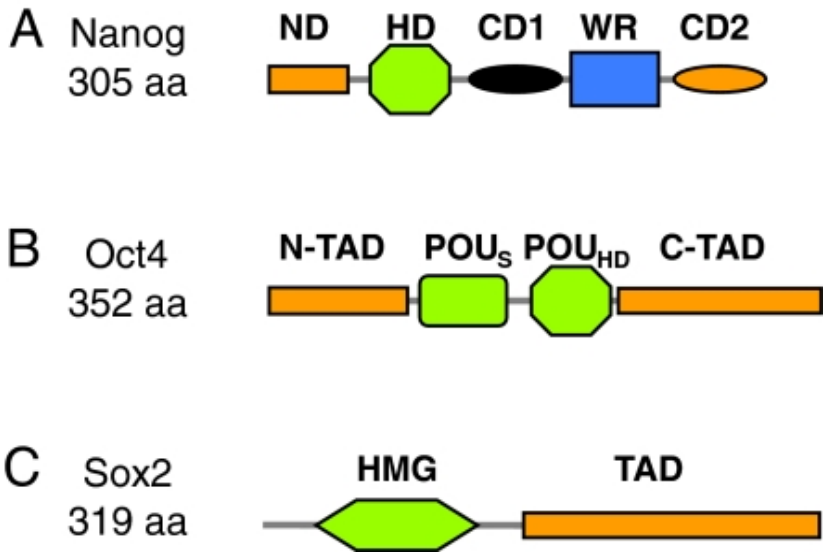

Figure 1.2 Nanog, Oct4 and Sox2 protein domains

(A) Nanog can be divided into an N-terminal and C-terminal half. The N-terminal half contains a DNA-binding homeodomain (HD) and an N-terminal domain (ND). The C-terminal half contains a tryptophan repeat (WR) domain, The WR repeat domain disconnects the C-terminal domain 1 (CD1) from the C-terminal domain 2 (CD2).
(B) Oct4 contains DNA-binding domains comprising a POU-specific DNA-binding domain (POU_S) and a POU-homeodomain (POU_{HD}), as well as transactivation domains located N-terminal (N-TAD) or C-terminal (C-TAD) to the POU domain.
(C) Sox2 contains a single HMG (High Mobility Group) DNA-binding domain and a transactivation domain (TAD).
The size of each protein is shown in amino acid residues (aa).
Copied from (Chambers and Tomlinson, 2009)

trophectoderm (Nichols et al., 1998; Niwa, 2001). Additional studies demonstrated that the stem cell fate depends on the precise Oct4 level (Niwa et al., 2000). Repression of Oct4 in ES cells induces differentiation along the trophectodermal lineage in accordance with the *in vivo* studies. When Oct4 is overexpressed ES cells differentiate into cells that express markers of mesoderm and endoderm (Niwa et al., 2000). This demonstrates that Oct4 is continuously required by ES cells in order to maintain their pluripotent identity. Interestingly, either the inhibition of Stat3 activity or the overexpression of Oct4 stimulates ES cells to differentiate into a similar cell population (Niwa et al., 2000). Therefore the existence of an undefined co-factor of Oct4 that is activated by Stat3 has been suggested (Niwa, 2001).

1.7.2 Sox2

Sox2 is a member of the Sox family of transcription factors that are defined by their relationship to the Y specific sex determining factor Sry (Sinclair et al., 1990) and by the presence of a High Mobility Group (HMG) box binding domain (Chambers and Tomlinson, 2009). The HMG-box DNA binding domain, bends DNA (50–90°) and specifically recognizes variations of the consensus sequence CTTTGTT (Williams et al., 2004). Sox2 regulates transcription of target genes in cooperation with Oct4 (Oct4/Sox2) binding both in ES cells and in pluripotent cells in vivo (Ambrosetti et al., 1997; Yuan et al., 1996). Sox2 occupies an important position in the maintenance of the pluripotent transcription factor network. ES specific binding sites for Oct4 and Sox2 have been identified in several genes, including Fgf4 (Yuan et al., 1996) Utf1 (Nishimoto et al.,

1999), Lefty 1 (Nakatake et al., 2006), Fbx15 (Tokuzawa et al., 2003) and Nanog (Chew et al., 2005; Kuroda, 2005; Rodda et al., 2005). More recent global chromatin studies have shown that Oct4 and Sox2 co-localise to many common sites throughout the ES cell genome (Boyer et al., 2005; Loh et al., 2006) Interestingly, the *Nanog*, *Oct4* and *Sox2* genes possess binding sites that are activated by the Oct4-Sox2 complex in ES cells (Okumura-Nakanishi, 2005).

The importance of Sox2 for the maintenance of the pluripotent state was emphasized by the finding that Sox2 deletion induced differentiation into multiple lineages (Ivanova et al., 2006). Also, inner cell mass explanted from embryos lacking Sox2 was unable to give rise to ES cells (Avilion et al., 2003). Although Sox2 heterozygote embryos develop normally, embryos lacking Sox2 died around E 6.5, which is a later time point in comparison to embryos lacking Oct4 (Avilion et al., 2003).

1.7.3 Nanog

The transcription factor Nanog was identified in two independent studies. The first method used expression cloning to identify cDNAs that were capable of directing self-renewal in the absence of LIF (Chambers et al., 2003). The second method used an *in silico* substraction method to identify genes specifically expressed in ES cells (Mitsui et al., 2003). Nanog when overexpressed can maintain ES cells in an undifferentiated state not only in the absence of LIF (Chambers et al., 2003) but also without BMP (Ying et al., 2003). Nanog is therefore considered a master regulator of self-renewal and pluripotency.

1.7.3.1 Nanog protein

Mouse Nanog is a 305 amino acid protein that is closely related to mouse NK2 family members (Chambers et al., 2003). However, < 70% identity within the homeodomain means that Nanog does not belong to the NK2 family (Chambers et al., 2003) and is a divergent homeodomain protein (Kappen et al., 1993). Homeodomain proteins often form homodimeric and heterodimeric complexes through their homeodomains. Nanog also forms dimers but in this case through interactions mediated by the tryptophan repeat domain (Mullin et al., 2008; Wang et al., 2008). Expression of a mutant form of Nanog in which the WR domain has been deleted, gives rise to a Nanog variant that cannot dimerize and that has lost the ability to confer LIF-independent self-renewal upon transfected ES cells (Mullin et al., 2008).

Prior work using reporter gene assays conducted in heterologous cells suggests that the N-terminal and C-terminal domains of mouse Nanog hold transactivator function (Pan and Pei, 2003). Only the C-terminal transactivation potential appears to be preserved in human Nanog (Oh, 2005). Furthermore, the mouse C-terminal domain was shown to contain two distinct transactivation domains: the WR and a second in CD2 (Pan and Pei, 2005).

1.7.3.2 Nanog expression and misexpression in vitro and in vivo

In contrast to Oct4 and Sox2, Nanog is not present as a maternal transcript and is not expressed during early cleavage stages. Rather, Nanog expression is first detectable by *in situ* methods at the morula stage (Figure 1.3), is then restricted to the inner cell mass

of the blastocyst but becomes down-regulated prior to implantation (Chambers et al., 2003; Mitsui et al., 2003). In the post-implantation embryo Nanog is expressed in the epiblast but is quickly down-regulated when cells proceed through the primitive streak to form mesoderm (Hart et al., 2004). Later in development Nanog expression can be detected in primordial germ cells (Chambers et al., 2003; Yamaguchi et al., 2005).

The in vivo phenotype of Nanog deletion shows that it is critical for early ICM cells to mature into pluripotent epiblast. Cells that are allocated to the ICM but that are *Nanog*$^{-/-}$ increasingly degenerate between E3.5 and E4.5 (Silva et al., 2009). Interestingly Nanog$^{-/-}$ cells fail to reactivate X inactivation and do not generate pluripotent cells in the embryo (Silva et al., 2009). This is of interest given that Nanog, Oct4, and Sox2 have been shown to bind within *Xist* intron 1 in undifferentiated ES cells (Navarro et al., 2008). The quick loss of all three factors from *Xist* intron 1 triggers ectopic accumulation of *Xist* RNA (Navarro et al., 2008). This has led to the conclusion that Oct4, Nanog and Sox2 cooperate to repress *Xist,* thus coupling the X-chromosome activation status to the control of pluripotency during embryogenesis (Navarro et al., 2008).

However Nanog is not essential for propagation of pluripotency *ex vivo* (Chambers et al., 2007). Nanog null ES cells are more inclined to differentiate but can be grown indefinitely *in vitro* and contribute extensively to somatic chimeras (Chambers et al., 2007).

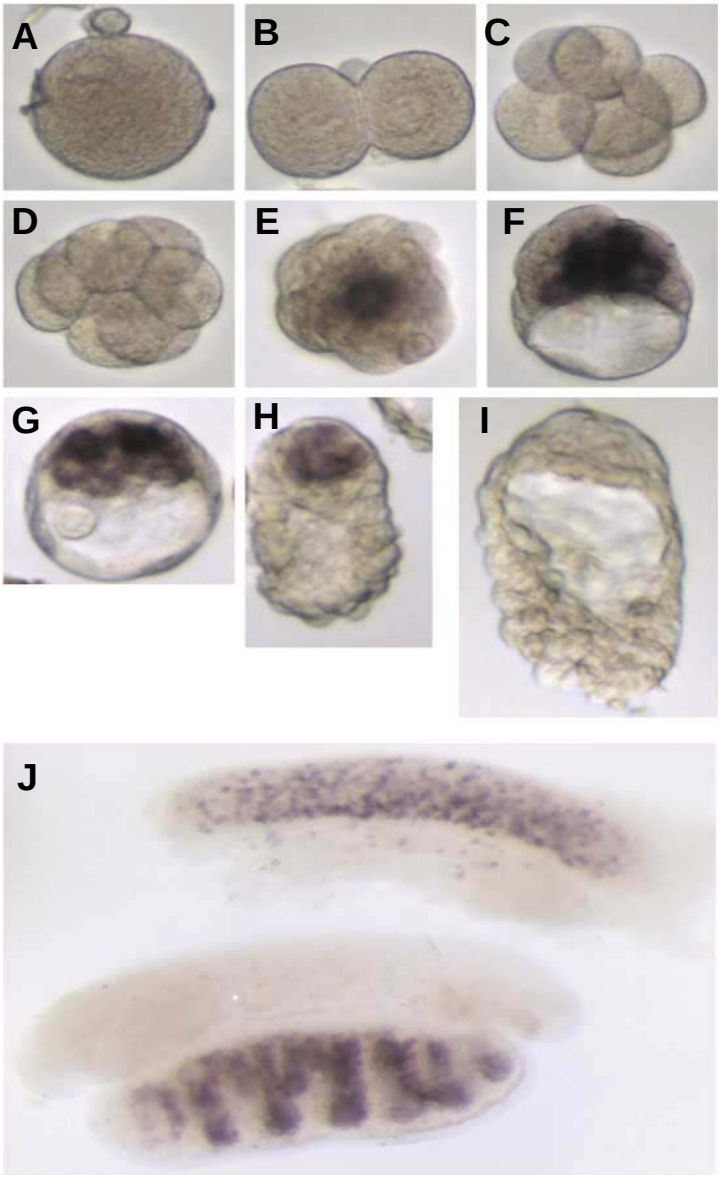

Figure 1.3 In situ hybridization showing Nanog mRNA expression during embryogenesis

In situ hybridization at different stages of mouse embryogenesis was used to detect Nanog mRNA. Panels show zygote (A), two cell (B), 6 cell (C), 8 cell (D), late morula (E), early blastocyst (F), expanded blastocyst, (G) hatched blastocyst (H), implanting blastocyst (I) and genital ridges (J).
Taken from (Chambers et al., 2003).

An interesting attribute of Nanog expression is that Nanog is heterogeneously expressed in the ICM of the mouse embryo in a salt and pepper distribution at E3.5 (Chazaud et al., 2006; Dietrich and Hiiragi, 2008). Interestingly the expression of Nanog is mutually exclusive to the expression of Gata6 which as well shows a random salt and pepper distribution in the ICM at E3.5 (Chazaud et al., 2006; Dietrich and Hiiragi, 2008). This salt and pepper distribution is resolved in the epiblast. In murine ES cells Nanog is also heterogeneously expressed in the Oct4 positive compartment with Nanog-negative cells showing an enhanced propensity towards differentiation (Chambers et al., 2007). Futhermore, Nanog low cultures can regenerate Nanog high cells. Therefore the transient downregulation of Nanog predisposes cells towards differentiation but does not necessary mark commitment (Chambers et al., 2007). Interestingly, this heterogenous expression is not exclusive to Nanog in ES cells. Further publications have reported that Stella (Hayashi et al., 2008), Rex1 (Toyooka et al., 2008), Hex (Canham et al., 2010) and Esrrb (van den Berg et al., 2008) are also heterogeneously expressed in ES cells.

1.7.3.3 Nanog regulation

A composite Oct4/Sox2 motif is present 180-166 bp upstream of the major transcription site of *Nanog* (Chambers and Smith, 2004). This motif is well conserved between mouse, rat and human. Mutagenesis of the Oct and Sox elements of this motif reduce the activity of luciferase constructs in transient expression assays (Kuroda, 2005; Rodda et al., 2005). Together with data from studies examining the localization of Oct4, Sox2 and Nanog to chromatin throughout the ES cell genome (Boyer et al., 2005; Loh et al., 2006), this led to the hypothesis that these transcription factors feedback positively on

each others genes to re-inforce gene expression. This would however imply that all cells expressing Oct4 should express Nanog, yet as we know from immunoflourescence data and from the activity of the Nanog:GFP allele, this is not the case (Chambers et al., 2007).

As Nanog heterogeneity has functional consequences for cell fate (since $Nanog^{low}$ cells are prone to commitment) it is important to understand how Nanog is regulated (Chambers et al., 2007). Amongst the various molecular pathways that have been reported to affect expression of Nanog, including p53 (Lin, 2005), Tcf3 (Pereira et al., 2006) and Satb1 (Savarese et al., 2009), the MEK pathway (Hamazaki et al., 2006; Kunath et al., 2007) stands out due to effects on the heterogeneity of expression patterns *in vivo*. Embryos lacking Grb2 and that consequently do not activate the MEK pathway did not form primitive endoderm and showed Nanog expression in all ICM cells (Chazaud et al., 2006). These results were recently confirmed in a study in which blockade of Erk signalling from the 8-cell stage suppressed development of the primitive endoderm (Nichols et al., 2009).

1.8 Aims of this thesis

Although the understanding of how Nanog heterogeneity is controlled is crucial for an appreciation of how different ES cell states are regulated, knowledge in this area is incomplete. Therefore, this thesis investigated the controls operating to produce Nanog heterogeneity. As self-renewal depends on the gene regulatory network surrounding Oct4 and Nanog the relationship between these two factors was a particular focus of attention.

Chapter 2

Materials and Methods

Chemicals described in this chapter were, unless otherwise stated, obtained from Fisher, and oligonucleotides were synthesised by vhBio. The water used for all procedures was milliQ water (Milipore) which was monitored for electrical resistance during purification, and used at 18.2 mΩ.

2.1 Culture and manipulation of mouse ES cells

2.1.1 Cell culture materials

SOLUTIONS/CHEMICALS	COMPANY	CATALOG NO
l-Glutamine 200 mM	Invitrogen	25030-024
Sodium pyruvate 100 mM	Invitrogen	11360-039
MEM Non-essential amino acids (100x)	Invitrogen	11140-036
Trypsin (100x) 2.5%	Invitrogen	15090-046
Penicillin /Streptomycin	Invitrogen	15140-122
Chick serum	Sigma	C5405
Tryptose Phosphate Broth	Sigma	T8159
Gelatin	Sigma	G1890
2-Mercaptoethanol	Sigma	M6250
G418 sulphate	PAA	P27-011
Puromycin dihydrochloride	Sigma	P8833
Hygromycin B (50 mg/ml)	Roche	843 555

Table 2.1 Overview of cell culture materials

Preparation :

(All aliquoted solutions are tested for contamination for 3 days before use)

Trypsin (1x):

500 ml PBS, add 0.186 g EDTA. Filter sterilised 5 ml chick serum and 5 ml concentrated Trypsin (2.5%) added and mixed. Final concentration of Trypsin: 0.025%.

Trypsin (4x):

As above, but with 20 ml concentrated Trypsin (2.5%). Final concentration of Trypsin: 0.1%.

Glutamate / pyruvate:

5.5 ml of Sodium pyruvate, 100 mM and 5.5 ml of l-Glutamine 200 mM.

Gelatin:

1% solution prepared in UHP water and autoclaved.

2-Mercaptoethanol:

200 µl of 2-Mercaptoethanol (14.3M) mixed with 28.2 ml UHP water. Final concentration 0.1 M.

Testers:

5 ml Tryptose Phospate Broth in universal.

LIF preparation:

Medium from transfected Cos7 cells is collected and is diluted with PBS to give a stock concentration of 100,000 Units/ml and frozen in 600µl aliquots.

ES cell Medium

500 ml GMEM (Sigma)

11 ml 50 mM Sodium pyruvate / 100 mM L-Glutamine (Invitrogen)

51 ml Foetal Calf Serum (Invitrogen)

5.5 ml 100x Non-essential amino acids (Gibco)

570 µl 0.1 M 2-mercaptoethanol (BDH)

570 µl LIF (prepared and titrated by ISCR staff and stock aliquoted at 100,000 units/ml)

2.1.2 Culturing mouse ES cells

1. Routinely cultured cells were passaged every 2-3 days when they were approximately 70- 80% confluent.
2. Cells were cultured on gelatin coated plates/flasks (Iwaki). 0.1% gelatin was applied to the flask 10-20 min before cells were trypsinised.
3. Spent ES cell medium was aspirated and cells were washed once with pre-warmed PBS (Sigma).
4. Enough Trypsin solution was added to cover the cells (0.5 -1.0 ml per $25cm^2$) and cells were incubated in the 37°C / 7% CO_2 incubator for approximately 1 min.
5. The plate/flask was tapped to dislodge the cells.
6. To neutralize the Trypsin, 4x volumes of ES cell media were added.
7. Cells were transferred into a universal tube and centrifuged at 1200 rpm; 3 min (ALC PK120; Annita III; 250xg).

8. The pellet was resuspended in ES cell media and cells were split 1:5-1:10 at each passage.
9. Cells were gassed with 5% CO_2/air for 15 sec and returned to the 37°C incubator.
10. Media was changed daily for wt ES cells (such as E14Tg2a) or every second day for some mutant cell lines.

2.1.3 Freezing mouse ES cells

1. Routinely 1-2 vials were frozen from a 80% confluent 25 cm^2 flask or 3-6 vials from a 75 cm^2 flask.
2. When mouse ES cells were to be frozen, trypsinised cells were prepared as in section 2.1.2 up to step 8.
3. Cells (~$5x10^6$) were resuspended in 1 ml culture freezing medium (ES cell media containing 10% DMSO), aliquoted into a cryotube (Nunc) and placed on ice.
4. Cells were stored as soon as possible in the 80^oC freezer overnight and transferred to a $N_{2(lq)}$ tank (-180°C) on the next day for long term storage. (It is important to cool down the cells gradually.)

2.1.4 Thawing mouse ES cells

1. A vial of frozen cells was taken from the $N_{2(lq)}$ tank and warmed quickly to 37^oC in the waterbath or by contact with hands. (It is important to thaw the cells as quick as possible.)
2. Cells were immediately transferred to a universal containing 10 ml of pre-warmed ES cell media and mixed gently.

3. Cells were centrifuged at 1000 rpm; 3 min (ALC PK120; Annita III; 200xg).
4. Media was aspirated carefully and cell pellet was gently resuspended in 5 ml pre-warmed ES cell media and transferred into a gelatinised flask.
5. Flask was placed in a 37°C/ 7% CO_2 incubator.
6. Appropriate changes were made to the $N_{2(lq)}$ storage book.

2.1.5 Colony forming assay

1. The colony forming assay was performed by seeding 600 cells in a well of a six well plate (60 cells/cm^2).
2. Cells were cultured in a 37°C/7% CO_2 incubator for 6 days in the presence or absence of LIF.
3. After 6 days cells were inspected and an alkaline phospatase staining was performed.

2.1.6 Alkaline phosphatase staining

This was performed using an Alkaline Phosphatase kit (Sigma Cat. # 86R-1KT). All components were stored at 4^0C until their expiration dates.

Fixative Solution (keep at 4^0C): 25 ml Citrate solution (18 mM Citric acid: 9 mM Sodium citrate: 12 mM NaCl), 8 ml Formaldehyde, 65 ml Acetone

Staining solution: 400 µl FRV alkaline solution and 400 µl Sodium Nitrite solution were combined and incubated at (RT). After 2 min of incubation the Alkaline/Nitrite mix was added to 18 ml dH_2O. At the end, 400 µl Napthol solution was added to the mix.

Procedure:

1. Medium was aspirated and cells were washed twice with warm PBS.
2. Enough fixative solution was added to cover each well (~2 ml in a six well) and cells were fixed for 45 sec. (Do not fix longer then 2 min.)
3. Fixative was aspirated and cells were washed in dH_2O.
4. Enough stain was added to cover each well (~2 ml in a six well) and cells were incubated in dark for 15 min (RT).
5. The staining solution was aspirated and cells were washed with dH_2O.
6. Plates were air dried before microscopic inspection.

2.1.7 Induction of ES cells differentiation

2.1.7.1 LIF withdrawal

Cells were prepared until step 8 of Chapter 2.1.2. Cell pellet was resuspended in complete medium not containing LIF. Cells were counted and replated at low density in complete medium but without LIF. The density of the cells varied from preferable 10^3 cells/cm^2 to 10^4 cells/cm^2. When cells were replated at higher density then 10^3 cells/cm^2 the proportion of undifferentiated ES cells in differentiating cultures was higher, however differentiation was still possible. If cells were replated at 10^3 cells/cm^2 the medium was changed daily after initial 72 hours.

2.1.7.2 Neural differentiation

Cells were prepared until step 8 of section 2.1.2. The cell pellet was resuspended in N2B27 medium (Stem Cells Sciences) and cells were carefully counted, as the plating

density is very important for neural induction. In my protocol most cell lines were replated at a density of 10^4 cells/cm^2 and left for one day in N2B27 medium containing LIF. On the second day the medium was changed into N2B27 only and changed daily for the time course of experiment. The first morphological changes were detected after 2-3 days and increased quickly over the following days.

2.1.8 DNA transfection into mouse ES cells

2.1.8.1 Stable transfection

1. Only healthy sub-confluent ES cells were used for transfection and medium was changed 2 h before electroporation was performed.
2. 9 cm diameter plates were gelatinised and 9 ml of ES cell medium was added into the plate and placed in the 37°C/ 7% CO_2 incubator.
3. Cells were pelleted at 1200 rpm; 3 min (ALC PK120; Annita III; 250xg), washed twice in 20 ml of PBS and counted using a haemocytometer.
4. 10^7 cells were pelleted at 1200 rpm; 3 min (ALC PK120; Annita III; 250xg) and resuspended in 0.7 ml PBS.
5. 100 µg of linearised DNA were resuspended in 0.1 ml 1x PBS and placed in a electroporation cuvette (Biorad).
6. 0.7 ml (10^7 cells) were added to the cuvette and mixed gently.
7. Electroporation was performed at 0.8 kV and 3 µF using a Gene Pulser (Biorad).
8. Cells were quickly aspirated with a plugged Pasteur pipette and added to 9.2 ml of pre-warmed ES cell media.

9. 1 ml ($1x10^6$) cell suspension was added to each 9 cm diameter plate and placed in the 37°C/ 7% CO_2 incubator.
10. Antibiotic selection was started 24-30h post-transfection.

2.1.8.2 Transient transfection

1. 10^6 cells were plated in a six-well plate and supplemented with 2 ml media.
2. Cells were placed in the 37°C/ 7% CO_2 incubator to attach.
3. For each transfection 3 µl Lipofectamine 2000 (Invitrogen) were resuspended in 250 µl serum-free medium and incubated at RT for 5 min.
4. For each transfection 3 µg plasmid DNA were resuspended in 250 µl serum-free medium and incubated at RT for 5 min.
5. The two solutions were combined, mixed gently and incubated at RT for 20 min.
6. The mixture was added directly to the cells and left for at least 24 hours in the 37°C/ 7% CO_2 incubator.
7. Antibiotic selection was started routinely 24-30 h post transfection.

ANTIBIOTIC	COMPANY	STOCK CONCENTRATION	WORKING CONCENTRATION
Blastocidin S HCL	Invitrogen	5 mg/ml	5-15 µg/ml
G418	PAA	200 mg/ml	200 µg/ml
Hygromycin	Roche	50 mg/ml	100-200 µg/ml
Puromycin	Sigma	5 mg/ml	1-2 µg/ml

Table 2.2 Antibiotic concentrations used for drug selection

2.1.8.3 Picking mouse ES cell colonies

1. ES cell colonies were grown for 8-14 days before they were picked.
2. Cells were washed once with pre-warmed PBS and a small amount of Trypsin (5µl) was picked up in a yellow tip and expelled gently onto the colony.
3. The colony was dislodged with the pipette tip and transferred into a gelatinised 96 well plate containing 200 µl of ES cell media.
4. Each colony was dispersed to ensure a break up of the colony.
5. The plate was placed in the 37^{o}C/7% CO_2 incubator.

2.2 Immunochemical techniques

2.2.1 Immunofluorescence analysis

1. Cells were rinsed once in PBS and fixed in 4% PFA for 10 min (RT).
2. Permeabilisation was performed by incubating in 0.3% Triton X 100/PBS twice for 5 min. If cells were not immediately processed they were stored in PBS at 4^{o}C.
3. Blocking was performed for >20 min in 1% BSA / 3% normal serum (from same species as Secondary antibody) in 0.3% Triton X 100/PBS (RT).
4. Primary antibodies were diluted in blocking solution and after addition, cells were incubated overnight at 4°C.
5. Cells were washed 3 times in 0.3% Triton X 100/PBS for 10 min.
6. Secondary antibodies conjugated to Alexa florophores (Molecular probes, Eugene Oregon, United States) were diluted 1:1000 in blocking solution and applied for 1 h (RT) in the dark.

7. Cells were washed 3 times in 0.3% Triton X 100/PBS for 10 min.
8. Cells were photographed or stained additionally with DAPI and stored in PBS at 4°C in the dark.

NAME	COMPANY	CATALOG NUMBER	ANTIBODY DILUTION	CLASS
75X36 Epitope: (SVGLPGPHSLPSSEE)	Produce in house	N/A	1:2000	Rabbit-HRP
Oct-4-C-10	Santa Cruz	sc-5279	1:1000	Mouse-HRP
TBX3	Santa Cruz	sc-17871	1:2000	Mouse-HRP
Sall4	Abnova	954-1053	1:1000	Mouse-IgG1
Esrrb	R&D Systems	PP-H6707-00	1: 2000	Mouse IgG2A
Klf4	R&D Systems	AF 3158	1:1000	Goat IgG
Sox2	Santa Cruz	sc-17320	1:1000	Goat IgG
Rex1	Santa Cruz	sc-50668	1:50	Goat IgG
pERK	Cell signaling	9106 S	1:50	Mouse IgG1
TUJI	Covance	MMS-435P	1:1000	Mouse IgG2a
Nestin	Hybridoma Bank	Rat-401-S	1:50	Goat IgG1

Table 2.3 Antibodies used for immunofluorescence analysis

2.2.2 FACS analysis

Cells were trypsinised and prepared as in section 2.1.2 until step 8. The pellet was resuspended in ice cold PBS/10% FCS at a density of $1x10^6$ cells/ml. Anti-SSEA1

antibody (mc480 IgM, Developmental Studies Hybridoma Bank, Department of Biological Sciences, University of Iowa, Iowa City, USA) was added to cells at 1:1,000 dilution, cells were incubated at 4^{o}C for 15 min and washed in PBS/10% FCS. Phycoerythrinconjugated anti-IgM mouse antibody (Jacksons Laboratories) was then added at a dilution of 1:1000 for 15 min at 4^{o}C in the dark. Propidium iodide (Sigma) was added to a dilution of 1:5000 to identify dead cells. FACS Calibur (Becton Dickinson) and FlowJo software was used for data analysis and presentation.

2.2.3 SDS-PAGE Electrophoresis and Immunoblotting

Running Buffer: MOPS Running Buffer (Invitrogen)

Transfer Buffer: 25 mM Tris, 0.21 M Glycine, 20% Methanol.

TBS: 10 mM Tris pH 7.6-8.0, 150 mM NaCl.

Immunoblot wash: 0.65 M NaCl, 10 mM Tris pH 7.8, 0.3% Triton X-100-TBS.

Stripping Buffer: 62.5 mM Tris pH 6.8, 2% SDS

2x Laemmli Buffer: 125 mM Tris pH 6.8, 4% SDS, 25% Glycerol, 0.01% bromophenol blue, 5% 2-mercaptoethanol.

1. Samples were prepared in 1x Laemmli buffer prior to loading. About 1x10^{6} cells were lysed in 200 µl 1x Laemmli buffer.
2. Running buffer was poured into the upper and lower chamber of the XCell*Surelock* module (Invitrogen).

3. If not otherwise quantified, 10 µl of lysate and 10 µl 'See Blue Plus 2' were loaded onto 10% Bis-Tris gels (Invitrogen). Electrophoresis was performed at 200 V for ~ 70 min at RT.
4. After electrophoresis the gel foot was cut off and the gel was soaked in ice cold transfer buffer.
5. Protein transfer was performed in the cold (4°C) at 395 mA constant for 70 min.
6. Directly after the transfer the membrane was washed briefly in TBS-T.
7. Blocking of non-specific binding was performed overnight in 10% non-fat dry milk in TBS-T.
8. Dilute solutions of primary antibodies were incubated for 2h (RT) with the membrane (Table 2.4). The antibodies were diluted in 5% non-fat dry milk in TBS-T.
9. The membrane was washed 3x; 15 min on a roller device (Denley/Spiramix2) in TBS-T.
10. Dilute solutions of secondary antibodies were incubated for 1h with the membrane. Antibodies were diluted in 5% non-fat dry milk in TBS-T.
11. The membrane was washed 3x; 15 min in TBS-T.
12. After the last wash, the membrane was incubated with Super-Signal West Pico reagent (Pierce) for 5 min (RT) and wrapped in cling film.
13. The membrane was exposed directly to Hyperfilm (Amersham) for several sec-min depending on the signal strength.
14. A SRX-101A developer (Konica-Minolta) was used to develop the film.

2.2.4 Stripping immunoblot membranes

Stripping buffer was warmed to 70°C. The membrane was incubated with stripping buffer in a universal at 70°C; 40 min. After the membrane was washed extensively 3x; 5 min the blot was ready for re-blocking and re-exposure.

ANTIBODY	COMPANY	CATALOG NUMBER	DILUTION	SECONDARY REAGENT
75X36	House Production	N/A	1:3000	Rabbit-HRP
Oct-4 C10	Santa Cruz	Sc5279	1:1000	Mouse-HRP
GFP	Sigma	MMS-101P	1:2000	Mouse-HRP
HDAC2	Upstate	05-814	1:1000	Mouse-HRP
mouse-HRP	Amersham	NA931	1:2000	N/A
rabbit-HRP	Amersham	NA934	1:2000	N/A

Table 2.4 Antibodies used for immunoblotting

2.3. Molecular biology techniques

2.3.1 Nucleic acid isolation

2.3.1.1 Plasmid isolation from bacterial cells

A colony of bacteria harboring the plasmid of interest was grown overnight at 37^{o}C with shaking at 225 rpm in LB broth supplemented with the appropriate antibiotic. Plasmid DNA isolation was performed using the Miniprep Kit (Qiagen catalogue no. 27104) or

the Maxiprep Kit (Qiagen catalogue no. 12163) following the instructions of the manufacturer. Plasmid concentration and purity (A_{260}/A_{280} and A_{260}/A_{230} values) were estimated using a NanoDrop® (ND-1000) spectrophotometer.

2.3.1.2 RNA isolation

RNA isolation was performed using the RNAEasy kit (Qiagen catalogue no. 74106) following the instructions of the manufacture. RNA concentration and purity (A_{260}/A_{280} and A_{260}/A_{230} values) were estimated using a NanoDrop® (ND-1000) spectrophotometer.

2.3.1.3 Genomic DNA isolation

DNA isolation was performed using the DNeasy Blood and Tissue kit (Qiagen catalogue no. 69504) following the instructions of the manufacturer. DNA concentration and purity (A_{260}/A_{280} and A_{260}/A_{230} values) were estimated using a NanoDrop® (ND-1000) spectrophotometer.

2.3.1.4 Ethanol precipitation of DNA

1. 1/10 or 1/15 volume of 3M Sodium acetate pH 4.8-5.2 were added to the DNA sample and mixed well.
2. 2-2.5 volumes of 100% Ethanol were added to the DNA/Sodium acetate mix and left at -20°C>30 min.
3. Sample was centrifuged at maximum speed at 4°C; 15 min.

4. The supernatant was carefully removed and the pellet was washed in 70% ice cold ethanol.
5. DNA sample was spun at full speed at 4°C; 15 min.
6. Ethanol was carefully removed and the pellet air dried.
7. Dry pellet was resuspended in the appropriate volume of water or TE.

2.3.2 DNA manipulation

2.3.2.1 Restriction endonuclease digestion

DNA was digested using restriction endonucleases from Roche or New England Biolabs according to the manufacture's instructions.

2.3.2.2 Blunt ending of 5' overhang

1. DNA was digested with the desired overhang-generating restriction enzyme.
2. To 1-4 µg of digested DNA, dNTP's (33µM as final concentration) and Klenow (1 unit per microgram DNA) were added and the reaction was incubated at RT; 15 min.
3. The reaction was stopped by adding EDTA to a final concentration of 10 mM and heating at 75°C; 10 min.

2.3.2.3 Polymerase Chain Reaction (PCR)

Routinely reactions were performed using *Taq* DNA polymerase. When a low mutation frequency was required, Phusion (Finnzymes), a high fidelity *Taq* DNA polymerase was used.

A 50 µl reaction contained the following;

DNA template (150ng cDNA/reaction)

300 nM oligo 1

300 nM oligo 2

200 µM dNTP's

1x PCR Buffer (Supplied by manufacturer)

0.5 µl Phusion (5U/µl) or *Taq* (5U/µl)

Make up to volume of a final 50 µl with milliQ H_2O.

The following programs were used on a GeneAmp®9700 thermocycler (Applied Biosystems).

For Phusion, high fidelity *Taq* DNA polymerase reaction:

1 cycle - 98°C 1- 5min

15-35 cyces - 98°C 15 sec-30 sec
T_m 15-60 sec
72°C 1min per kb

1 cycle - 72°C 10 min

For *Taq* DNA polymerase reaction:

1 cycle - 95°C 1- 5 min

15-35 cycles - 95°C 15 sec-30 sec
T_m 15-60 sec
72°C 1 min per kb

1 cycle - 72°C 10 min

5-10 µl of PCR reaction mixture was subjected to TBE or TAE agarose gel electrophoresis to visualise the product.

2.3.2.4 Agarose gel electrophoresis

1. For a 1% gel, 1g agarose powder (Seakem) was measured and added to 100 ml 0.5xTBE or 1x TAE buffer (45 mM Tris- borate, acetate, 1 mM EDTA).
2. The agarose was melted in a microwave until the solution became clear.
3. When the agarose solution has cooled to about 50°C (e.g. by running under a cold tap), Ethidium bromide was added to a final concentration of 0.25µg/ml and the solution was poured directly into the casting tray, ensuring that no bubbles got into the gel.
4. Gels were run routinely at 100 V in a gel tank, with the DNA in 1x Ficoll Blue DNA loading buffer (6x stock; 15% w/v Ficoll 400 (Amersham) in dH_2O/0.02% bromophenol blue (BHD)).
5. After running the gel, the DNA was visualised using a GeneFlash Imager (Syngene).

2.3.2.5 Preparing new DNA molecules

2.3.2.5.1 Purification of restriction DNA fragments

1. 2-10 µg plasmid DNA were digested routinely according to the manufacture's instructions (New England Biolabs or Roche).

2. Digested plasmid DNA was loaded onto a TAE agarose gel and separated according to size by gel electrophoresis.
3. The bands were located with a long-wavelegth UV light-box.
4. The gel slice containing the DNA fragment was excised using a clean scalpel and placed in a 1.5 mL eppendorf tube.
5. The DNA was extracted from the gel using the QIAquick gel extraction kit (Qiagen) following the manufacturer's instructions.

2.3.2.5.2 Ligation

1. Routinely ligation reactions were performed using either T4 DNA Ligase or QuickLigase (New England Biolabs) in a volume of 20 µl.
2. The vector: insert ratio was set as 1:1 or 1:3 using 100 ng of the vector fragment.
3. The ligation was performed at 16^0C overnight or at RT;30 min.
4. Following the ligation, the DNA was transformed by adding 6 µl of the ligation mix to 50 µl DH5α *E.coli* or One Shot® Chemically Competent *E. coli.*

2.3.2.5.3 Cloning of blunt and PCR products

For blunt ending the Zero Blunt® TOPO® cloning kit was used (Invitrogen) following the manufacturer's instructions. The pCR®-Blunt II- TOPO® vector contains *Eco*RI flanking the insert site which enables a first screening of transformants via *Eco*RI digestions. Subsequently, cloned PCR products were confirmed by sequencing. This was performed at the school of Biological Sequencing Service – University of Edinburgh or

the University of Dundee. The analysis of the data was performed using the Seqman software (Lasergene).

2.3.3 Transformation of plasmid DNA into *E.coli*

Autoclaved Luria Broth (LB) agar (1.5% w/v agar in LB, 1% w/v tryptone (Difco), 0.5% w/v yeast extract (Difco), 5 mM NaCl) was melted and cooled to about 50°C. The appropriate antibiotics were added to the agar at the concentrations indicated in Table 2.5. A thin layer of LB Agar was poured into a sterile Petri dish.

1. DH5α *E.coli* (Invitrogen) or One Shot® Chemically Competent *E. coli* (Invitrogen) were placed directly on ice after removing from -80^{o}C storage.
2. 1- 10 ng plasmid or 6 µl of a ligation reaction were added to DH5α *E.coli* or One Shot® Chemically competent *E. coli* with a sterile pipette.
3. Cells were mixed very gently (do not pipette up and down) and incubated on ice for 30 min.
4. Cells were heat shocked for 30 sec at 42°C and tubes were placed immediately on ice for at least 2 min.
5. The transformation mixture was added to 950 µl LB broth (DH5α) or 250 µl SOC medium (One Shot®).
6. Cells were shaked at 225 rpm in 37°C for 1 h in an orbital shaker.
7. Serial dilutions were spread onto the appropriate antibiotic containing plates (Table 2.5) under sterile conditions.
8. Plates were left undistured until the inoculum was absorbed and then inverted.

9. Plates were incubated overnight at 37°C and stored at 4°C (until transformation was successful).
10. Transformation efficiency was monitored by transfecting a 5 pg of pUC19 plasmid.

ANTIBIOTIC	STOCK CONCENTRATION	WORKING CONCENTRATION
Ampicillin	100 mg/ml in dH_2O	50 µg/ml
Carbenicillin	100 mg/ml in dH_2O	50 µg/ml
Kanamycin	10 mg/ml in$ENRATdH_2O$	20 µg/ml
Zeocin	100 mg/ml in dH_2O	25 µg/ml

Table 2.5 Antibiotic concentrations for selection of transformants in *E.coli.*

2.3.3.1 Screeing for correct ligation products

~ 200-400 ng of Miniprep DNA was digested with at least 2 or 3 restriction endonucleases to define the specific restriction fragment length pattern upon agarose gel electrophoresis.

2.3.4 Analysis of ES cell RNA

2.3.4.1 First strand cDNA synthesis

First strand cDNA was synthesised from 1-2 µg of total RNA using the superscript® II reverse transcriptase (Invitrogen catalogue no. 12371-019) following the instructions of the manufacturer.

2.3.4.2 Quantitative PCR

Q-PCR was performed by using the primers listed in Table 2.6 with a LightCycler 480 probes master kit (Roche Cat. no. 04707494001) and LightCycler 480 Sybr Green 1 master kit (Roche Cat. no. 04707516001) with cDNA equivalent to 25 ng total RNA. New oligos have been designed with the "Universal probe library" software (Roche; www.universalprobelibrary.com).

Thermal cycles monocolour hydrolysis probe protocol:

1 cycle - 95 ^{o}C for 5 min

45 cycles - 95 ^{o}C, 10 sec
61 ^{o}C, 10 sec

Thermal cycles Sybr Green protocol:

1 cylce - 95^{o}C for 5 min

45 cycles - 95 ^{o}C, 0.5sec
60 ^{o}C, 10 sec
72 ^{o}C, 20 sec
81 ^{o}C ,1 sec.

2.3.4.3 Fluidigm gene expression analysis

Protocols are copied from BioMark Advanced Development Protocol: "Gene expression Analysis Using Assays designed with Probes from the Universal Probe Library (Roche Applied Sciences). Number 8.

Preparing primer stocks:

1. Primer stocks were prepared at 200 µM using TE Buffer

2. A 100x mixture of forward and reverse primers for each of the assays was prepared by preparing a 1/10 dilution of the original stock.

3. A 4x primer mixture for specific target amplification was prepared by pooling by pooling the primer mixes in Step2 for each assay. The concnentration of each primer in the 100x stock is 20 µM and the final concentration of each primer should be 200 nM in the 4x mix.

For the Specific Target Amplification the following Ingredients were mixed:

Ingredients	Volume µl
cDNA (from 1 to 25 ng total RNA)	2.5
4x Multiplex primer Mix	2.5
2X TaqMan PreAmpMaster Mix (PN 4391128)	5
Total	10

Thermal cycles

1 cycle – 95^{o}C, 10 min

14 cycles – 95^{o}C, 15 sec
60^{o}C, 4 min

Samples were diluted by adding 40 µl TE. Stored thereafter at -20^{o}C.

The 10x Assay Mix was prepared as follow:

Ingredients	Volume µl (per assay inlet)
DA Assay Loading Reagent (PN 85000735)	2.5
100X Primer Pair Mix	0.5
Probe from library	0.5
Water	1.5
Total	5.0

Sample Mix for 48 Samples:

Ingredients	Volume µl
TaqMan Universal PCR Master Mix (PN 4304437)	200
GE Sample Loading Reagent (PN 85000746)	20
Total	2

1. 4 µl of the Sample Mix were added to each of the 48 well or tubes
2. 2.5 µl of Sta Sample were added to each of the 48 wells or tubes

Running the Chip

Thermal cycles:

1 cycle – 50°C, 2 min

1 cycle – 95°C, 10 min

40 cycles – 95°C, 15 sec
70°C, 5 sec
60°C, 1 min

PRIMER	FORWARD SEQUENCE	REVERSE SEQUENCE
Oct4	GTTGGAGAAGGTGGAACCAA	CTCCTTCTGCAGGGCTTTC
Oct6	CATCTCCACCCGCAAGAC	CGTTCGTTAAGGCCAGGAG
Bbx	TGTGTGCCTCCCATTTACCT	TCAGAACTTCCAGCTTCTGTGA
Brachyury	CAGCCCACCTACTGGCTCTA	GAGCCTGGGGTGATGGTA
Dnajb6	TCCGGAACCCAGATGATG	CACCTCGGCTTCTATTTCCTC
Dusp6	CTGGTGGAGAGTCGGTCCT	CGGCCTGGAACTTACTGAAG
Esrrb	TGAGGGTAACCTTTCCTTGC	ACGACATTCGGTTCAGCAG
Fabp7	AACCAGCATAGATGACAGAAACTG	ACTTCTGCACATGAATGAGCTT
Fgf5	GTTTCCAGTGGAGCCCTTC	CTTTGCCATCCGGGTAGAT
Gata6	GGTCTCTACAGCAAGATGAATGG	TGGCACAGGACAGTCCAAG
Intronic26	GGTGATACGTTGGCCTTCTAGT	TTCTCAAATACACACAAGAGCCTA
Intronic28	AGCCCAGTACTCAGGCTTGT	AGCATCACAACACGCACCT
Intronic29	GCCAGCAGATGGCATAATTT	TGATGGCAATGCTGAGGTTA
Intronic32	GATTCTATTCACCCAGCACCA	CCTTCTGAGTGGAGGTTTATCC
Intronic33	CCATCTCAGCTACTGGAGCA	ATTAGAACCGTGACCGCATC
Klf2	CTAAAGGCGCATCTGCGTA	TAGTGGCGGGTAAGCTCGT
Klf4	CGGGAAGGGAGAAGACT	GACTTCCTCACGCCAACG
Mybl2	TTAAATGGACCCACGAGGAG	TTCCAGTCTTGCTGTCCAAA
Nanog	CCTCCAGCAGATGCAAGAA	GCTTGCACTTCATCCTTTGG
Nestin	CTGCAGGCCACTGAAAAGT	TTCCAGGATCTGAGCGATCT
Nfatc4	TGGTGTTCGGAGAGGAAAAG	CATGGAGGGGTATCCTCTGA

Nfkb1	CACTGCTCAGGTCCACTGTC	CTGTCACTATCCCGGAGTTCA
Notch3	AGCTGGGTCCTGAGGTGAT	AGACAGAGCCGGTTGTCAAT
p53	ATGCCCATGCTACAGAGGAG	AGACTGGCCCTTCTTGGTCT
Pax6	GTTCCCTGTCCTGTGGACTC	ACCGCCCTTGGTTAAAGTCT
PBGD	AAAGTTCCCCAACCTGGAAT	CCAGGACAATGGCACTGAAT
Pitx2	CCTTACGGAAGCCCGAGT	AAAGCCATTCTTGCACAGC
Rex1	CAGCTCCTGCACACAGAAGA	ACTGATCCGCAAACACCTG
Satb1	ATGGCGTTGCTGTCTCTAGG	CTTCCCAACCTGGATGAGC
Sox2	GTGTTTGCAAAAAGGGAAAAGT	TCTTTCTCCCAGCCCTAGTCT
TBP	GGGGAGCTGTGATGTGAAGT	CCAGGAAATAATTCTGGCTCA
Tbx3	TTGCAAAGGGTTTTCGAGAC	TGCAGTGTGAGCTGCTTTCT
Tcfap2c	CGCGGAAGAGTATGTTGTTG	CGATCTTGATGGAGAAGGTCA
Tcfcp2l1	GGGGACTACTCGGAGCATCT	TTCCGATCAGCTCCCTTG
Tuji	GCGCATCAGCGTATACTACAA	TTCCAAGTCCACCAGAATGG
UTF1	GTCCCTCTCCGCGTTAGC	GGGGCAGGTTCGTCATTT
Zfp36	TCTCTTCACCAAGGCCATTC	CATGGCTCATCGACTGGA
Zfp57	TGGCTAGAAGCAGTCTGGAAT	CTGGATGGCTGGGAAGACT

Table 2.6 Primers used for quantitative PCR

2.3.5 Analysis of ES cell genomic DNA

2.3.5.1. Southern Blot analysis

Digestion of DNA

1. 4-5 µg of DNA in 40 µl total volume were digested for 1 hour at 37°C with 10 Units of restriction enzyme. A second aliquot of 10 Units was then added and incubation continued for a further hour at 37°C.
2. 4 µl of 10X loading dye were added and the sample loaded onto a 0.8% TAE gel.
3. One large gel tray - 24.4 x 15cm, was used to prepare a > 300 ml unstained gel. The gel tank was filled with 1X TAE and electrophoresis was performed overnight at 30V.

Blotting Gel

20X SSC 3M Sodium Chloride (174.2 g/litre)
0.3M Tri Sodium Citrate (88.2 g/litre)

Solution 1 0.5M Sodium Hydroxide (20 g/litre)
1M Sodium Chloride (58.4 g/litre)

Solution 2 0.5M Tris (30.28 g/500 ml)
3M Sodium Chloride (87.6 g/500 ml)
Dissolve Tris and NaCl in dH_2O pH 7.4

1. The Gel was put in a tray and stained with 500 ml dH_2O containing 1 µg/ml ethidium bromide for 30 min gentle rocking.
2. The gel was transferred to a new tray (using the large scoop) and photographed with a fluorescent ruler at the side. The gel was exposed for 1 min to 245nm UV. Using a short wave transilluminator (Herolab UVT-28S).
3. The gel was washed in 500 ml of solution 1; 15 min.
4. The gel was removed and the solution discarded. The step above was repeated with the remaining solution 1.
5. Solution 1 was poured off and the gel was rinsed briefly in dH_2O and washed in 500 ml of solution 2; 45 min.
6. 3 mm paper was prepared as follow:

   2 x 24 cm wide by length of paper

   4 x size of gel
7. Hybond XL membrane was cut to fit the gel, and labeled and soaked in 2X SSC.
8. The tray was set up with 20X SSC and glass plate was put on top.
9. 2 large pieces of 3mm paper were soaked together and placed on top of glass plate with the ends tucked into the 20X SSC beneath.
10. Air bubbles were rolled out with a pipette.
11. Gel was put onto plate and the top of the gel was cut through the wells with a blade. Gel was sandwiched with another glass plate and turned over.
12. More 20X SSC was added to the paper and gel was placed on top with no air bubbles.
13. Saran wrap was placed up to the edges of the gel on all sides.

14. The membrane was placed (soaked in 2X SSC) on top with marked side down. Wells were marked with a pencil.
15. 2 small pieces of 3 mm paper soaked in 2X SSC were placed on top.
16. 2 small dry pieces of 3 mm paper were placed on top.
17. 1 pack of paper towels was split and placed on top side by side.
18. A metal plate and a 500 ml bottle were placed on top.
19. Blot was left overnight.
20. Next day, the paper towels and paper were carefully removed and the membrane turned upright (DNA is on top) into a tray containing 2X SSC to wash.
21. Membrane was placed on to 3 mm paper to dry and then and baked for 2 h at 80ºC.

Following picture shows the blotting apparatus:

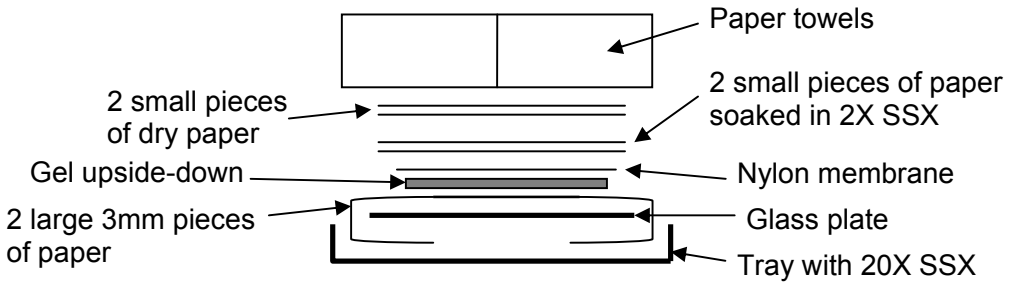

Pre-hybridisation

1. The hybridisation bottle was washed and blue and white caps were fitted on. A small amount of water was put in to the bottle and warmed up in the oven at 65ºC.
2. 1:100 (120 µl) salmon sperm DNA (Sigma) was added to 12 ml Perfecthyb (Sigma, H7033) in a 50 ml corning tube and warmed up in the 65ºC oven.
3. The filter was soaked in 2X SSC.
4. The water was tipped out of the bottle. The filter was rolled up and put into the bottle (marked corner near the white end) and unrolled without any air bubbles.
5. The Perfecthyb/salmon sperm DNA mix was added to the bottle and left for pre-hybridisation for at least 1 h while the probe was prepared.

Labeling Probe DNA

1. 2-25 ng of probe DNA were diluted into 45µl of TE.
2. DNA was boiled for 5 min, then snap frozen and centrifuged briefly.
3. DNA was added to rediprime tube (GE Healthcare Catalogue no. RPN1633) (not mixed).
4. 5 µl $dCTP^{32}$ were added and mixed by pipetting 12 times.
5. Incubation was performed at 37ºC; 10 min.
6. 5 µl 0.2M EDTA were added to stop the reaction.
7. Micro Bio-Spin 30 Chromatography Columns (Bio-RAD) were spuned at 2000 rpm; 3 min.

8. Meanwhile the volume of the probe was made up to 100 µl (45 µl dH_20 were added).
9. After the Column was centrifuged, the probe was added to the centre of the spin column and spinned again at 2000 rpm; 3 min.
10. The probe was boiled for 5 min and added to warmed Perfecthyb buffer (second pre-heated 12 ml containing salmon DNA).
11. The pre-hyb was tipped off from the filter and the probe was added.
12. Incubation was performed overnight at 65ºC.

Washes

1. The probe was tipped off and the membrane was rinsed with 0.5X SSC 0.1% SDS at room temperature (filtered solution).
2. Membrane was washed with 50 ml of pre-warmed 0.5X SSC 0.1% SDS at 65ºC ; 40 min.
3. Membrane was washed again with 50 ml of pre-warmed 0.5X SSC 0.1% SDS at 65ºC; 15 min.
4. At the end membrane was wrapped in cling film and placed in a cassette and exposed at first overnight at -80ºC.

Chapter 3

Oct4 influences *Nanog* expression

3.1 Introduction

Self-renewal depends on several extrinsic and intrinsic cues including a gene regulatory network centered around the transcription factors Nanog, Oct4 and Sox2. Existing ChIP data (Boyer et al., 2005; Loh et al., 2006) together with data from reporter assays (Chew et al., 2005; Kuroda, 2005; Rodda et al., 2005; Tomioka et al., 2002) have been interpreted to suggest that Oct4, Sox2 and Nanog positively regulate each other (Figure 3.1). This would suggest that all Oct4 positive cells express Nanog. However, as Oct4 positive cells exist that do not express Nanog (Chambers et al., 2007) the effects of alterating Oct4 expression upon Nanog heterogeneity were investigated in this Chapter.

3.2 Results

3.2.1 Functional Oct4 heterozygote ES cells express elevated level of Nanog mRNA and protein

Evidence has been presented that Oct4 positively regulates Nanog through binding to an Oct4/Sox2 element (Kuroda, 2005; Rodda et al., 2005) located 180 bp upstream of the mapped transcription initiation site (Chambers, 2004a). This suggests that cells expressing lower Oct4 levels should express reduced levels of Nanog.

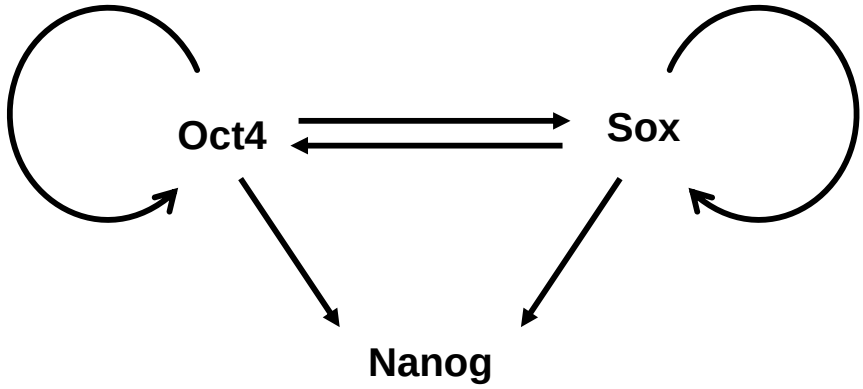

Figure 3.1 Model of Oct4, Sox2 and Nanog interaction

The drawing depicts a network pattern resulting from a simple positive feedback between the three core transcription factors Nanog, Oct4 and Sox2.

This was investigated by comparing Nanog expression in three ES cell lines (Table 3.1) genetically modified at the *Oct4* locus (ZHBTc4.1, ZHTc6 and OKO160) with three control ES cell lines, unmodified at the *Oct4* locus (E14Tg2a, CGR8 and Zin40). Surprisingly, all cell lines in which Oct4 expression was reduced harboured elevated levels of Nanog mRNA (Figure 3.2 A). Immunoblot analysis confirmed that this increase in mRNA was reflected in elevated levels of Nanog protein (Figure 3.2 B).

3.2.2 Functional Oct4 heterozygote ES cells express Nanog relatively homogeneously

To investigate how the elevated Nanog expression in ES cells expressing reduced Oct4 protein was reflected at the single cell level, immunofluorescence analysis was performed on colonies formed from individual cells. Nanog was detected at widely varying levels in individual nuclei within E14Tg2a colonies (Figure 3.3). In contrast, all cell lines expressing reduced Oct4 protein expressed Nanog more uniformly throughout the colonies and at levels comparable to those present in high Nanog expressing nuclei in E14Tg2a colonies. Additional ES cell specific genes such as Esrrb and Rex1 have been reported to be heterogeneously expressed in ES cells (Toyooka et al., 2008; van den Berg et al., 2008). Therefore, I investigated expression of Esrrb and Rex1 in the same cell lines by immunofluorescence (Figure 3.4 and 3.5). Esrrb (Figure 3.4) and Rex1 (Figure 3.5) were detected at widely varying levels in E14Tg2a cells, but were more uniformly expressed in ES cells expressing reduced Oct4 levels. To investigate the

CELL LINES	DERIVED FROM	GENETIC MODIFICATIONS
E14TG2a	129/ Ola mouse strain	Deficient in HPRT
CGR8	129/ Ola mouse strain	No modifications
ZIN40	129/ Ola mouse strain	Express a randomly integrated lacZ-ires-neo transgene
OKO8	E14Tg2a	An IRES-βgeopA cassette has been introduced into one Oct4 allele by homologous recombination
OKO160	CGR8	An IRES-βgeopA cassette has been introduced into one Oct4 allele by homologous recombination
ZHTc6	CGR8	Contains a Dox-suppressible Oct4 transgene. One allele has been inactivated by targeted intergration of an IRESzeopA cassette.
ZHBTc4.1	CGR8	As ZHTc6 cells but the second Oct4 allele has been inactivated by targeted integration of an IRESBSDpA cassette.
D7A3 PE	E14Tg2a	*Lif*$^{-/-}$ cells

Table 3.1 Overview of cell lines used in this chapter

The table summarizes name, origin and genetic modification made in each individual cell line. This table can be additionally found in the Appendix.

A

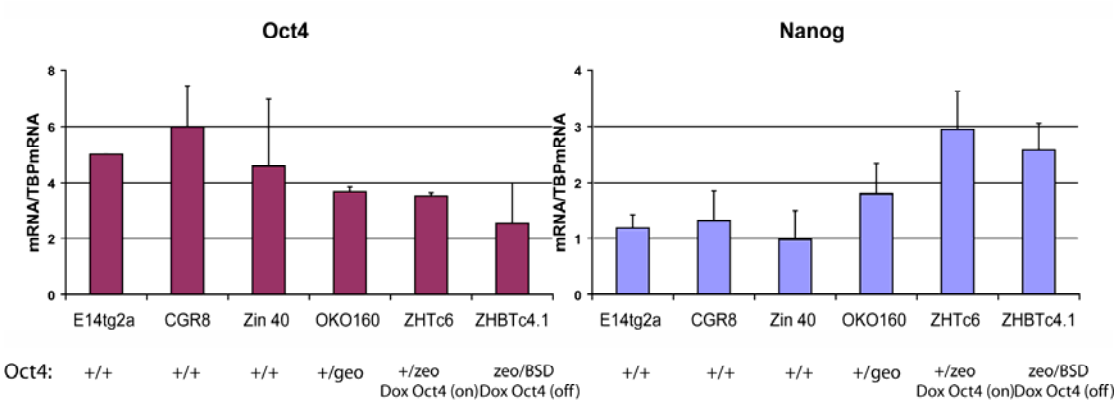

B

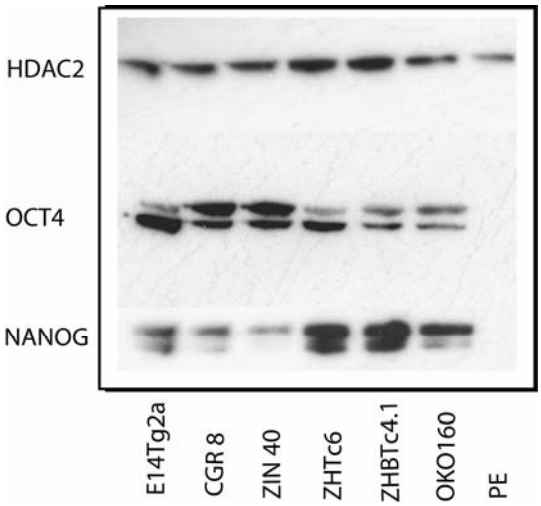

Figure 3.2 Oct4 functional heterozygote cells express elevated level of Nanog mRNA and protein

A: Q-PCR analysis for Nanog and Oct4 in ES cell lines carrying the indicated genetic modifications at the Oct4 locus (see Table 3.1 for details). mRNA expression is normalised to TBP mRNA expression. Average of three biological samples is shown; error bars represent standard deviation of the mean (n=3).
B: Western Blot analysis for Nanog, Oct4 and HDAC in the same cell lines shows an elevated Nanog protein level in functional Oct4 heterozygote cells. This immunoblot was performed by Alessia Gagliardi.

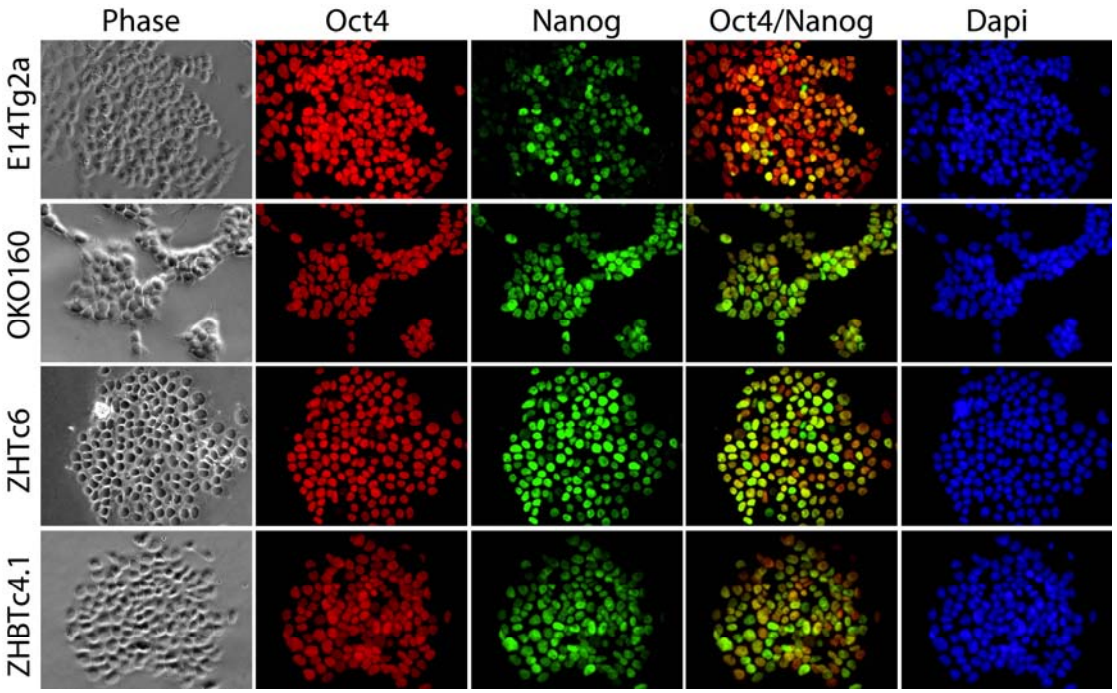

Figure 3.3 Nanog heterogeneity is reduced in functional Oct4 heterozygote ES cells

Immunofluorescence analysis in E14Tg2a ($Oct4^{+/+}$), OKO160 ($Oct4^{+/geo}$), ZHTc6 ($Oct4^{+/zeo}$; Oct4 transgene off) and ZHBTc4.1 cells ($Oct4^{zeo/BSD}$; Oct4 transgene on) for Nanog (Green), Oct4 (Red) and DAPI. Nanog expression pattern is more homogeneous in functional Oct4 heterozygote ES cells (OKO160, ZHTc6 and ZHBTc4.1) in comparison to the wild type Oct4 ES cell line E14Tg2a.

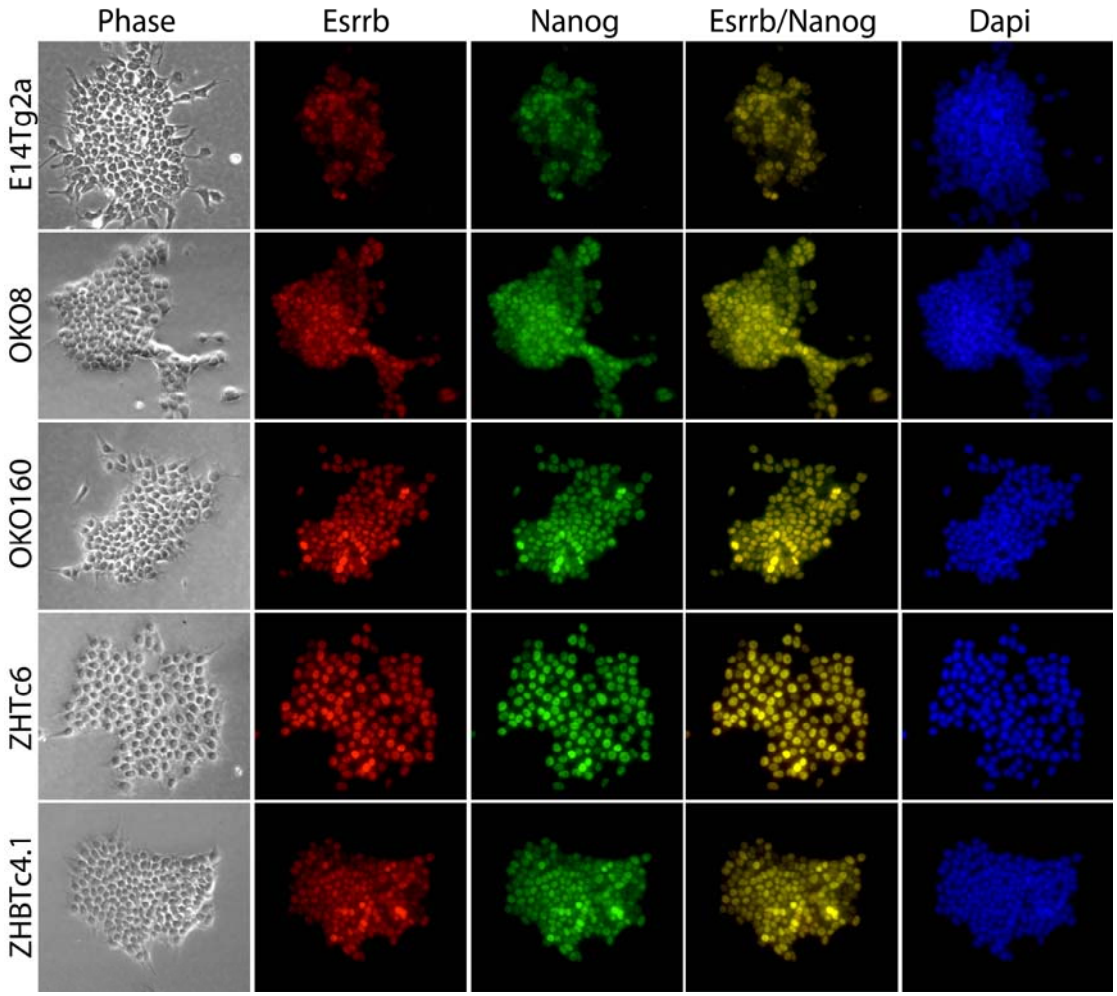

Figure 3.4 Esrrb heterogeneity is reduced in functional Oct4 heterozygote ES cells

Immunofluorescence analysis in E14Tg2a ($Oct4^{+/+}$), OKO8 ($Oct4^{+/geo}$), OKO160 ($Oct4^{+/geo}$), ZHTc6 ($Oct4^{+/zeo}$; Oct4 transgene off) and ZHBTc4.1 cells ($Oct4^{zeo/BSD}$; Oct4 transgene on) for Nanog (Green), Esrrb (Red) and DAPI. Esrrb expression pattern is more homogeneous in functional Oct4 heterozygote ES cells (OKO8, OKO160, ZHTc6 and ZHBTc4.1) in comparison to the Oct4 wild type ES cell line E14Tg2a.

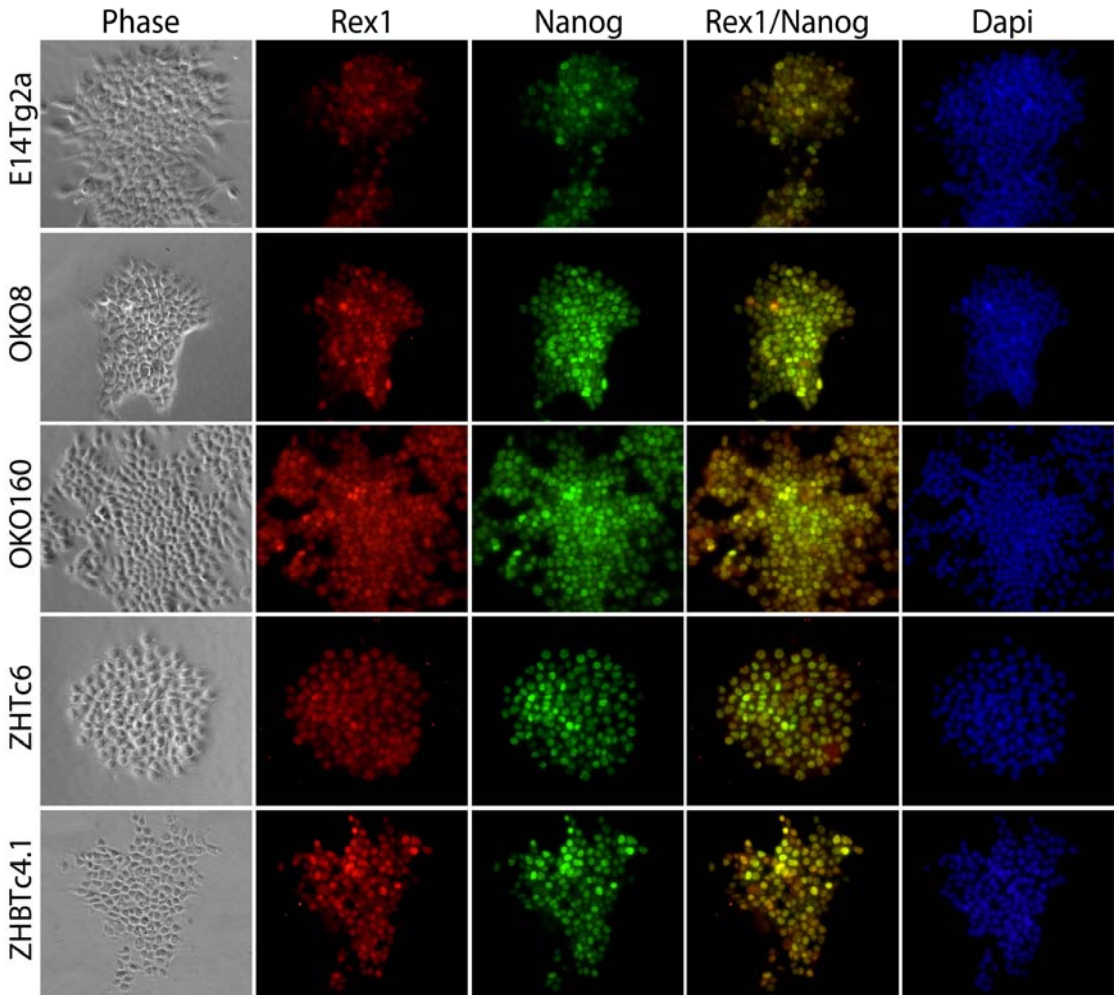

Figure 3.5 Rex1 heterogeneity is reduced in functional Oct4 heterozygote ES cells

Immunofluorescence analysis of E14Tg2a ($Oct4^{+/+}$), OKO8 ($Oct4^{+/geo}$), OKO160 ($Oct4^{+/geo}$), ZHTc6 ($Oct4^{+/zeo}$; Oct4 transgene off) and ZHBTc4.1 cells ($Oct4^{zeo/BSD}$; Oct4 transgene on) for Nanog (Green), Rex1 (Red) and DAPI. Rex1 expression pattern is more homogeneous in functional Oct4 heterozygote ES cells (ZHBTc4.1, ZHTc6 and OKO160) in comparison to the Oct4 wild type ES cell line E14Tg2a.

heterogeneity in Nanog expression further, ZHBTc4.1, ZHTc6 and OKO160 cells were modified by homologous recombination to introduce a GFP reporter at the *Nanog* locus (details of the *Nanog* locus modifications are in Figure 3.6 and an overview of the resulting cell lines is in Table 3.2). Southern analysis was used to evaluate the success of the homologous recombination (Figure 3.6). Correctly targeted clones of each genotype were expanded in Puromycin-containing medium for 6 days. This selects for expression for the targeted *Nanog* locus and produces uniformly GFP^+ populations. Cultures of TNG, ZHTNG, ZHBTNG and OKOTNG were then replated in the absence of Puromycin. All cell lines expressed high GFP levels in a tight relatively homogenous pattern at the beginning of the experiment (Figure 3.7). By day 6, TNG cells had developed a broad range of GFP expression levels. However, all cell lines with reduced Oct4 protein expression retained a tight, relatively homogenous pattern of GFP expression until at least day 16 (Figure 3.7).

3.2.3 Titration of Oct4 restores Nanog heterogeneity

The preceding results suggest that the homogeneous expression of Nanog is due to a reduction in Oct4 levels in functional Oct4 heterozygotes cells. To determine whether elevating the expression of Oct4 in such cells would restore a heterogeneous pattern of Nanog expression, ZHTNG cells were deployed. These cells contain a GFP reporter at the *Nanog* locus, a Doxycycline suppressible Oct4 transgene and a Zeocin gene trap replacement of one of the endogenous Oct4 alleles. These cells are cultured in Doxycycline to keep the Oct4 transgene off. Removal of Doxycycline causes

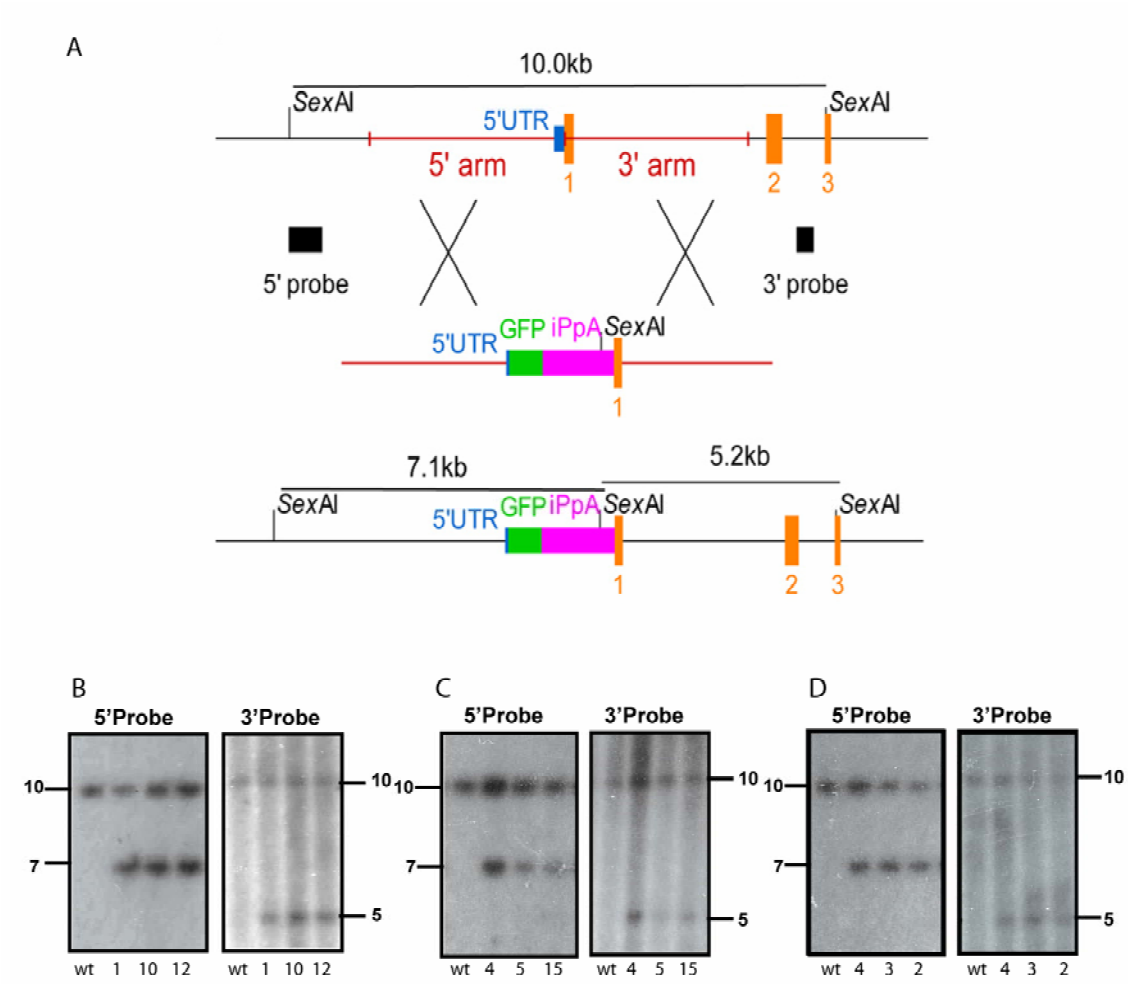

Figure 3.6 Genetic construction of Nanog:GFP reporter derivatives of functional Oct4 heterozygotes

A. The 5' end of the Nanog gene is shown schematically at the top. Exons, orange; 5'UTR, blue; homology arms used for construction of the targeting vector, red. eGFP was inserted between the homology arms precisely at the Nanog AUG codon in the targeting construct shown in the middle. GFP expression is linked through an IRES to puromycin resistance encoded by the *pac* gene and followed by a polyA site (iPpA); taken from Chambers *et al*., (2007).
B. Southern Blot analysis of *Sex* AI digested genomic DNA from targeted clones from ZHBTc4.1 (B), ZHTc6 (C) and OKO160 (D) cells which had undergone homologous recombination. Southern shows one wild type clone with a 10 kb band only and three clones from each cell line which showed the expected pattern for homologous recombinants with a 10 kb wild type band and a 7.1 kb mutant band at the 5' end and a mutant band of 5.2 kb at the 3' end.

CELL LINE	DERIVED FROM	GENETIC MODIFICATIONS
TNG	E14Tg2a	An eGFP IRESpacpA cassette has been inserted at the AUG codon of Nanog into one allele of the Nanog gene by homologous recombination
OKOTNG	OKO160	An IRES-βgeopA cassette has been introduced into *one* allele of the Oct4 gene by homologous recombinations. In addition, an eGFP IRESpacpA cassette has been inserted at the AUG codon of Nanog into one allele of the Nanog gene by homologous recombination.
ZHTNG	ZHTc6	Contains a Dox-suppressible Oct4 transgene in an $Oct4^{+/-}$ background. ES cells maintained with 1000ng/ml Doxycycline. In addition, an eGFP IRESpacpA cassette has been inserted at the AUG codon of Nanog into one allele of the Nanog gene by homologoues recombination.
ZHBTNG	ZHBTc4.1	Contains a Dox-suppressible Oct4 transgene, in an $Oct4^{-/-}$ background. ES cells maintained in the absence of Doxycycline. In addition, an eGFP IRESpacpA cassette has been inserted at the AUG codon of Nanog into one allele of the Nanog gene by homologoues recombination.

Table 3.2 Overview of the Nanog:GFP reporter cell lines

The table summarizes the new name, the origin and the genetic modifications made in the Nanog:GFP reporter cell lines. This table can be additionally found in the Appendix.

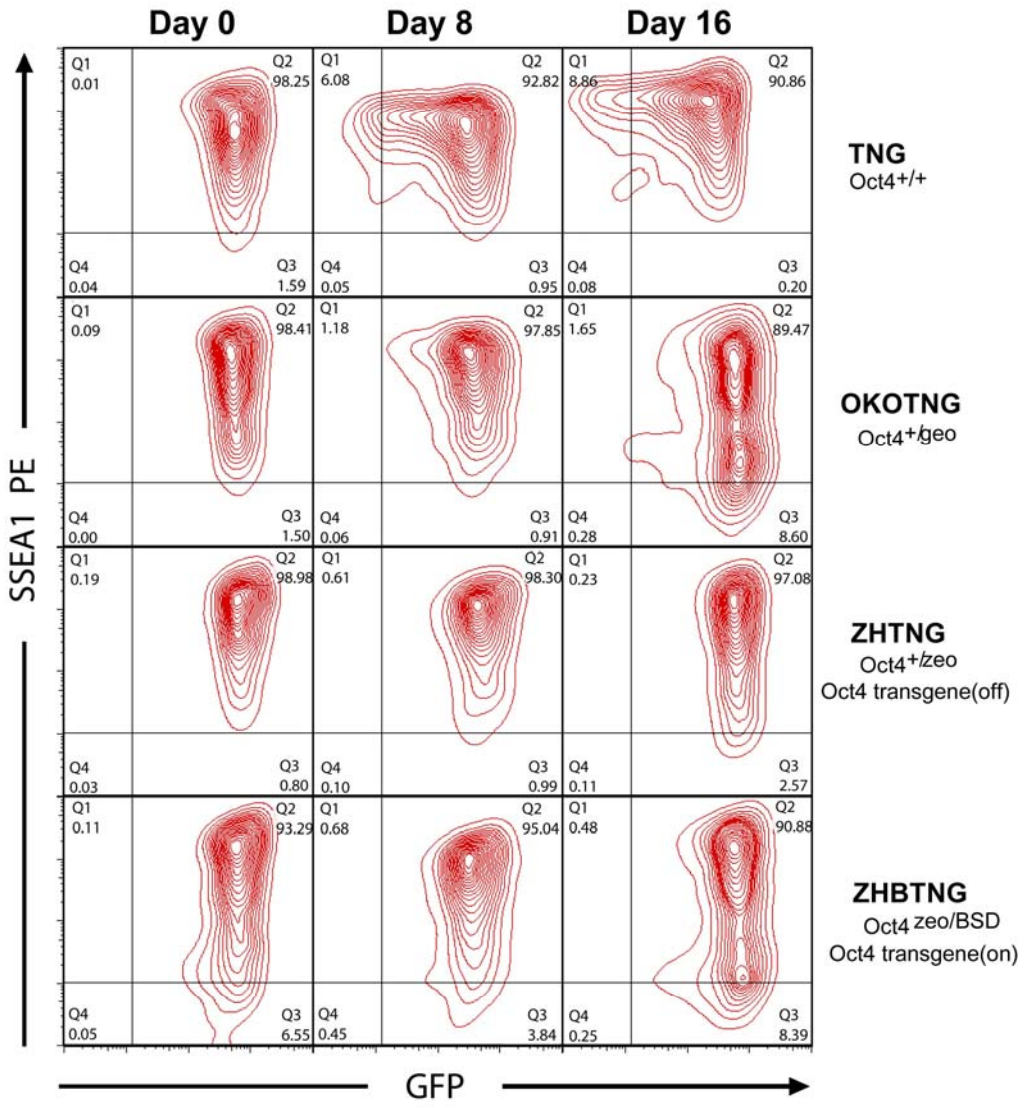

Figure 3.7 FACS analysis in Nanog:GFP reporter cell lines

FACS analysis for GFP and SSEA1 expression in Oct4 wild type ES cells (TNG) and functional Oct4 heterozygote ES cells (ZHBTNG, ZHTNG, OKOTNG). Cells were selected for Nanog using the selection marker Puromycin (Day 0). The expression of GFP (Nanog) in the $SSEA1^{+}$ undifferentiated compartment was monitored by FACS at day 0, 8 and 16 of experiment. The Q1 and Q4 quadrants represent the GFP negative compartment. The Q2 and Q3 quadrants represent the GFP positive compartment. The Q4 and Q3 quadrants represent the SSEA1 negative compartment.
In contrast to TNG cells which express Nanog heterogeneously, functional Oct4 heterozygote ES cells express Nanog more homogenously, even until day 16.

overexpression of Oct4 and induces differentiation of parental ZHTc6 cells. To determine whether heterogeneity of GFP can be restored, ZHTNG cells were treated with dilutions of Doxycycline (1000, 1, 0.3, 0.1, 0.03 and 0 ng/ml). Complete removal of Doxycycline from the parental ZHTc6 cells causes an upregulation of differentiation markers (e.g. GATA4, FGF5) at 96 hours (Niwa *et al.*, 2000). In order to eliminate differentiated cells from the analysis, Zeocin was added to select for expression of the *Oct4* locus. Figure 3.8 shows that at concentrations from 1000 to 0.3 ng/ml, no changes in GFP expression were detectable by FACS. However at 0.1 ng/ml Doxycycline, cells expressing reduced GFP could be observed by day 3. This broader GFP expression pattern developed further by day 6. Importantly, reduction in GFP expression was not accompanied by a change in SSEA1 expression (Figure 3.8). To confirm that Oct4 protein was being induced and to visualise the relationship between Oct4 protein and GFP expression, cells were examined by immunofluorescence for Oct4 at day 6 (Figure 3.9). Consistent with the FACS data, no increase in the Oct4 protein level was observed at concentrations of Doxycycline from 1000 ng/ml to 0.3 ng/ml (Figure 3.9). However, a dramatic increase in the Oct4 protein level was detected upon a further semi-log dilution of Doxycycline. Importantly, this upregulation of Oct4 coincided precisely with a shift in the GFP profile. To determine if the cells in which GFP was downregulated were still undifferentiated, staining with the pluripotency marker Sall4 was performed at day 6 of this experiment (Figure 3.10). Sall4 was detected in GFP high and as well GFP low cells of ZHTNG cells, confirming that these cells were still undifferentiated.

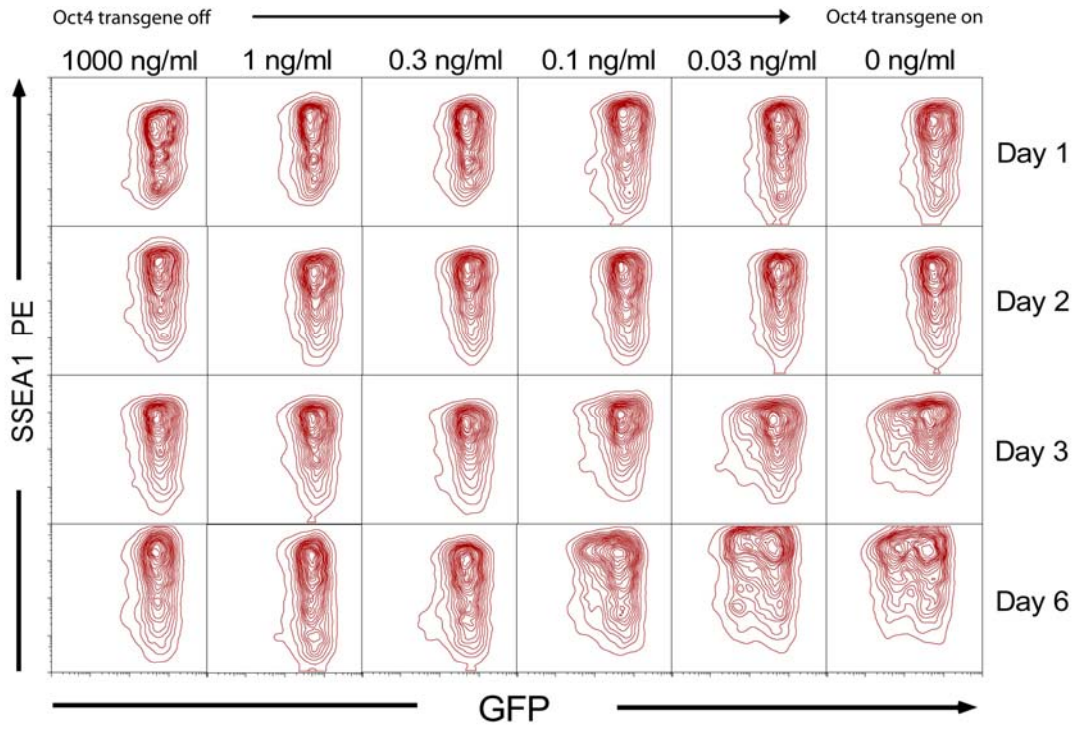

Figure 3.8 Nanog heterogeneity can be restored by titrating back in Oct4 protein

FACS analysis for GFP (X-axis) and SSEA1 (Y-axis) expression in ZHTNG cells ($Oct4^{+/zeo}$; $Nanog^{+/GFP}$; contain a Doxycycline suppressible Oct4 transgene). Cells were cultured in the presence of Zeocin, treated with the indicated dilution of Doxycycline (top) and were analysed at day 1, 2, 3 and 6 of treatment. Heterogeneity in GFP expression appeared at day 3 at concentrations from 0.1 to 0 ng/ml of Doxycyline and continued to increase over the next days. To avoid dense cell culture conditions, cells were passaged every 2-3 days.

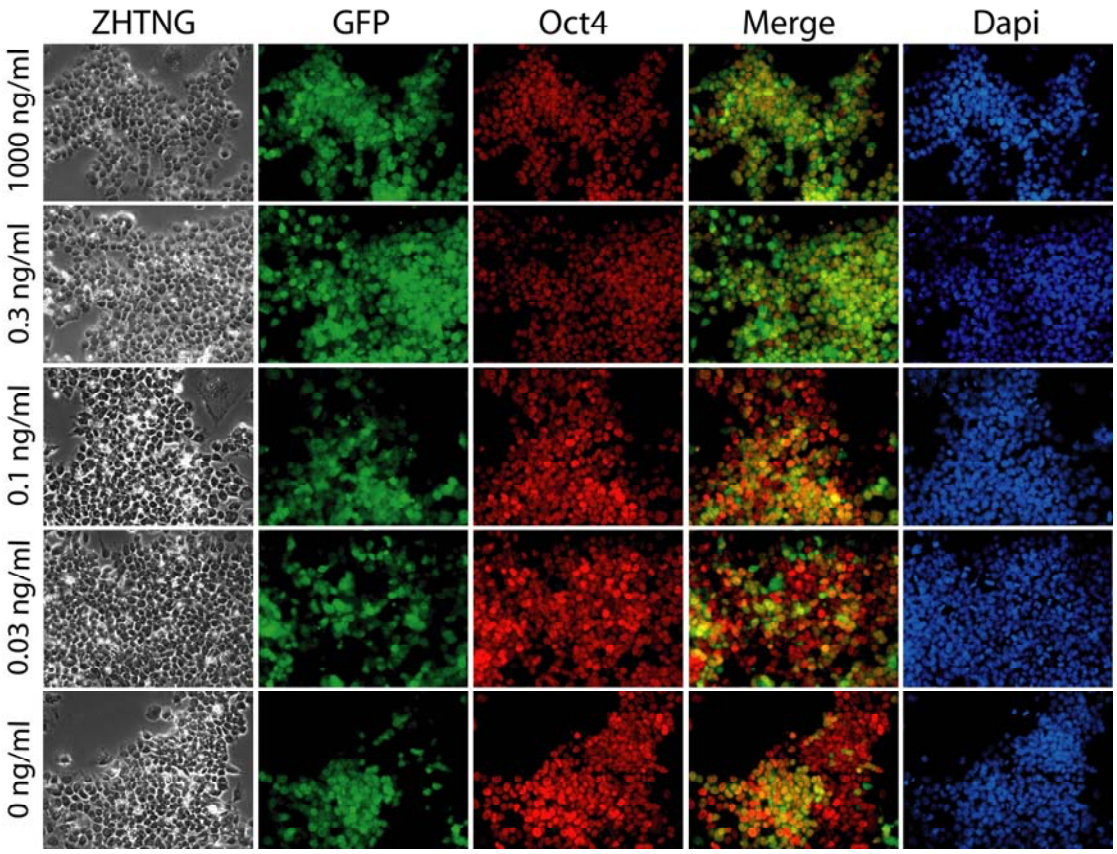

Figure 3.9 Development of Nanog heterogeneity is related to Oct4 increase

Figure shows immunofluorescence analysis for GFP (Nanog), Oct4 (Red) and DAPI in ZHTNG cells ($Oct4^{+/zeo}$; $Nanog^{+/GFP}$; contain a Doxycycline suppressible Oct4 transgene) treated with the indicated dilutions of Doxycycline (left margin) at day 6 of experiment. Staining confirmed an increase of Oct4 protein at concentrations in which GFP heterogeneity appeared (0.1-0ng/ml of Doxycycline).

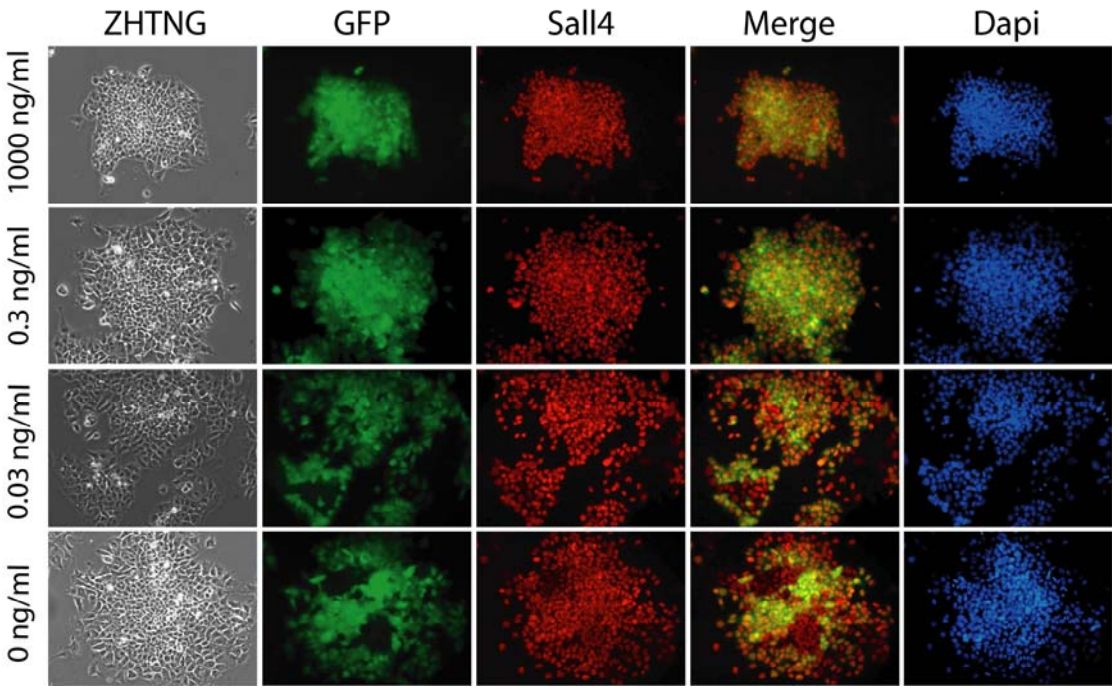

Figure 3.10 GFP low expressing cells still express pluripotency markers

Immunofluorescence analysis for GFP (Nanog), Sall4 (Red) and DAPI in ZHTNG cells ($Oct4^{+/zeo}$; $Nanog^{+/GFP}$; contain a Doxycycline suppressible Oct4 transgene) at day 6 of the Doxycycline titration experiment. The Doxycycline dilutions are indicated on the left. Staining confirmed that GFP low cells still express the pluripotency marker Sall4.

3.2.4 Heterogenous Nanog expression within the undifferentiated compartment is reversible

It was previously reported (Chambers et al., 2007) that Nanog low cells can convert back to a high Nanog expressing state. This raises the question of whether GFP low cells from heterogenous ZHTNG cells after Oct4 induction have a similar capability to reverse Nanog expression. Therefore, TNG and ZHTNG (1000 ng/ml Doxycycline) cells were cultured in parallel in the presence of Puromycin for five days, to select for Nanog expression. Cells were then replated without Puromycin, to enable TNG cells to develop a heterogenous Nanog expression. ZHTNG cells were cultured without Doxycycline (to induce Oct4 transgene expression) and in the presence of Zeocin (to select for continued expression from the Oct4 locus and thus against differentiation). After 6 days, $SSEA1^{+}$ cells were sorted into GFP^{low} and GFP^{high} populations. The purity of both populations in both cell lines was > 99% (Figure 3.11 top). Directly after the sort, cells from both populations were replated into separate wells at a density of 4000 cells per cm^2. TNG cells were cultured without Puromycin. ZHTNG cells were also cultured without Puromycin but in these cells further expression of transgenic Oct4 was suppressed by the addition of 1000 ng/ml of Doxycycline, in order to prevent Oct4 induced differentiation Zeocin was removed from these cultures.

TNG cells behaved as expected (Chambers et al., 2007). The GFP^{low} TNG population produced GFP^{high} cells whose numbers increased in proportion over a 4 day period. The GFP^{high} TNG population on the other hand produced cells with reduced GFP expression by day 1 and these cells increased in proportion over the following three days. The

GFP^{low} ZHTNG cells showed a similar behaviour to the GFP^{low} TNG cells, producing GFP^{high} cells, by day 1 which increased in proportion over the next 3 days. In contrast the GFP^{high} ZHTNG population did not produce GFP^{low} cells.

3.2.5 Nanog kinetics during Oct4 induction

When the Oct4 transgene is induced in ZHTNG cells Nanog expression becomes heterogenous. Therefore it was important to examine more carefully the kinetics of Nanog and Oct4 expression during Oct4 induction in ZHTNG cells. First however, ZHTNG cells were treated with Puromycin for five days to ensure homogenous Nanog expression. Cells were then replated in the presence of Zeocin, either with 1000 ng/ml or without Doxycycline and were investigated by Q-PCR (Figure 3.12). Q-PCR analysis for Oct4 and Nanog over this timecourse showed that the upregulation of Oct4 mRNA happened slowly. Only small differences in Oct4 mRNA were seen over the first 2 days. However, at day 3 Oct4 mRNA increased ~2.5 fold (Figure 3.12). Interestingly, this change was not only abrupt but was also stable as similar levels were maintained for the next 2 days. Nanog mRNA showed initially a positive correlation with Oct4 mRNA. At day 2 the 30% increase in Oct4 mRNA was accompanied by a 50% increase in Nanog expression. However at day 3 when Oct4 was over two fold upregulated, Nanog mRNA decreased to 65% of its expression at 1000 ng/ml of Doxycycline. Whereas the Oct4 mRNA level was stable from day 3-5, Nanog mRNA declined between day 3-4 before stabilizing. Nanog pre-mRNA (Figure 3.12 bottom) was also investigated and was strongly correlated with Nanog mRNA.

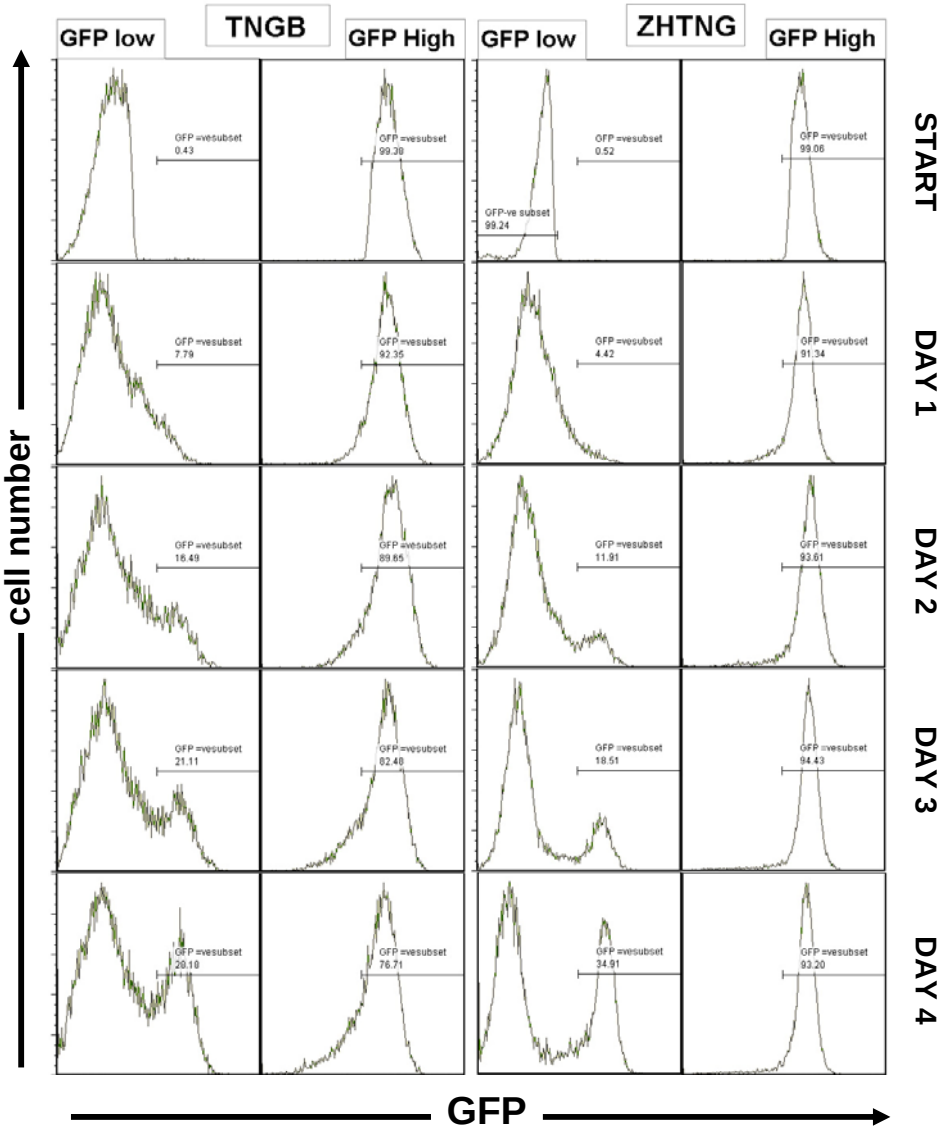

Figure 3.11 Nanog expression is reversible

FACS analysis of sorted ZHTNG (Oct4$^{+/zeo}$; Nanog$^{+/GFP}$; contain a Doxycycline suppressible Oct4 transgene) and TNG (Oct4$^{+/+}$; Nanog$^{+/GFP}$) cells. Both cell lines were sorted for the GFP^{low} and the GFP^{high} populations in the SSEA1^{+} compartment. Cells were replated directly after the sort and analysed at day 1, 2, 3 and 4 of culture for GFP expression in both populations. Analysis showed that GFP expression is reversible in cells in which GFP expression was reduced through the induction of Oct4 similarly to the re-expression of GFP^{high} cells in the GFP^{low} TNG cells.

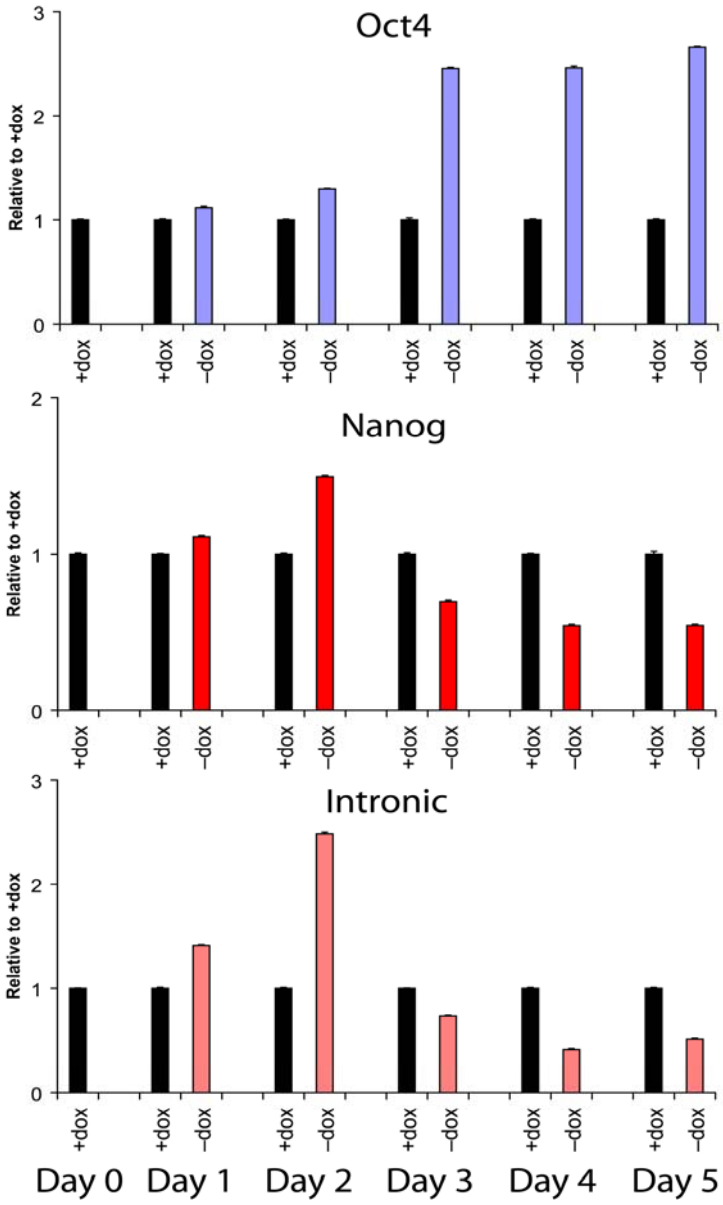

Figure 3.12 Q-PCR analysis in an Oct4 induction experiment

Q-PCR analysis for Oct4, Nanog and Nanog's pre-mRNA (Intronic) in ZHTNG cells ($Oct4^{+/zeo}$; $Nanog^{+/GFP}$; contain a Doxycycline suppressible Oct4 transgene) treated with 1000 ng/ml (+dox) and 0 ng/ml (-dox) of Doxycycline over the time course of five days. mRNA expression, normalised to TBP mRNA expression, is represented relative to (+dox), which is set as 1. Errors bars represent the standard deviation of the mean (n=3).

3.2.6 Kinetics of Nanog expression through Oct4 downregulation

The kinetics of Oct4 induction in ZHTNG cells, showed that the relationship between Nanog and Oct4 is not simple. For that reason it was of importance to investigate this relationship under conditions in which Oct4 was downregulated. For that reason ZHBTc4.1 cells in which two Oct4 alleles were inactivated and which carry a Doxycycline suppressible Oct4 transgene as the only source for Oct4 expression, were examined following Doxycycline treatment. Cells were examined by immunofluorescence and Q-PCR analysis after 0, 6, 12, 18, 24, 48 or 72 hours of Doxycycline treatment. Oct4 mRNA was quickly downregulated (Figure 3.13) and was almost undetectable at 12 hours post Doxycycline treatment. Nanog however showed a more complicated expression pattern. Initially up to 12 hours of Doxycycline induction the mRNA expression correlated with Oct4 downregulation. However at 12 hours, when Oct4 mRNA was undetectable, Nanog mRNA was expressed at 50% of its initial level. Interestingly, after this initial decrease, Nanog was upregulated to a level similar to that at the start of the experiment. This re-expression was followed by a linear downregulation which was completed by 72 hours (Figure 3.13 top). A similar expression pattern was observed by immunofluorescence for Nanog, which showed a decrease in Nanog protein until 12 hours (Figure 3.14). Subsequently, Nanog was upregulated at 24 hours before being completely downregulated by 72 hours (Figure 3.14). This expression pattern of Nanog raised the question of whether Nanog, was the only gene with this complex expression pattern. To investigate this, Q-PCR analysis was performed for other pluripotency genes (Figure 3.13 middle and bottom). Interestingly, although some genes such as Rex1 were linearly downregulated, other genes showed a

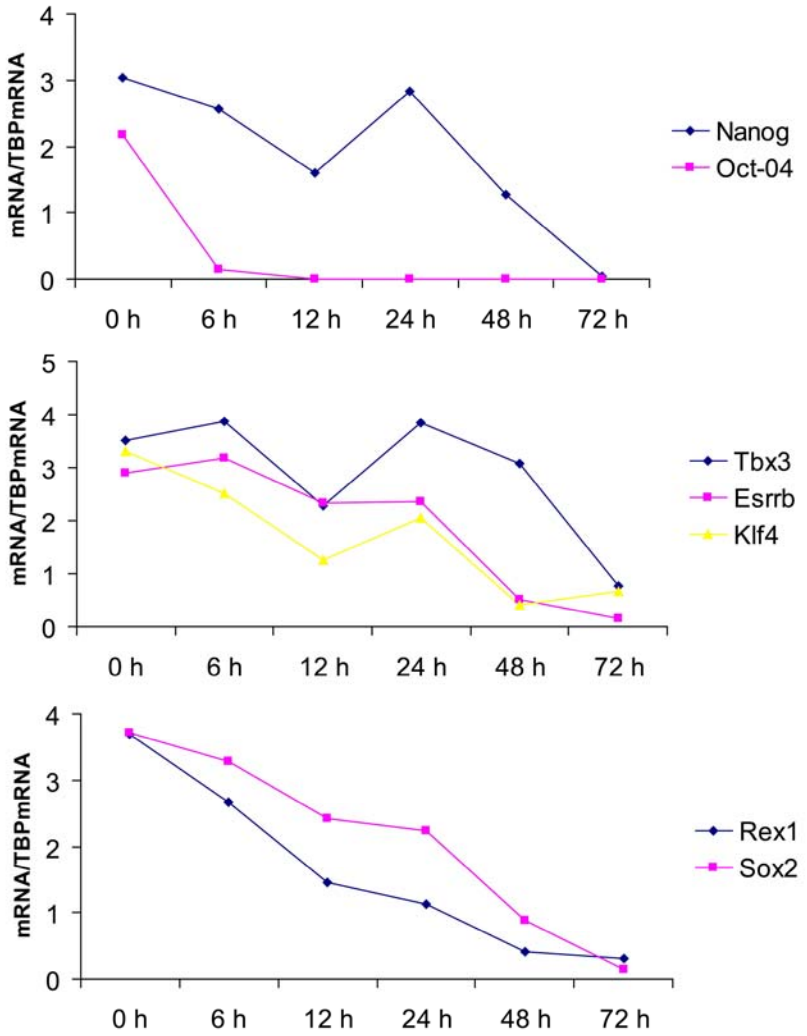

Figure 3.13 Kinetics of Nanog and Oct4 mRNA after Oct4 downregulation in ZHBTc4.1 cells

Q-PCR analysis for Nanog and Oct4 mRNA in ZHBTc4.1 cells ($Oct4^{zeo/BSD}$; contain a Doxycyclin suppressible Oct4 transgene) treated with 1000 ng/ml of Doxycycline over the indicated timecourse represented in hours (h), showed, that Nanog's downregulation is disrupted through a second increase at 24 hours after treatment. This secondary relief of suppression evolved after Oct4 was completely downregulated (top). The same expression pattern was observed for Klf4 and slightly for Esrrb. TBX3 showed the strongest upregulation of all genes at 24 hours (middle). Rex1 and Sox2 showed a progressive decrease overtime. mRNA expression was normalised to TBP mRNA expression.

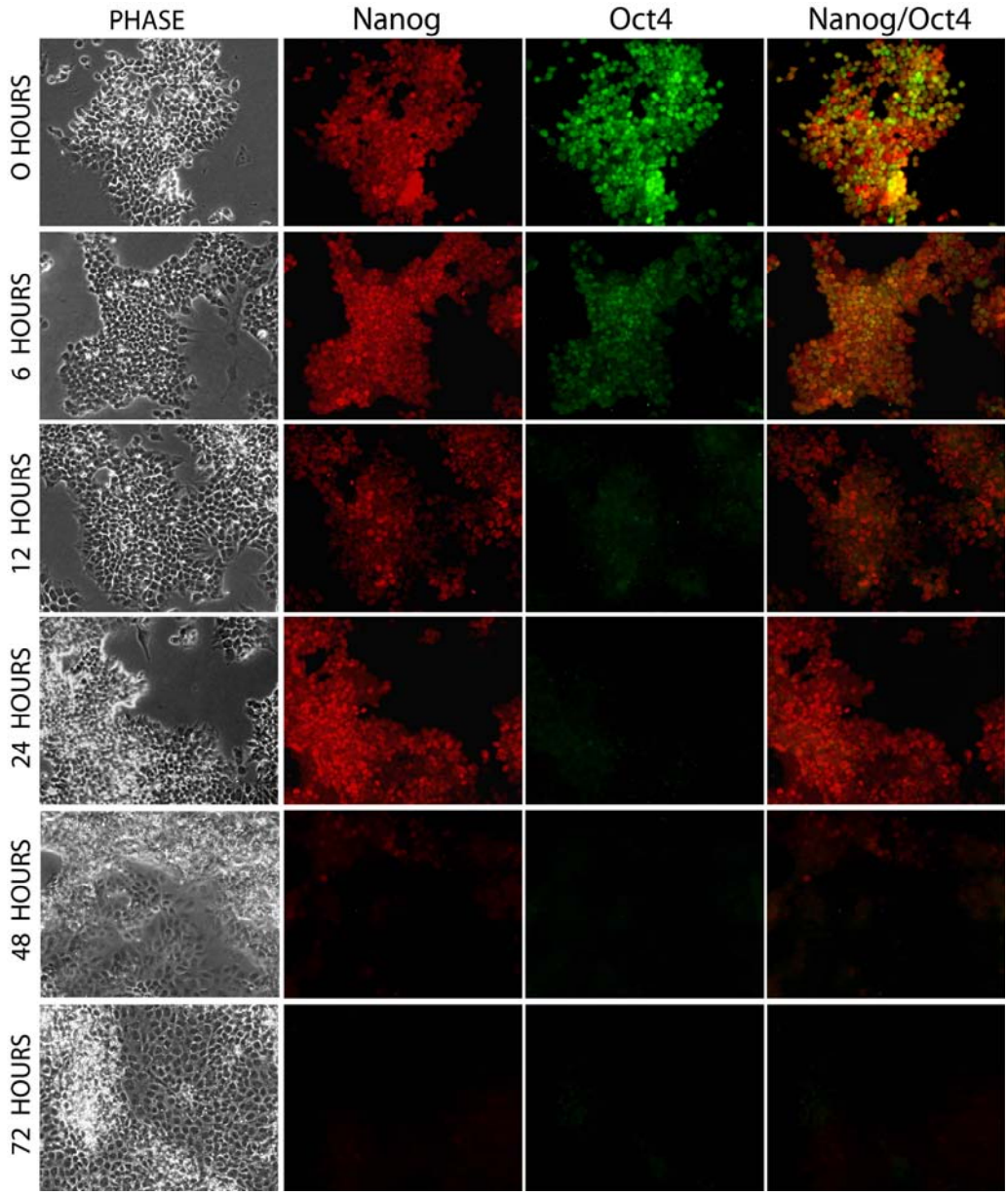

Figure 3.14 Immunofluorescence analysis in ZHBTc4.1 cells after Oct4 downregulation

Panel shows immunofluorescence analysis for Nanog and Oct4 in ZHBTc4.1 cells ($Oct4^{zeo/BSD}$; contain a Doxycycline suppressible Oct4 transgene) treated with 1000 ng/ml of Doxycycline over the indicated timecourse (left margin).

re-induction pattern between 12-24 hours similar to Nanog. Klf4 and Tbx3 behaved in this way, while Sox2 and Esrrb levels appeared to plateau between those time points. (Figure 3.13 middle and bottom).

3.3 Discussion

The data presented in this chapter demonstrates that functional Oct4 heterozygote ES cells express Nanog less heterogeneously than Oct4 wild type cells. Furthermore Nanog mosaicism can be restored by directly raising Oct4 levels in Oct4 functional heterozygote ES cells. Sorting of ZHTNG cells into GFP^{high} and GFP^{low} cells, shows that high GFP expression can be restored to the GFP^{low} population by adding Doxycycline back to the culture. Interestingly, neither downregulation nor upregulation of Oct4 is accompanied by a linear down or upregulation of Nanog, but shows a more complex regulation pattern.

3.3.1 Nanog expression in functional Oct4 heterozygote ES cells

Oct4 heterozygote ES cells express elevated level of Nanog mRNA and protein (Figure 3.2) and importantly express Nanog more homogenously (Figure 3.3 and 3.7). This was unexpected and suggested that Oct4 might directly or indirectly suppress *Nanog* when expressed at wild type levels. Interestingly, the general increase of Nanog mRNA and protein was not associated with an overall increase in expression in all cells in the population but rather reflected a reduction in the number of cells in the Nanog low population. This was not only the case for Nanog but also for Esrrb and Rex1 (Figure

3.4 and 3.5), suggesting that Esrrb and Rex1 may be subject to similar upregulation as Nanog. In addition, an overall decrease in Oct4 expression may through feedback mechanisms act to restore Oct4 expression towards wild type levels. Therefore, genes that act to sustain pluripotency through activation of Oct4 would be increased in such cells. This would implicate Nanog, Esrrb and Rex1 as potential positive regulators of Oct4 (Chen et al., 2008; Kim et al., 2008). These findings are, in my opinion, significant and important for the stem cell field as they indicate a potential origin of transcription factor heterogeneity within the intrinsic circuitry of the pluripotency gene regulatory network and de-mystify the original observation of Niwa that an increase in Oct4 can cause differentiation. Rather then being a direct consequence of Oct4 action at elevated concentrations, these results show that Oct4 acts by providing a population of Nanog low cells responsive to differentiation cues.

3.3.2 Titration of Oct4 restores Nanog heterogeneity

The preceding results suggest that homogeneous Nanog expression is due to a reduction in Oct4 concentration in functional Oct4 heterozygote cells. To determine whether increasing the expression of Oct4 in such cells would restore Nanog heterogeneity, ZHTNG cells were deployed. In this case, Nanog-low cells could be obtained by decreasing the Doxycycline dosage and therefore increasing the Oct4 concentration. This proved that changes in Nanog expression were caused by the decrease of Oct4 expression from wild type levels. Importantly, the reduction of Nanog:GFP expression (Figure 3.8) did not represent as a simple shift of the whole population towards the GFP

low compartment but reflected an increase of the Nanog middle and low compartments, therefore resembling Nanog expression in wild type ES cells. These results indicate that the relationship between Oct4 and Nanog that I have proposed is robust and eliminate the possibility that effects on Nanog expression are due to unrelated genetic alterations in these cells.

Immunofluorescence analysis showed that the shift in GFP expression coincided precisely with a total increase of Oct4 protein in functional Oct4 heterozygote ES cells (Figure 3.9), confirming that Nanog reduction is associated with an increase of Oct4 protein. The changes in GFP expression appeared in the SSEA1 positive compartment. To confirm their undifferentiated status, cells were examined by immunofluorescence for Sall4. Sall4 is a pluripotency marker that is expressed homogeneously in ES cells and whose downregulation is associated with differentiation (Lim et al., 2008; Zhang et al., 2006). Sall4 is detectable throughout the GFP negative colonies. It would be of interest to examine expression of additional pluripotency markers in future experiments.

When ZHTNG cells were sorted into GFP high and GFP low populations (Figure 3.11), the GFP low population was able to switch back to a Nanog:GFP high expressing state. This indicates that these cells remain undifferentiated (Chambers et al., 2007) and that these changes indeed can be attributed to the levels of Oct4 expression, as the switch was possible when Oct4 expression from the transgene was suppressed. It will be important in future to eliminate the possibility that these results are attributed to contamination of the GFP low population with GFP high cells by replating GFP low

cells as single cells in individual wells and following GFP reacquisition. It will also be of interest to determine whether cells can switch back to GFP high state without suppression of the Oct4 transgene to discover alternative regulatory mechanisms unrelated to Oct4 levels.

3.3.3 Kinetics of Nanog expression through Oct4 upregulation

The kinetics of Nanog expression during Oct4 induction in ZHTNG were examined to more fully explore the relationship between these two genes. Initially, Nanog mRNA showed a positive correlation with Oct4 mRNA. An increase of Oct4 at day 2 was accompanied by an increase in Nanog expression. However at day 3, when Oct4 was over two fold upregulated, Nanog mRNA decreased to 65% of its expression at 1000 ng/ml of Doxycyline and continued to decrease over the next 2 days. These results revealed a more complex relationship between Oct4 and Nanog. In future experiments it would be of importance to examine why Oct4 levels switch to a new steady state rather then increasing linearly. The design of primers distinguishing between expression from the endogenous *Oct4* allele and from the transgene should help to address this question. Furthermore it would be helpful to visualize the expression of Oct4 and Nanog directly with fluorescence reporters. In this way the exact kinetics could be ascertained at the single cell level. Such an approach would be important for establishing the hierarchical relationship between these genes and the exact levels at which a switch was thrown. In this way the interaction between these two genes could be more precisely observed dynamically, particularly by time-lapse video microscopy.

Such an approach could profitably be extended to other pluripotency regulators including for example Sox2, Esrrb, Klf4 and Tbx3. However this would stretch the current capabilities of fluorescence reporter systems (Schroeder, 2008; Tsien) although variant reporters with specific subcellular localisation could be beneficial here (Okita et al., 2004). It would also be of interest to investigate the expression of Sox2, Essrb, Klf2 and Tbx3 more precisely during the induction of Oct4 in ZHTNG cells. This would help to define whether Nanog heterogeneity could be induced through manipulation of these genes in the Oct4 functional heterozygote ES cells. Such experiments could help to unravel feedback controls operating on the gene regulatory network in ES cells.

3.3.4 Kinetics of Nanog expression through Oct4 downregulation

The kinetics of Oct4 induction in ZHTNG cells suggest a complex relationship between Nanog and Oct4. For further understanding ZHBTc4.1 cells were examined following Doxycycline mediated extinction of Oct4. This treatment causes trophectodermal differentiation (Niwa et al., 2000). Although Oct4 mRNA levels declined linearly upon Doxycycline treatment and were almost undetectable by 12 hours (Figure 3.13), changes in Nanog expression were more complicated. Initially, Nanog mRNA expression correlated with Oct4 downregulation, being reduced by 50% at 12 hours. Subsequently, Nanog was upregulated at 24 hours to a level similar to that at t=0, before being progressively and completely downregulated by 72 hours (Figure 3.13 top). A similar expression pattern was observed for Nanog protein by immunofluorescence. This non-linear pattern suggests the elimination of an Oct4 dependent inhibitor of Nanog. In this regard potential Nanog supressors (e.g. Tcf3) may warrant investigation. In addition,

decreased expression of Oct4 in ZHBTc4.1 cells has been associated with a decrease in Prc2 activity (Endoh et al., 2008). A further candidate would be Nanog. It would, therefore be interesting to determine whether Nanog overexpression could restore heterogeneity in Oct4 functional heterozygote ES cells, similar to the action of Oct4 (Figure 4.8). A possible approach to distinguish, whether Oct4 indirectly suppresses *Nanog* through Nanog upregulation would be to upregulate Oct4 expression in 44Cre6 (*Nanog* null cells carrying the TNG reporter at one *Nanog* allele). If an increase in *Nanog* heterogeneity was observed in these cells, this would indicate that the repressive activity of Oct4 acted in a Nanog-independent manner.

Chapter 4

Functional consequences of manipulating the levels of Oct4

4.1 Introduction

When TNG cells expressing the undifferentiated cell surface marker SSEA1 were sorted into GFP^{low} and GFP^{high} populations and replated, the GFP^{low} population lost SSEA1 expression faster then the GFP^{high} population (Chambers et al., 2007). Together with the reversibility of Nanog expression this suggested a model in which Nanog low cells had an increased propensity for differentiation (Figure 4.1). As functional Oct4 heterozygote cells lack a $Nanog^{low}$ population, such ES cells may be retarded in their differentiation kinetics compared to wild type ES cells. To investigate this hypothesis, differentiation assays were performed. Cultures were first selected for undifferentiated cells by adding Zeocin to ZHBTc4.1/ZHTc6 cells, G418 to OKO160/OKO8 and Puromycin to Oct4GIP cells to select for undifferentiated cells. After 7 days, selection was removed and cells were replated in two distinct differentiation conditions.

4.2 Functional Oct4 heterozygote ES cells are retarded in their differentiation capacity

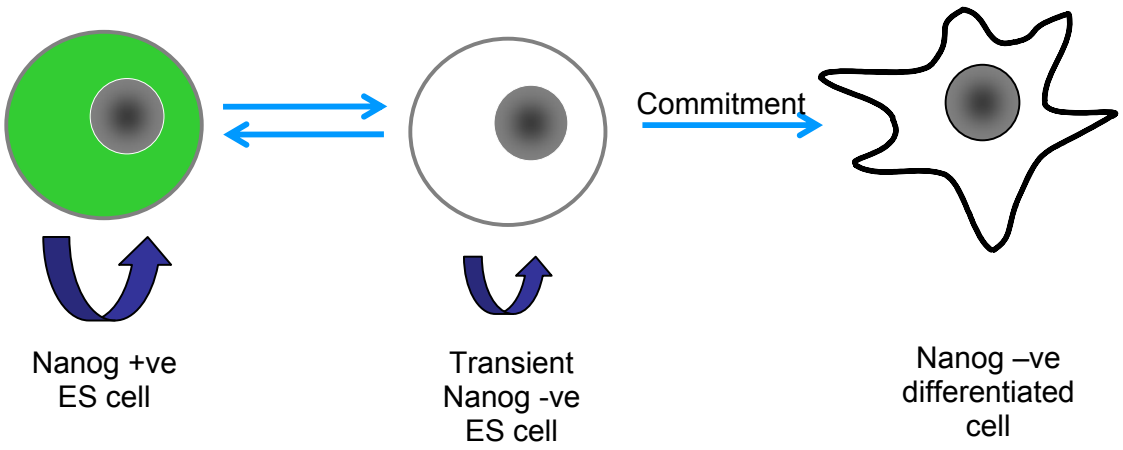

Figure 4.1 Model of the relationship between levels of Nanog and self-renewal and differentiation capacity of ES cells

Model (Chambers et al., 2007) underlines the importance of Nanog mosaic expression for self-renewal and differentiation of ES cells, suggesting that Nanog acts to safeguard self-renewal by countering the effects of differentiation inducers and preventing progression to commitment. In this context Nanog low cells give an opportunity for an ES cell to differentiate.

4.2.1 LIF withdrawal

Upon LIF withdrawal, wild type ES cells began to show morphological signs of differentiation by day 2, which became more clearly apparent by day 3. In contrast, all functional Oct4 heterozygote ES cells retained an undifferentiated morphology in the majority of cells at day 3 (Figure 4.2). Q-PCR analysis showed a delay in the loss of pluripotency markers Rex1 and FGF4 as well as a delay in the upregulation of the mesodermal gene Brachyury in functional Oct4 heterozygote ES cell lines (Figure 4.3).

4.2.2 Neural differentiation

The same cell lines were assessed during neural differentiation. Cells were examined by microscopy each day for 8 days. Subsequently, cells were fixed and stained for the expression of Nestin, βIII Tubulin and Oct4. Immunofluorescence analysis showed that βIII Tubulin and Nestin were readily detectable in E14Tg2a and Oct4GIP cells, whereas only isolated cells with poorly developed axonal processes were detected in OKO8, OKO160, ZHTc6 and ZHBTc4.1 cultures (Figure 4.4 and 4.5). To determine if cells were unable to make the transition to the neural lineage because they remained undifferentiated, rather then differentiating into non-neural cells, immunofluorescence analysis for Oct4 was performed. Oct4 was readily detectable in all functional heterozygote ES cells at day 8 but was expressed only in isolated colonies in E14Tg2a and Oct4GIP cultures (Figure 4.4). Q-PCR analysis confirmed the Oct4 immunofluorescence data. This also showed that all Oct4 functional heterozygote ES were impaired in downregulation of Rex1 (Figure 4.5 A) and in expression of the neural markers Nestin βIII Tubulin and Pax6 (Figure 4.5 B).

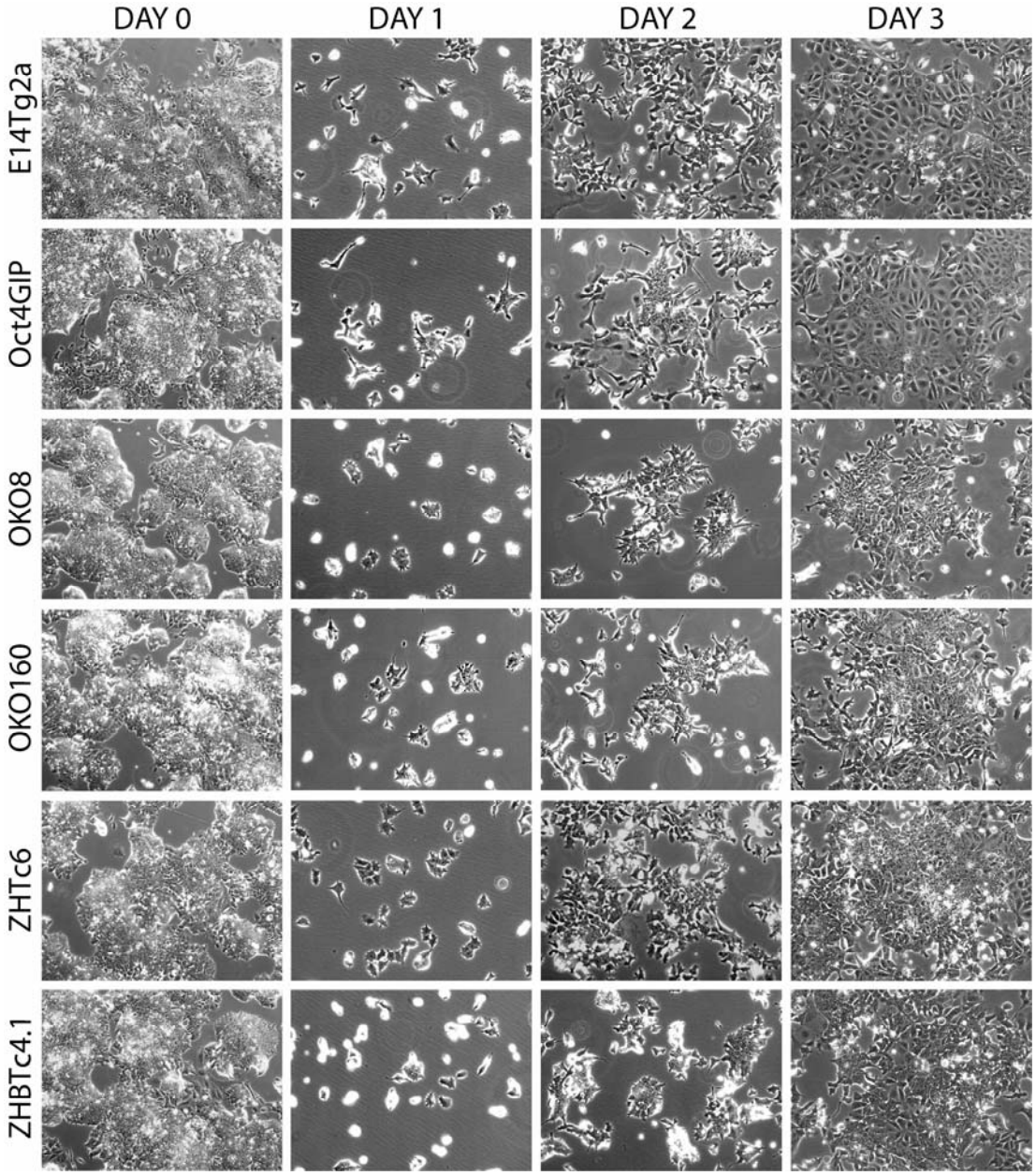

Figure 4.2 Morphological changes in the LIF withdrawal differentiation assay

The panel shows morphological changes in Oct4 wild type (E14Tg2a ($Oct4^{+/+}$), Oct4GIP ($Oct4^{+/+}$)) and functional Oct4 heterozygote cells (OKO8 ($Oct4^{+/geo}$), OKO160 ($Oct4^{+/geo}$), ZHTc6 ($Oct4^{+/zeo}$; Oct4 transgene off), ZHBTc4.1 ($Oct4^{zeo/BSD}$; Oct4 transgene on) in an LIF withdrawal differentiation assay over the timecourse of three days.

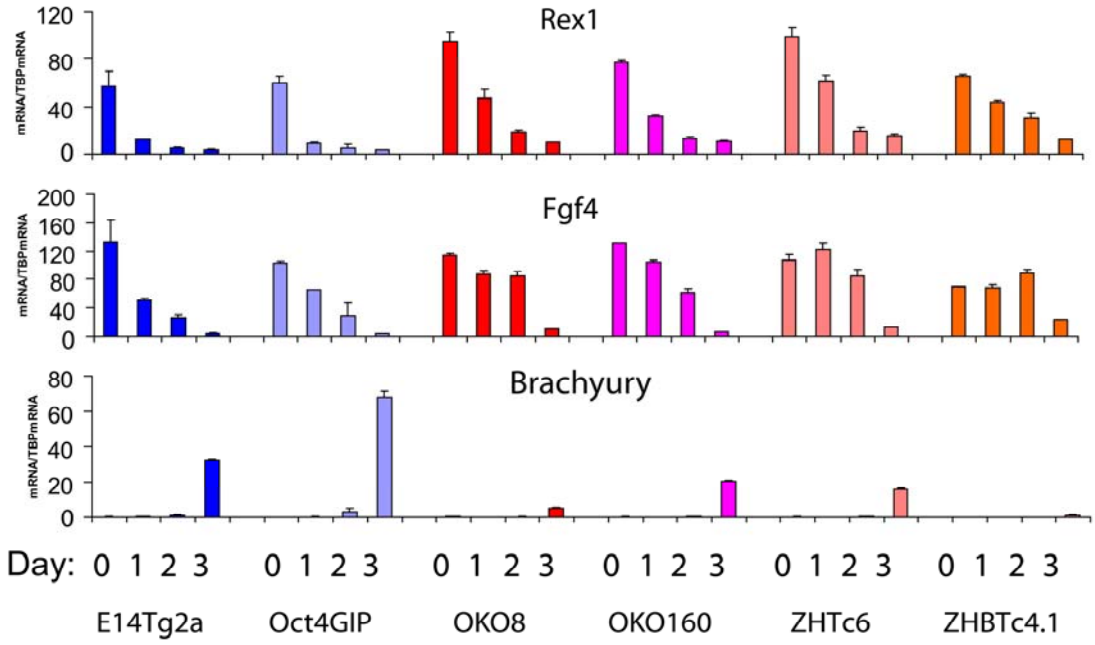

Figure 4.3 Q-PCR analysis during the LIF withdrawal differentiation assay

Q-PCR analysis shows that all functional Oct4 heterozygote ES cell lines (OKO8 ((Oct4$^{+/geo}$), OKO160 (Oct4$^{+/geo}$), ZHTc6 (Oct4$^{+/zeo}$; Oct4 transgene off), ZHBTc4.1 (Oct4$^{zeo/BSD}$; Oct4 transgene on) express pluripotency markers like Rex1 and FGF4 longer than Oct4 wild type cells (E14Tg2a (Oct4$^{+/+}$), Oct4GIP (Oct4$^{+/+}$)) during the differentiation protocol. Furthermore, the figure shows a significant decrease in the expression of Brachyury which is highly expressed at day 3 in the two Oct4 wild type cell lines. mRNA expression was normalised to TBP mRNA expression. Errors bars represent the standard deviation of the mean (n=3).

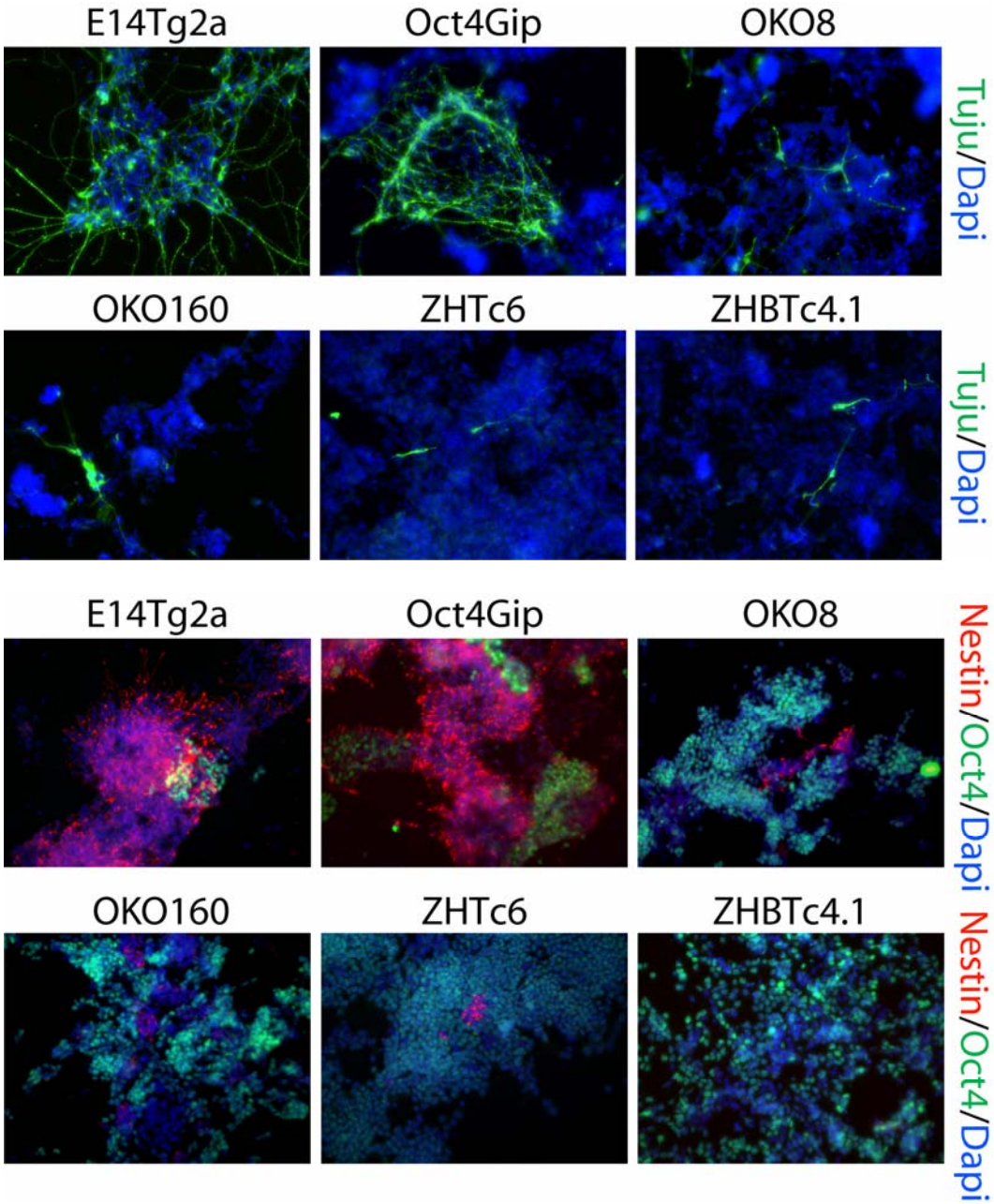

Figure 4.4 Immunofluorescence analysis for neural marker

Immunofluorescence analysis for βIIITubulin (Tuji) and Dapi (top panels) as well as Nestin, Oct4 and Dapi (bottom panels) at day 8 of a neural differentiation protocol in Oct4 wild type cells (E14Tg2a ($Oct4^{+/+}$), Oct4GIP ($Oct4^{+/+}$)), and functional Oct4 heterozygote ES cell lines (OKO8 ($Oct4^{+/geo}$), OKO160 ($Oct4^{+/geo}$), ZHTc6 ($Oct4^{+/zeo}$; Oct4 transgene off), ZHBTc4.1 ($Oct4^{zeo/BSD}$; Oct4 transgene on)).

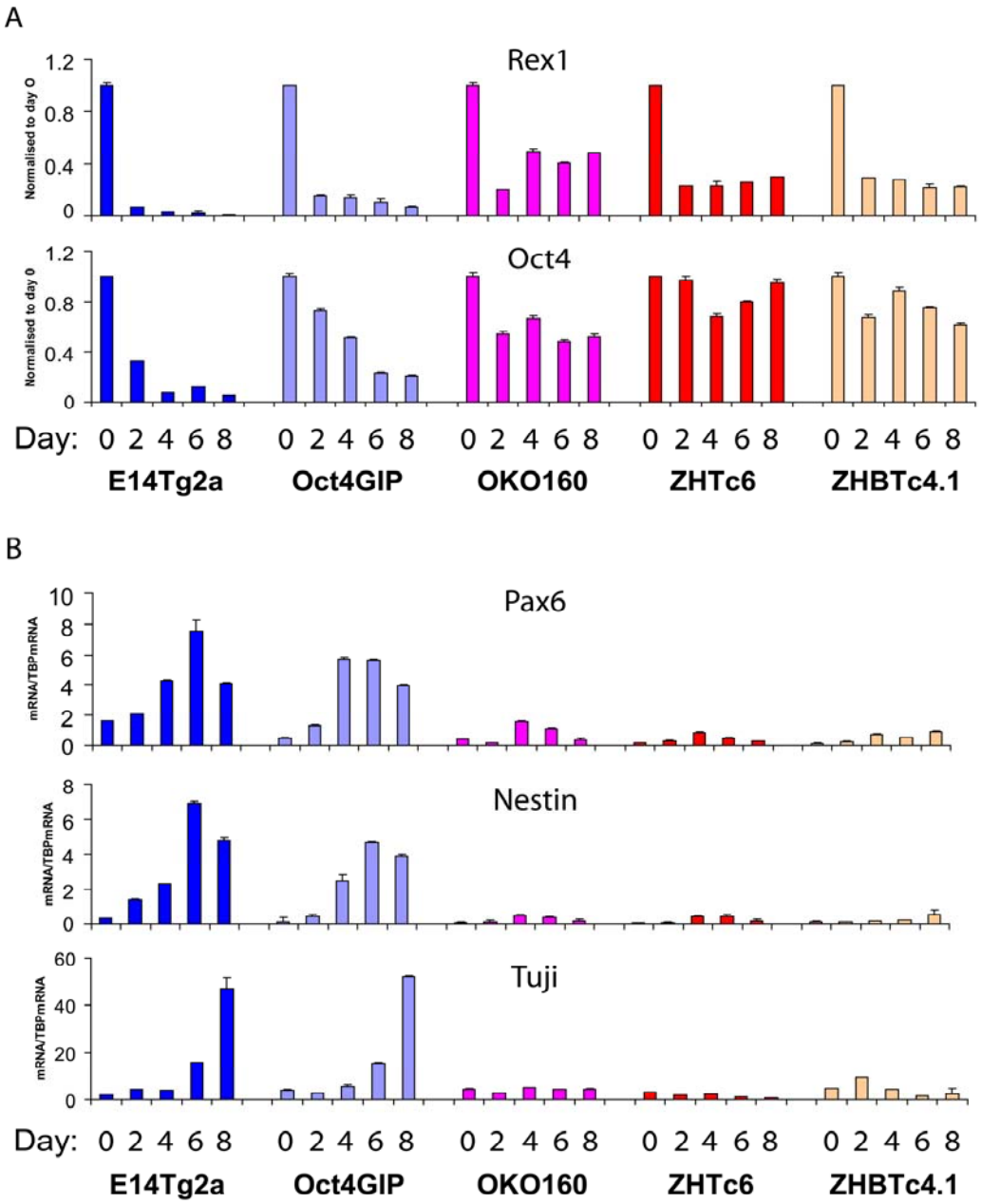

Figure 4.5 Q-PCR analysis during the neural differentiation assay

Q-PCR analysis for pluripotency markers: Rex1 and Oct4 (A) and neural markers: Nestin, βIII Tubulin (Tuji) and Pax6 (B) over the indicated time course (0-8 days). mRNA expression was normalised to TBP mRNA expression. Errors bars represent standard deviation of the mean (n=3).

4.3 Retarded differentiation capacity can be rescued by restoring Nanog heterogeneity via induction of Oct4

4.3.1 LIF withdrawal

According to the hypothetical model (Figure 4.1) the block in differentiation was predicted as a consequence of the loss of Nanog heterogeneity in functional Oct4 heterozygote cells. To investigate whether the retarded kinetics in Oct4 functional heterozygotes ES cells could be restored by re-establishing the heterogeneity in Nanog expression in these cells, Oct4 protein was titrated back into the cells. ZHTNG cells were therefore treated with Puromycin for 7 days to obtain a culture of cells with homogenous Nanog expression. After 7 days, cells were passaged in two conditions (Figure 4.6 outlines the experimental set up). In the first condition, cells were kept in the presence of Zeocin and 1000 ng/ml of Doxycycline. In the second condition, cells were kept in Zeocin but were treated with 0.03ng/ml of Doxycycline to relieve the suppression of the Oct4 transgene in ZHTNG cells. At day 4, cells treated with 1000 ng/ml of Doxycycline expressed GFP homogenously whereas cells treated with 0.03 ng/ml were heterogenous for Nanog in the $SSEA1^{+}$ compartment (Figure 4.7 top left). To demonstrate that this heterogeneity in GFP expression was related to the increase in Oct4 expression, cells were investigated for Nanog and Oct4 mRNA expression at the start of the differentiation experiments (Figure 4.7 top right). Indeed cultures in which Oct4 was upregulated showed a strong decrease in Nanog expression (Figure 4.7 top right). Cells were washed twice with PBS and medium was replaced with standard medium without LIF. At start of the differentiation assay, cells which were previously treated with 1000 ng/ml were supplemented further with 1000 ng/ml of Doxycycline

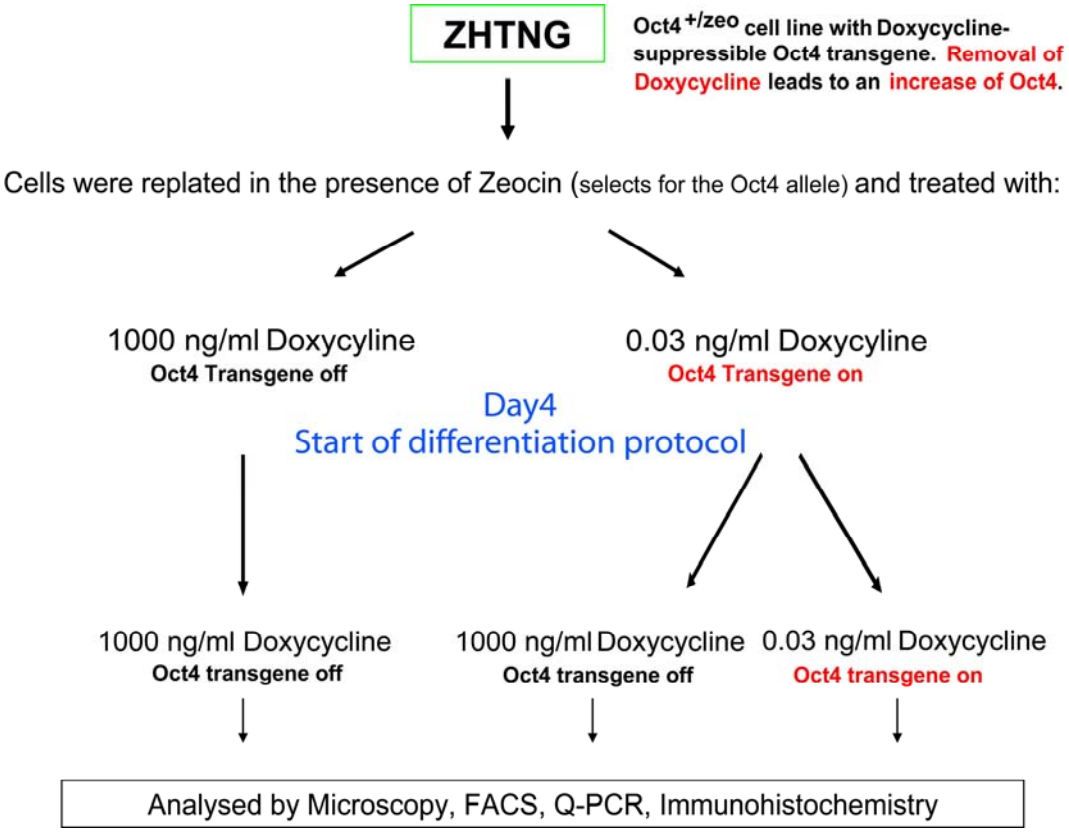

Figure 4.6 Schematic representation of experimental set up

Graph depicts a schematic representation of the experimental set up described in this section. Shown is the treatment of ZHTNG cells ($Oct4^{+/zeo}$; $Nanog^{+/GFP}$; contain a Doxycycline suppressible Oct4 transgene) before and after the differentiation assays were started (blue). The LIF withdrawal differentiation assay was conducted over 3 days and the neural differentiation protocol over 8 days. The activation of the Oct4 transgene due to a dilution of Doxycycline is indicated in red. At the end of the differentiation protocol cells were investigated by some of the indicated possibilities.

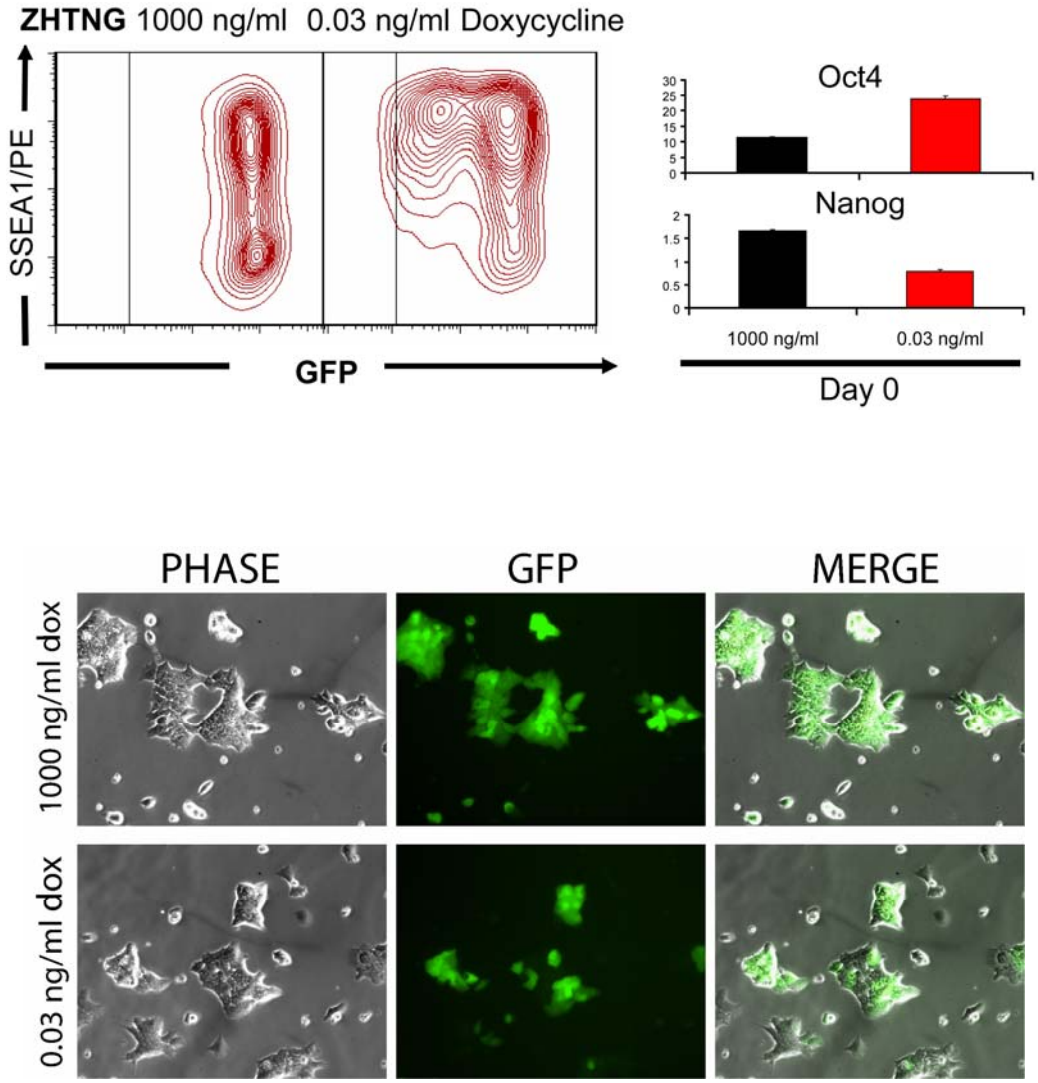

Figure 4.7 Investigations of ZHTNG before start of differentiation assays

Top left panel shows FACS analysis for GFP and SSEA1 in ZHTNG cells ($Oct4^{+/zeo}$; $Nanog^{+/GFP}$; contain a Doxycycline suppressible Oct4 transgene) treated either with 1000 ng/ml or 0.03 ng/ml of Doxycycline directly before the LIF withdrawal and neural differentiation assays were performed. Top right panel shows the corresponding Q-PCR results for Nanog and Oct4 to cultures represented by FACS.
Bottom panel shows the microscopy analysis of the particular ZHTNG cultures analysed at the top. As visible by morphology, cells heterogenous for GFP were morphologically undifferentiated before differentiation was induced.

for the whole time course of experiment. This monitored effects of continued suppression of the Oct4 transgene. Cells which had been treated with 0.03 ng/ml of Doxycycline and which showed a heterogenous GFP expression pattern (Figure 4.7) were divided into two experimental conditions. In the first, treatment with 0.03 ng/ml of Doxycycline was continued. This allowed monitoring of the effects of continued high level expression of Oct4. In the second condition, the full Doxycycline dose of 1000 ng/ml was added back to block further expression of the Oct4 transgene during the timecourse of experiment. In this situation the results could be unambiquously attributed to the induced heterogeneity in GFP expression at the beginning of experiment rather than secondary effects of ectopic Oct4 expression (Niwa et al., 2000). Differentiation was conducted over three days with medium being changed twice daily. ZHTNG cells treated with 1000 ng/ml (Figure 4.8) showed a similar morphology to ZHTc6 previously described in (Figure 4.2). At day two and at day three most of the cells appeared morphologically undifferentiated. In contrast, cells which were heterogenous for GFP before the start of experiment, had a higher proportion of differentiated cells, which increased in number at day 3 (Figure 4.8).

4.3.2 Neural differentiation

To monitor neural differentiation capacity, ZHTNG cells were treated first with Puromycin to obtain uniform Nanog expression and were then treated with Doxycycline as described in section 4.3.1 to produce an undifferentiated population of cells expressing Nanog homogenously or heterogenously. Medium was then removed, cells were washed twice in PBS and supplemented with N2B27 media. Cells were then

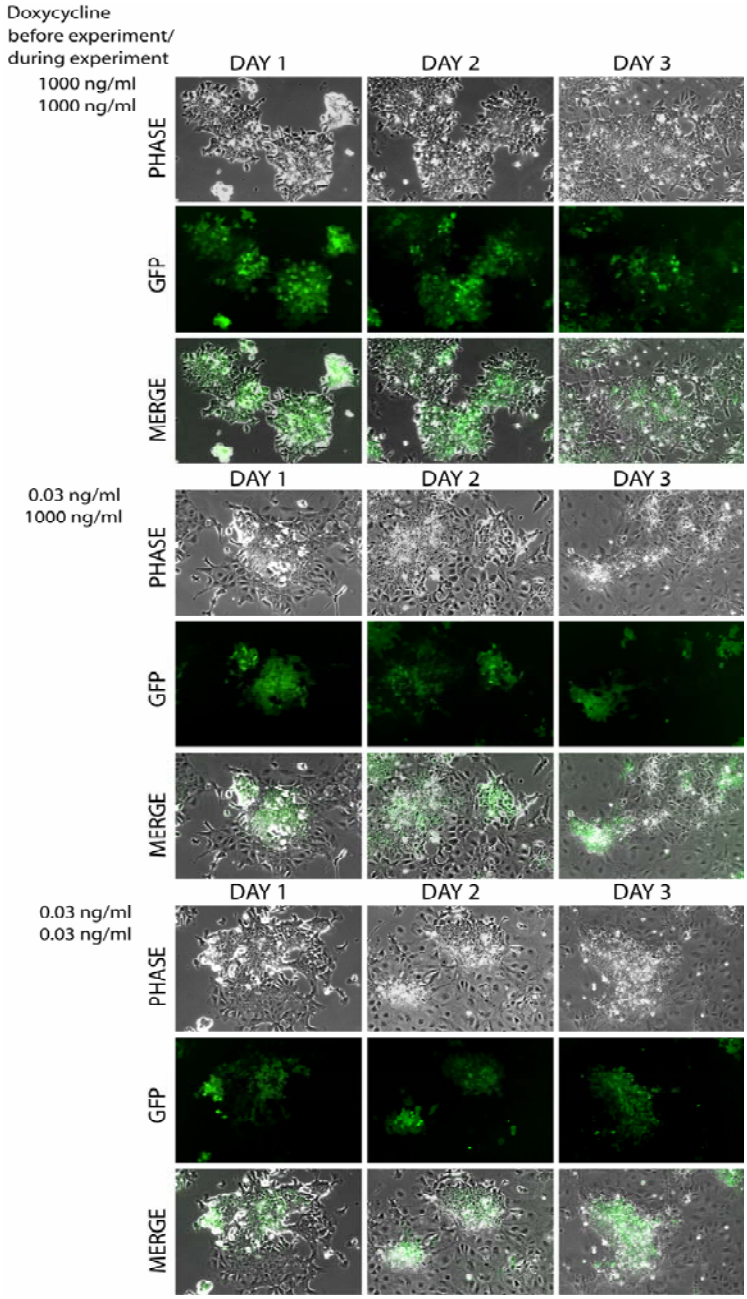

Figure 4.8 Morphological changes in the LIF withdrawal assay

Panel shows morphological changes in ZHTNG cells ($Oct4^{+/zeo}$; $Nanog^{+/GFP}$; contain a Doxycycline suppressible Oct4 transgene) treated with the indicated dose of Doxycycline during the LIF withdrawal differentiation assay over the time course of three days. Cells treated with 0.03 ng/ml of Doxycycline before the start show a significant higher proportion of differentiated cells.

separated into three experimental conditions described in section 4.3.1. Cells were observed daily by microscopy and collected every second day for RNA. Q-PCR analysis showed that the neural progenitor markers Nestin and Pax6 (Figure 4.9) were strongly upregulated during differentiation of cultures in which Nanog heterogeneity had been induced. At day 8, cells were fixed and stained for Nestin, βIII Tubulin (Tuji) and DAPI. The immunofluorescence analysis showed that in ZHTNG cultures treated before and during the experiment with the full dose of Doxycycline, Nestin and βIII Tubulin were barely detectable (Figure 4.10), yet Nanog:GFP was broadly expressed in most cells. However, ZHTNG cultures which were heterogenous for Nanog:GFP at beginning of the neural differentiation assay and which were treated with 1000 ng/ml of Doxycycline through the 8 days of the neural differentiation protocol showed a much higher proportion of Nestin and βIII Tubulin positive cells by immunofluorescence (Figure 4.9 and 4.10).

The proportion of Nestin and βIII Tubulin positive cells was further increased in cells in which the expression of the transgene was not blocked through the continuous treatment with 0.03 ng/ml of Doxycycline (Figure 4.9 and 4.10). In summary, these experiments show that the induction of Nanog heterogeneity in cultures lacking a Nanog low compartment increases their differentiation ability.

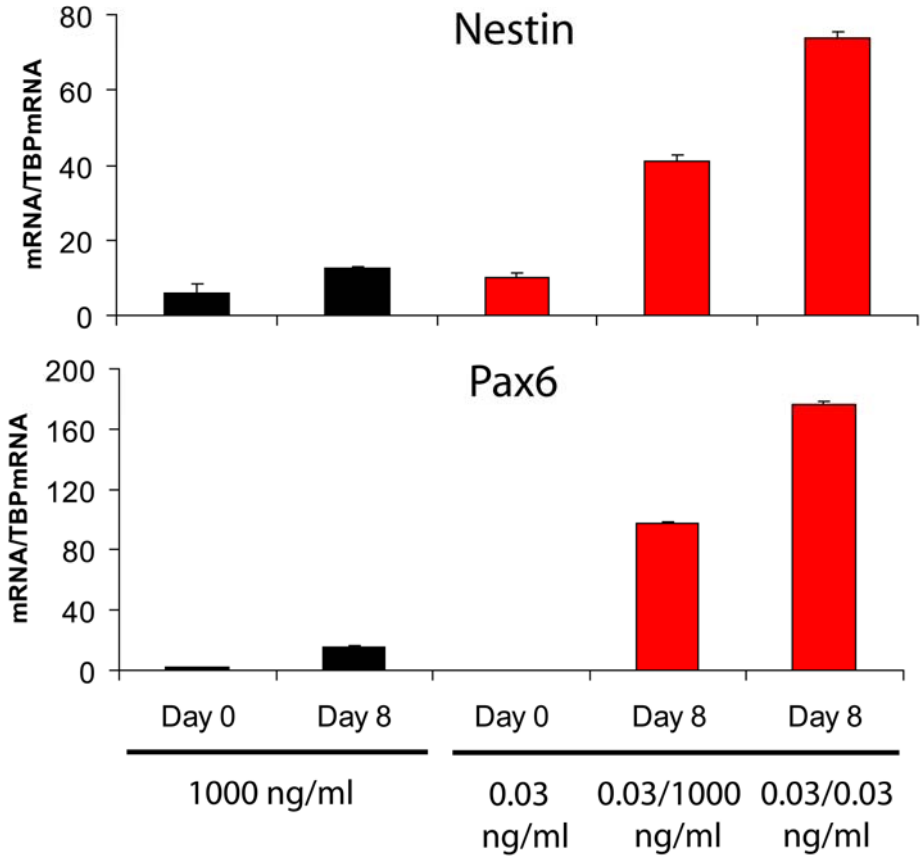

Figure 4.9 Q-PCR for neural progenitors

Q-PCR analysis for Nestin and Pax6 at day 0 and day 8 of neural induction. Cultures treated either with 1000 ng/ml or 0.03 ng/ml of Doxycycline before start of experiment (Day 0). The first numbers indicate the Doxycycline concentrations before start of neural induction and the second numbers indicate the Doxycycline concentrations used during the time course of experiment. mRNA expression was normalised to TBP mRNA expression.

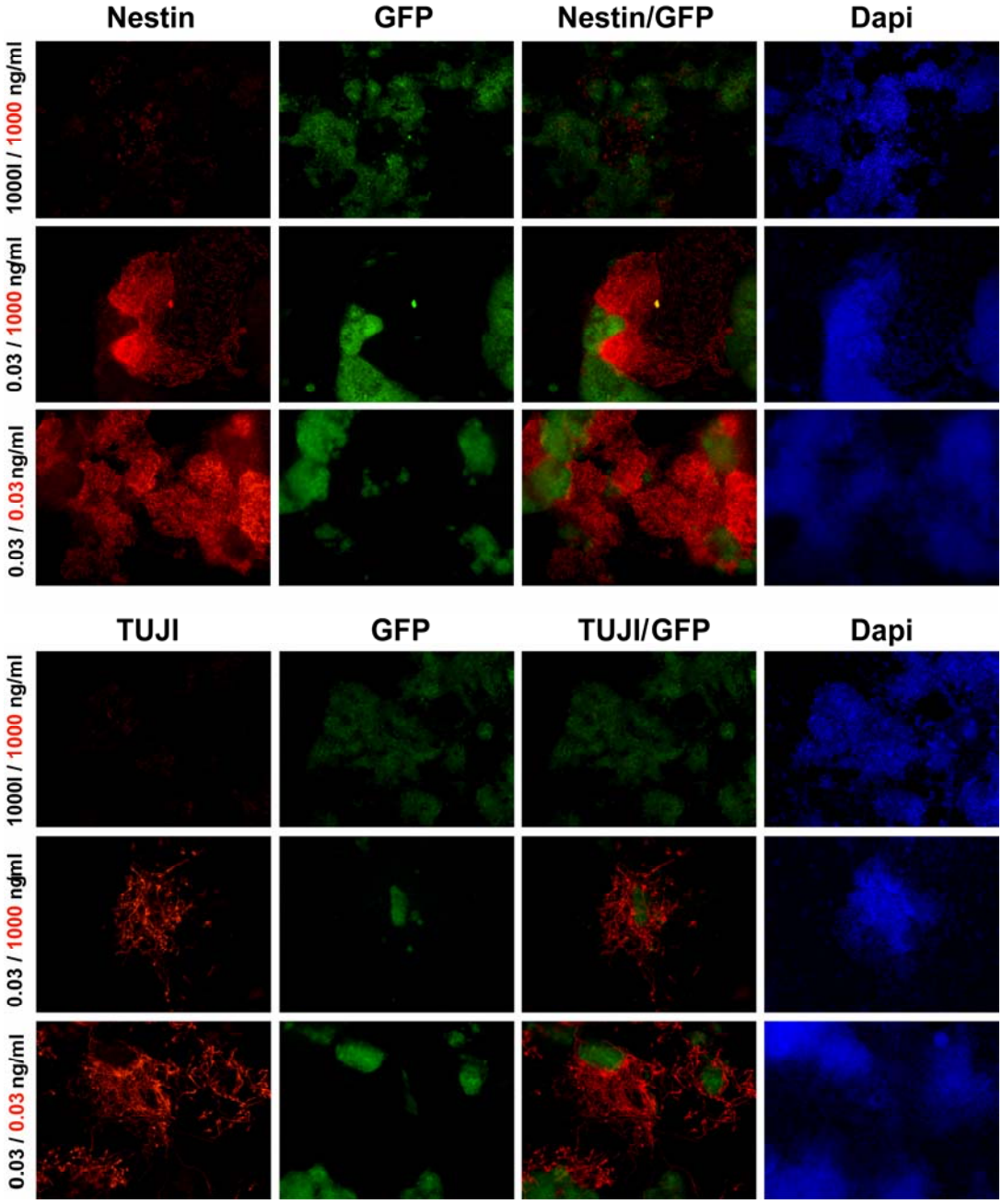

Figure 4.10 Immunofluorescence analysis for neural markers

Immonuflourescence analysis in ZHTNG ($Oct4^{+/zeo}$; $Nanog^{+/GFP}$; contain a Doxycycline suppressible Oct4 transgene) for Nestin (top panels), Tuji (bottom panels) and DAPI at day 8 of neural differentiation assay. Doxycycline dose at start of experiment is represented in black (left margin) and concentrations used during the time course are shown in red (left margin).

4.4 Discussion

The data in this chapter show that differentiation of functional Oct4 heterozygote ES cells is delayed due to a lack of a Nanog negative undifferentiated population. This delayed differentiation can be rescued by raising the Oct4 level in functional heterozygotes and restoring heterogenous Nanog expression.

The unexpected finding that functional Oct4 heterozygote ES cells are less mosaic than wild type ES cells, enabled me to investigate how a culture system lacking Nanog mosaicism responds to differentiation cues compared to cultures with heterogeneous Nanog expression. According to (Chambers et al., 2007), low levels of Nanog may constitute a window of opportunity in which extrinsic or intrinsic perturbations enable a lineage commitment decision. Therefore, I have postulated that the functional Oct4 heterozygote cells could be retarded in their differentiation kinetics compared to wild type ES cells due to a smaller Nanog low compartment. To investigate this hypothesis a LIF withdrawal and a neural differentiation assay were performed to determine if Nanog heterogeneity is important to drive cells more efficiently into commitment. As shown in Figure 4.2–4.3 during the LIF withdrawal protocol, ES cells homogenous for Nanog (OKO8, OKO160, ZHTc6 and ZHBTc4.1) showed delayed morphological changes, a delayed loss of pluripotency markers, as well as a delayed upregulation of the mesodermal gene Brachyury in comparison to cells heterogeneous for Nanog (E14Tg2a and Oct4 GIP) (Figure 4.3). The same cell lines were assessed during neural differentiation. Immunoflourescence analysis showed that in E14Tg2a and Oct4GIP

cells, βIIITubulin and Nestin were detectable, whereas in OKO160, ZHTc6 and ZHBTc4.1 cultures, only isolated cells expressing βIIITubulin could be found and these showed poor axonal development (Figure 4.4 and 4.5). To determine if cells remained undifferentiated rather than made a transition into other lineages staining for the pluripotency marker Oct4 was performed. Oct4 was detectable in all functional heterozygote ES cells at day 8 of experiment but was only expressed in isolated colonies in E14Tg2a and Oct4GIP cultures (Figure 4.4). Q-PCR analysis confirmed the immunofluorescence data (Figure 4.5). Consequently a missing Nanog negative compartment is significant for cell fate.

Nanog has previously been shown to block differentiation when overexpressed (Chambers et al., 2003). The experiments in this chapter suggest that in addition ES cells that express wild-type Nanog levels but that do so uniformly have an impaired differentiation capacity. These results are of interest in relation to the report by Shimozaki et al., that upregulated Oct4 expression enhanced neuronal differentiation of ES cells via an unknown mechanism (Shimozaki et al., 2003). One of the experiments performed by Shimozaki was to increase Oct4 levels driven from the transgene in ZHTc6 cells (Niwa et al., 2000). They showed that ZHTc6 cells have an impaired neural differentiation capacity relative to ZHTc6 cultures in which Oct4 was upregulated. These results may therefore be explained by a restoration in Nanog heterogeneity, as shown in this chapter.

To further investigate these findings, the kinetics of sorted Nanog^{high} and Nanog^{low} cells from ZHTNG and TNG cells should be compared. This would establish whether reciprocal interactions between the populations were dispensable for enhanced differentiation of the Nanog^{low} cells.

A similar mechanism might be important in the mouse embryo. Palmieri et al., reported a transient increase in Oct4 protein in the primitive endodermal cells of the blastocyst prior to its final downregulation (Palmieri et al., 1994). In this context recent publication by (Nichols et al., 2009) showed that that blockade of Erk signalling from the 8-cell stage suppresses appearance of Nanog^{low} cells within the ICM and blocks primitive endoderm development. This indicates that the development of the hypoblast is dependent on Erk signaling possibly downstream of FGF. As Oct4 can directly upregulate FGF4 (Yuan et al., 1996), it will be important in further experiments to link the results represented in my thesis to the ground state theory (Ying et al., 2008).

Chapter 5

The consequences of deleting the Oct4 binding site in the *Nanog* promoter on *Nanog* expression

5.1 Introduction

The Oct4/Sox2 site in the *Nanog* promoter has been shown by mutagenesis to mediate a positive effect of Oct4 in luciferase assays (Kuroda, 2005; Rodda et al., 2005). However, experimental evidence in support of the action of Oct4 at this site on the endogenous *Nanog* gene is lacking. In this chapter, I have investigated the function of this site on *Nanog* regulation.

5.2 Results

5.2.1 Oct4 is a direct activator of Nanog

As functional Oct4 heterozygote ES cells express Nanog homogenously and as Oct4 induction in these cells induces heterogenous Nanog expression, we investigated the effect of mutating the Oct4 site in the context of a TNG allele at the endogenous *Nanog* locus. A mutation in the Oct4 site at 181 bp was made in the TNG targeting vector (Figure 5.1A) by replacing the Oct4 binding sequence TTTTGCAT with a *Sex*A1 restriction site to simultaneously abolish Oct4 binding and enable selection of the correctly targeted clones by Southern analysis (Figure 5.1B). The presence of the correct

A

B

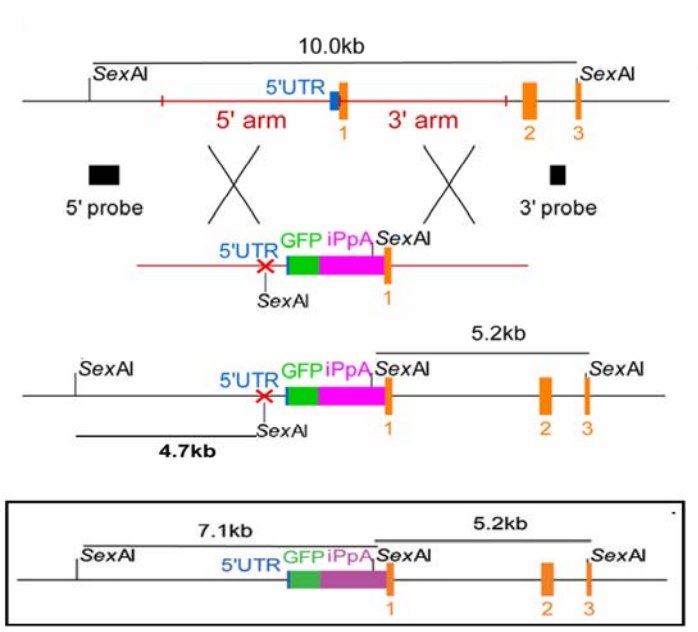

Figure 5.1 Oct4 mutant vector

A: Panel shows the Nanog promoter sequence around the Oct4 binding sites (red). Indicated are as well the binding sites for Essrb (blue) and Sox2 (green) (top). The sequence containing the Oct4 site mutation (red) is represented on the bottom of panel A. B: The 5' end of the *Nanog* gene is shown schematically at the top. Exons are shown in orange; 5'UTR in blue; homology arms used for construction of the targeting vector in red. eGFP was inserted between the homology arms precisely at the Nanog AUG codon in the targeting construct shown in the middle. The Oct4 binding site (red cross) was mutated into a *Sex*A1 restriction sequence in the targeting vector. This mutated Oct4 binding site lies 3250 bp from the 5' end and 370 bp from the 3'end of the 5' homology arm. The positions of the flanking probes used for Southern analysis and the fragment sizes produced by *Sex*AI digestion are indicated. Black box at the bottom indicates the non mutated TNG allele.

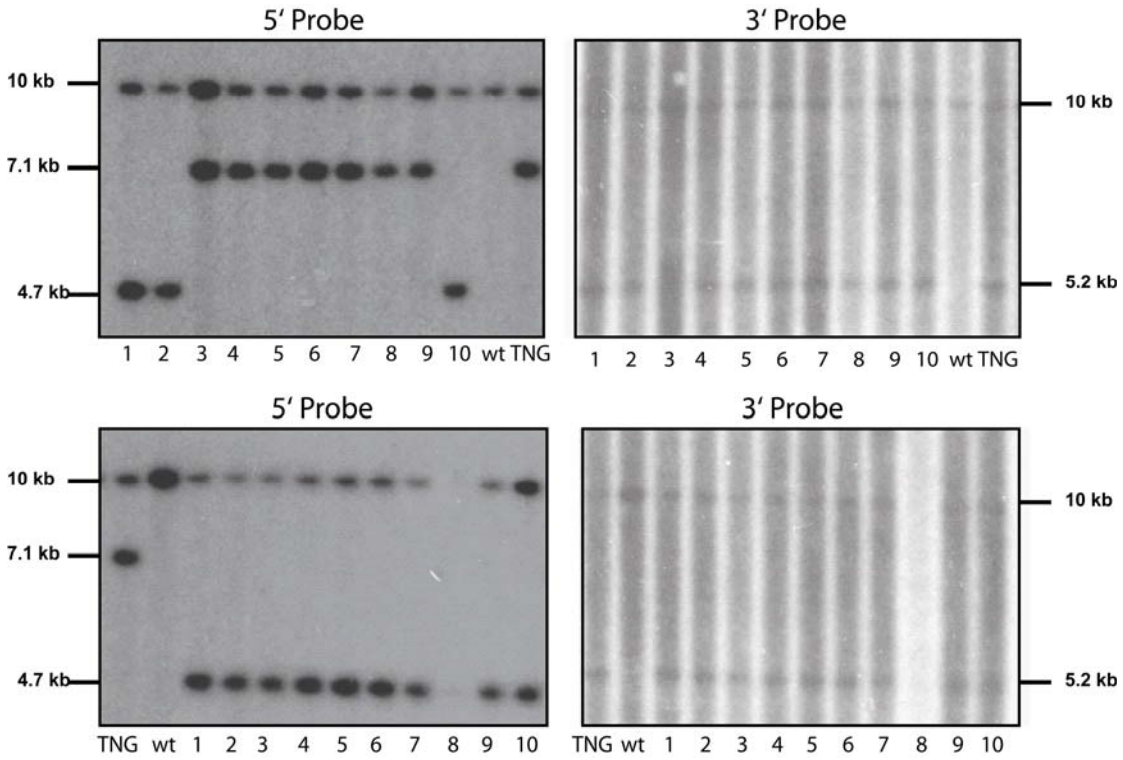

Figure 5.2 Southern Blot analysis in Oct4 mutant clones

Southern Blot analysis of *Sex* AI digested genomic DNA from E14tg2a (top) and ZHBTc4.1 (bottom) cells in which the Oct4 mutant targeting vector was introduced by homologous recombination. The loss of the Oct4 binding sequence is visible in the 5' Blot in the appearance of a 4.7 kb band. The 3' Blot should show for mutated and non-mutated cells a 10 and 5.2 kb band. Wild type cells show one 10kb band only.
Clone 1 and 2 from the top panel and clone 4 and 5 from the bottom panel were analysed further.

sequence in the targeting vector was confirmed by enzyme digestion and sequencing (not presented here). The construct was linearised and introduced into the wild type cell line E14Tg2a and the functional Oct4 heterozygote cell line ZHBTc4.1. Southern analysis of *Sex*A1 digested genomic DNA from both cell lines was performed to identify homologous recombinants (Figure 5.2). Correctly targeted cells were identified for both E14Tg2a (3/10) and ZHBTc4.1 (9/9) derivatives and are referred to as mutant TNG (mTNG) and mutant ZHTNG (mZHTNG). To investigate the consequences of the Oct4 site mutation, two clones from each cell line (clone 1 and 2 for mTNG and clone 4 and 5 for mZHTNG) were examined in more detail.

In the first instance, TNG, mTNG, ZHTNG and mZHTNG cells were plated in parallel in the presence of 0.5 μg/ml of Puromycin for 4 days. Cells were then replated at the same density and were treated with a dilution series of Puromycin, the selection drug for the targeting event (0.5, 0.75, 1 and 1.25 μg/ml), to examine directly the promoter activity in these cells. Cells were analysed by FACS and microscopy to observe the GFP intensities and the survival capacity of cells under these conditions. The basic hypothesis behind the experiments was, that if Oct4 acts as a direct repressor of Nanog, deletion of the Oct4 site might result in an increase of Nanog expression. FACS analysis of the two TNG mutant clones (Figure 5.3 top (clone 1 and 2)) showed a general shift of the GFP peak towards the GFP low compartment in comparison to TNG cells, suggesting that the mutated cells expressed Nanog at lower levels. In addition, cells showed a shoulder towards GFP low expression that was more pronounced than in the TNG cells. Microscopy (Figure 5.3 bottom) confirmed this general decrease in GFP expression.

Additionally, compared to TNG cells, mTNG cells showed lower survival at Puromycin concentrations of 1 μg/ml and higher. The expression pattern for the mZHBTNG clones also showed a slight general shift towards the GFP low compartment in both clones but in this case without a shoulder of decreased expression (Figure 5.4). Microscopy showed a higher survival capacity of these cells at high Puromycin concentrations compared to mTNG.

However it was also of interest to examine the consequences of the Oct4 mutation on Nanog heterogeneity. To enable similar starting conditions and starting populations, the TNG and ZHBTNG cells were expanded in GMEMβ/FCS/LIF in the presence of 0.75 μg/ml of Puromycin and were double sorted for GFP high cells in parallel with all Oct4 mutant clones. The purity of the sorts is represented in Figure 5.5. Cells were replated in GMEMβ/FCS/LIF without Puromycin and observed over the next 18 days by FACS. The top panel in Figure 5.6 shows an overlap of GFP expression of TNG cells (black) and the two TNG-Oct4 mutant clones (red and orange). TNG-Oct4 mutant cells showed a high heterogenous GFP expression pattern and a general shift in GFP expression towards the negative compartment. However it was possible to culture the cells for many passages without a complete loss of GFP expression, suggesting that Oct4 is not the only activator of Nanog. Microscopy confirmed that the cells were more heterogenous for GFP than TNG cells at day 18 (Figure 5.6 bottom). The mZHBTNG clones were similarly treated and investigated by FACS and microscopy over the time course of 18

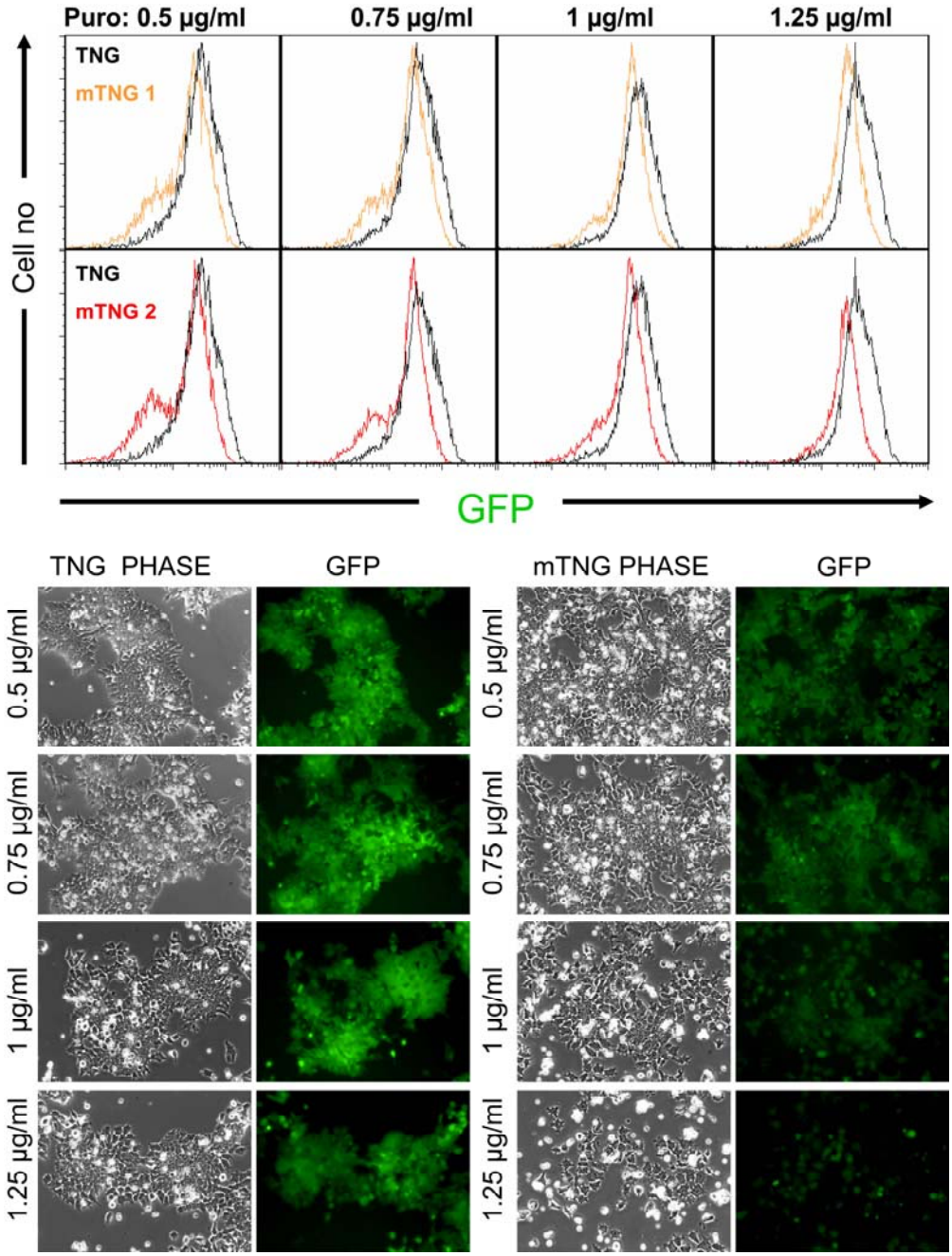

Figure 5.3 Nanog expression is reduced in mTNG cells

Top panel shows FACS analysis of TNG ($Oct4^{+/+}$; $Nanog^{+/GFP}$) (black) and two mTNG clones (red and orange). Bottom panel shows brightfield and GFP photos of TNG cells and one representative mTNG clone treated in parallel with the indicated dose of Puromycin.

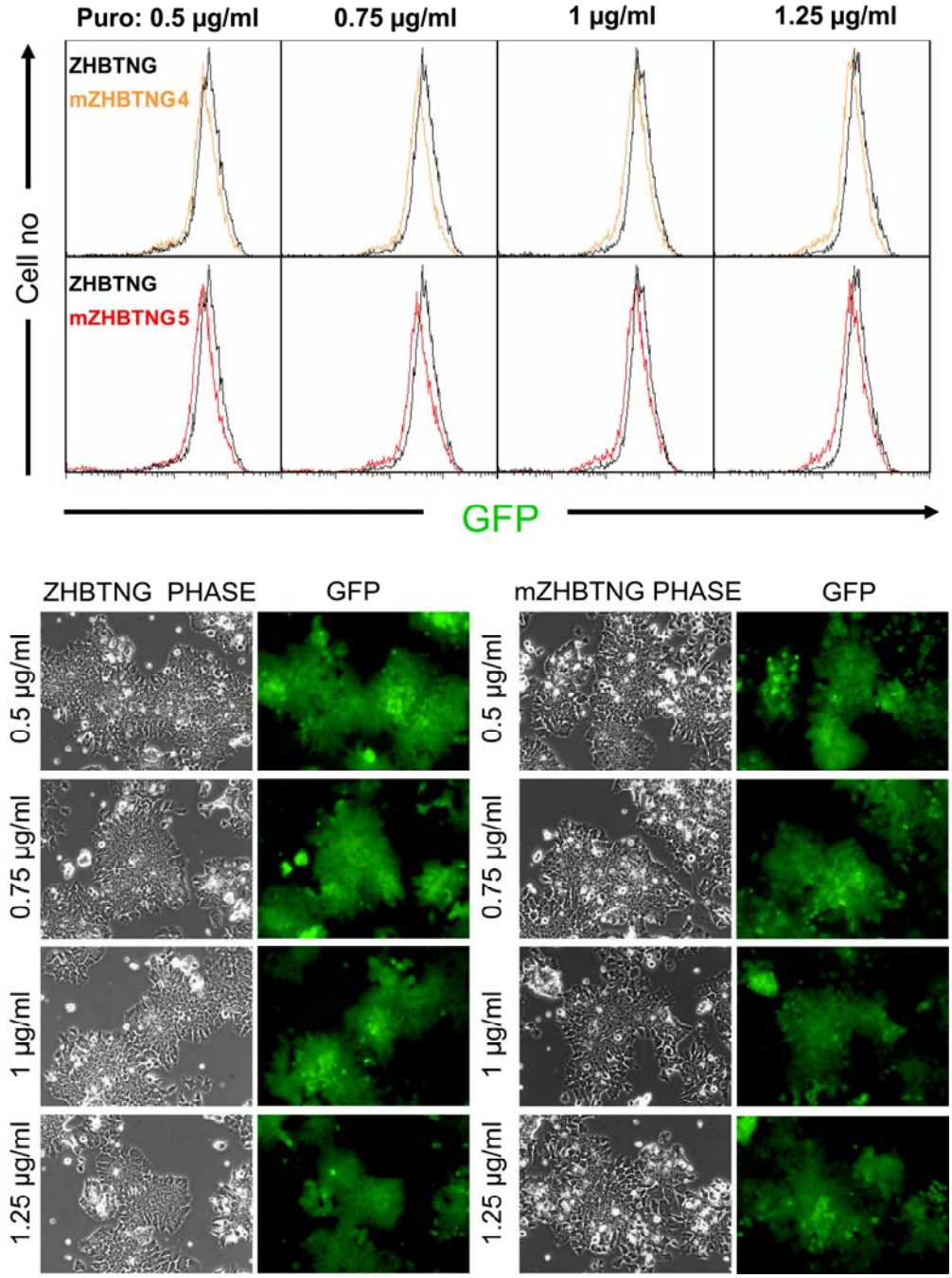

Figure 5.4 Nanog expression is reduced in mZHBTNG cells

Top panel shows FACS analysis of ZHBTNG (Oct4$^{zeo/BSD}$; Nanog$^{+/GFP}$; Oct4 transgene on)(black) and two mZHBTNG clones (red and orange). Bottom panel shows brightfield and GFP photos of ZHBTNG cells and one representative mZHBTNG clone treated in parallel with the indicated dose of Puromycin.

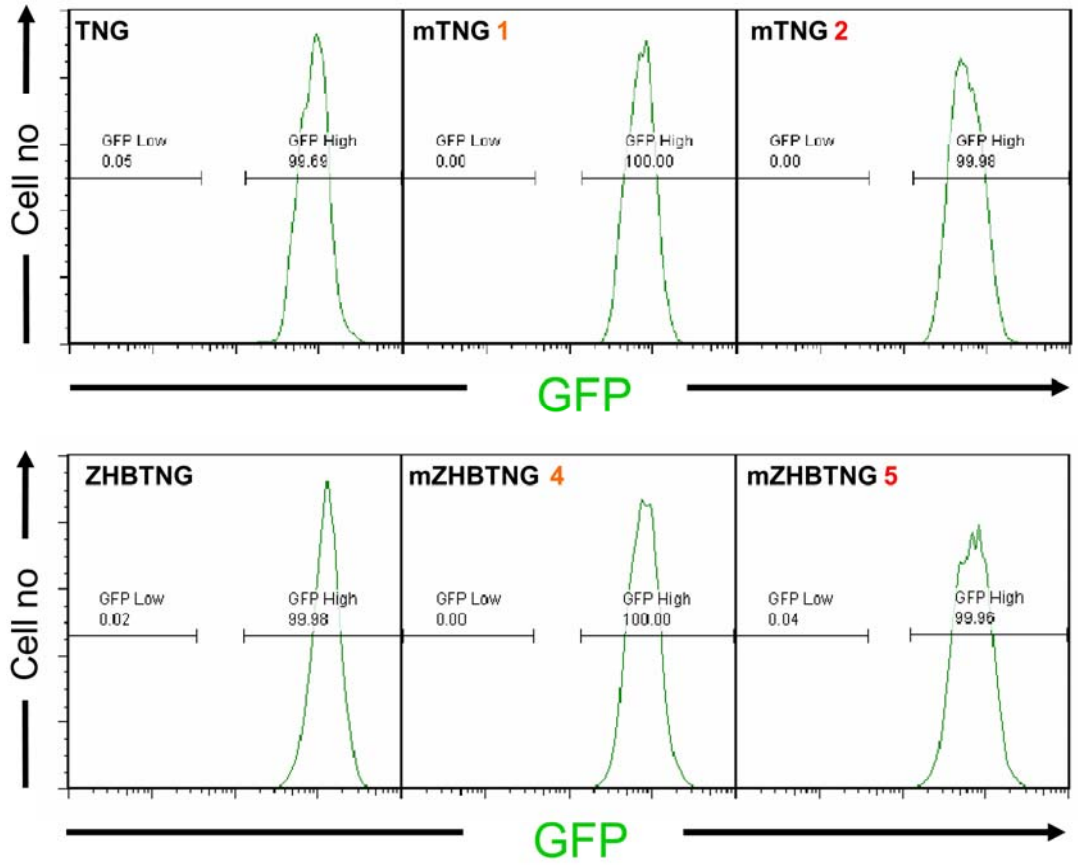

Figure 5.5 Purity analysis of sorted TNG, ZHBTNG and Oct4 mutant cells

FACS purity analysis of TNG ($Oct4^{+/+}$; $Nanog^{+/GFP}$), ZHBTNG ($Oct4^{zeo/BSD}$; $Nanog^{+/GFP}$; Oct4 transgene on) and two mTNG and two mZHBTNG clones directly after sorting for GFP high expressing cells. The purity of the investigated population is indicated in percent of cells representing either the GFP^{high} or the GFP^{low} compartment.

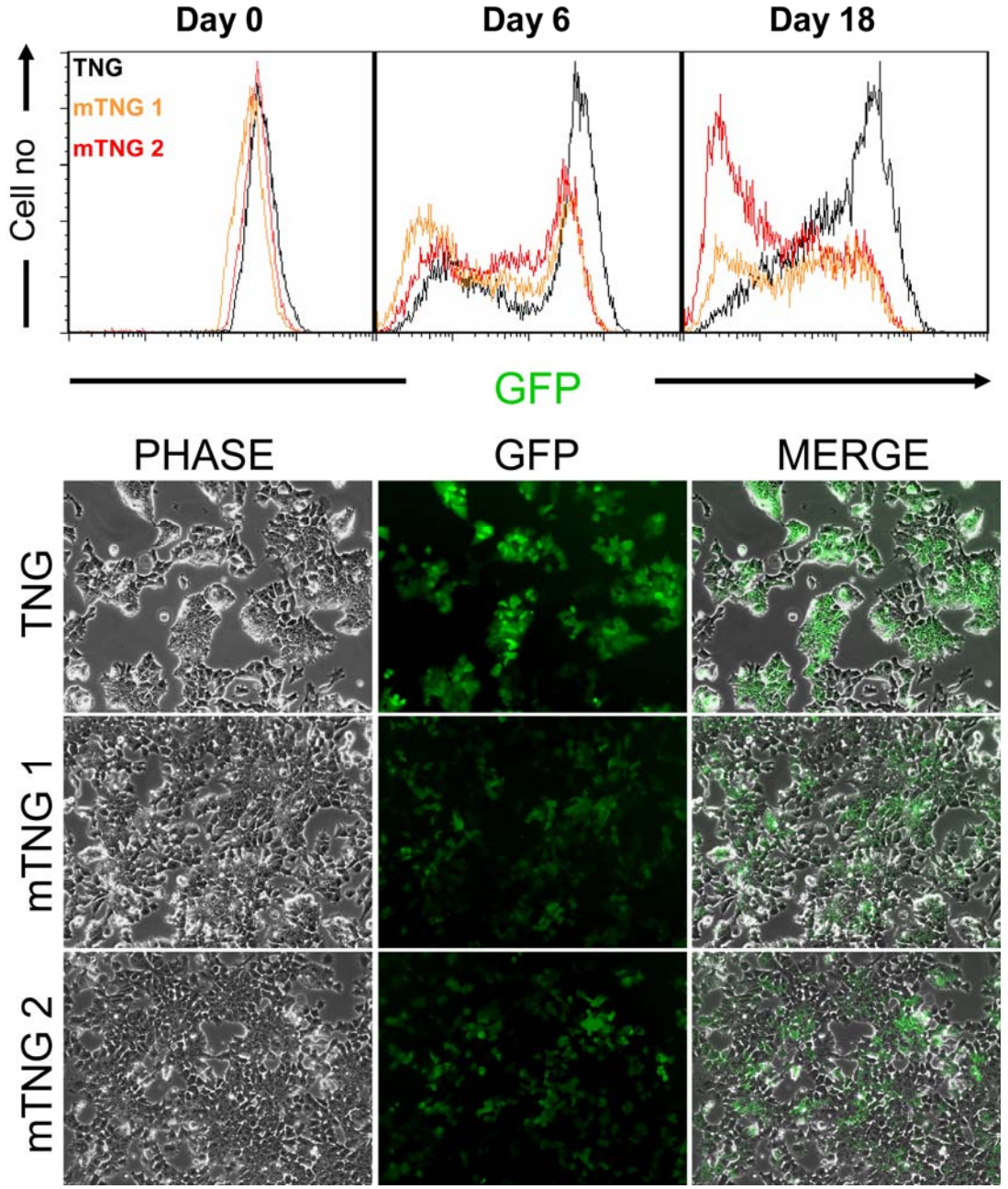

Figure 5.6 GFP heterogeneity is increased in mTNG cells

Top panel shows FACS analysis of TNG ($Oct4^{+/+}$; $Nanog^{+/GFP}$) (black) and two mTNG clones (red and orange) at day 0, 6 and day 18 of experiment. mTNG cells show a reduction in GFP expression and therefore an increase in GFP heterogeneity. Bottom panel shows brightfield and GFP photos of TNG cells and the two mTNG clones at day 18 of experiment.

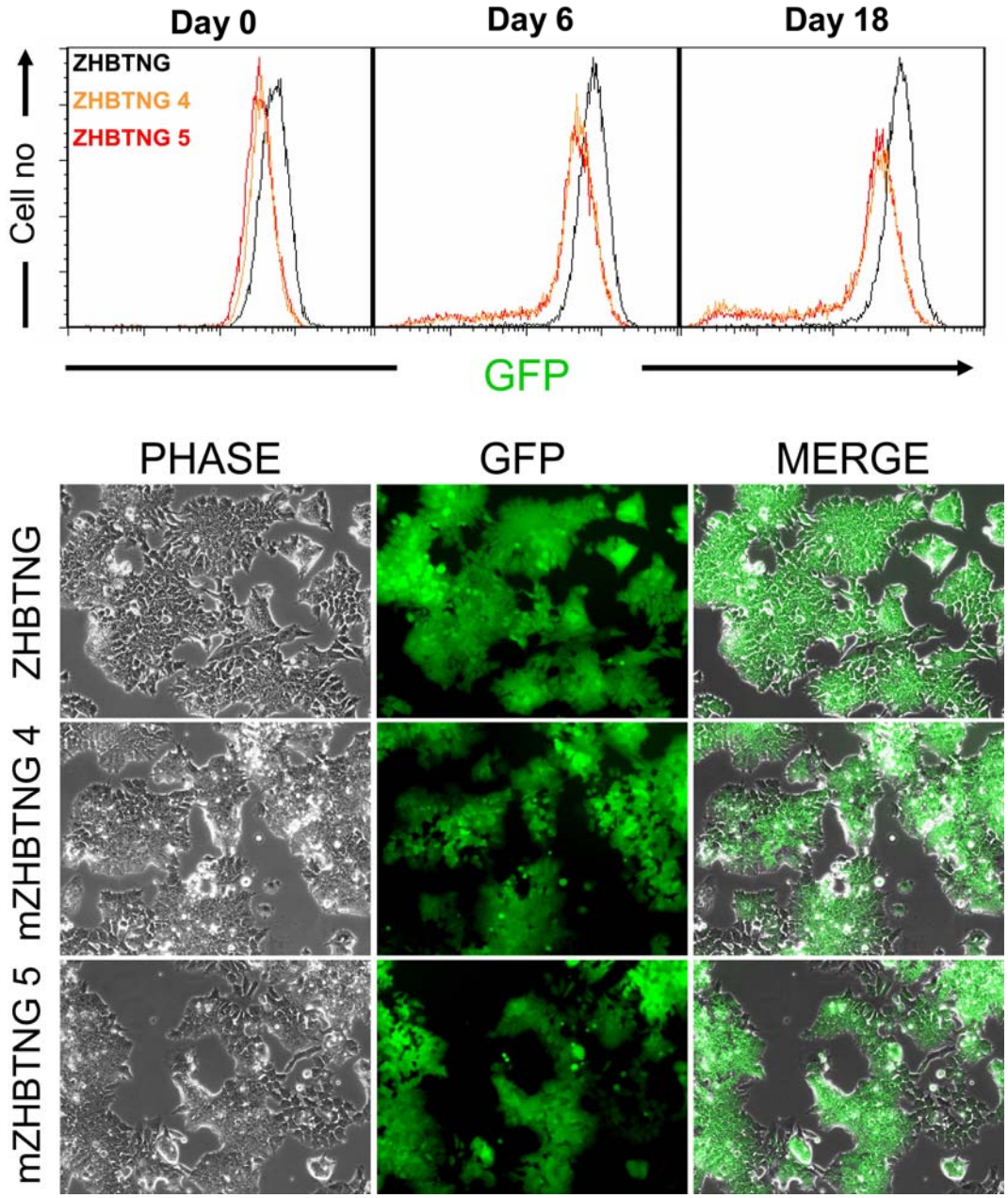

Figure 5.7 GFP heterogeneity is increased in mZHBTNG cells

Top panel shows FACS analysis of ZHBTNG (Oct4$^{zeo/BSD}$; Nanog$^{+/GFP}$; Oct4 transgene on) (black) and two mZHBTNG clones (red and orange) at day 0, 6 and day 18 of experiment. mZHBTNG cells show a reduction in GFP expression and an increase in GFP heterogeneity. Bottom panel shows brightfield and GFP photos of ZHBTNG cells and the two mZHBTNG clones at day 18.

days. These cells expressed GFP in a heterogenous pattern, but not such highly mosaic as observed for TNG-Oct4 mutant or even TNG cells (Figure 5.7). To confirm the exact expression levels, RNA was prepared at day 18 and analysed by Q-PCR for Oct4, Nanog and GFP expression (Figure 5.8). Oct4 mRNA was expressed at the same level in the mutant clones and the respective parental cells. Primers located in *Nanog* Exon 3 and 4 that measure expression from the unmodified *Nanog* allele produced similar signals in both mutant clones compared to the parental lines. Dramatic differences however were observed in the GFP expression, which showed a 3 fold decrease in the mTNG cells, and a 2 fold decrease in mZHBTNG cells compared to TNG and ZHBTNG cells. This result confirmed the previous observations and showed that at this site Oct4 acts as a positive activator.

5.3 Discussion

In order to determine the role of the proximal Oct4 binding site on regulation of the endogenous *Nanog* gene, I made a Nanog:GFP targeting vector in which the Oct4 site was mutated. This vector was introduced into wild type E14Tg2a cells to directly visualise effects upon heterogeneity. The same vector was introduced into ZHBTc4.1 cells to monitor effects upon the more homogenous Nanog expression pattern of these cells.

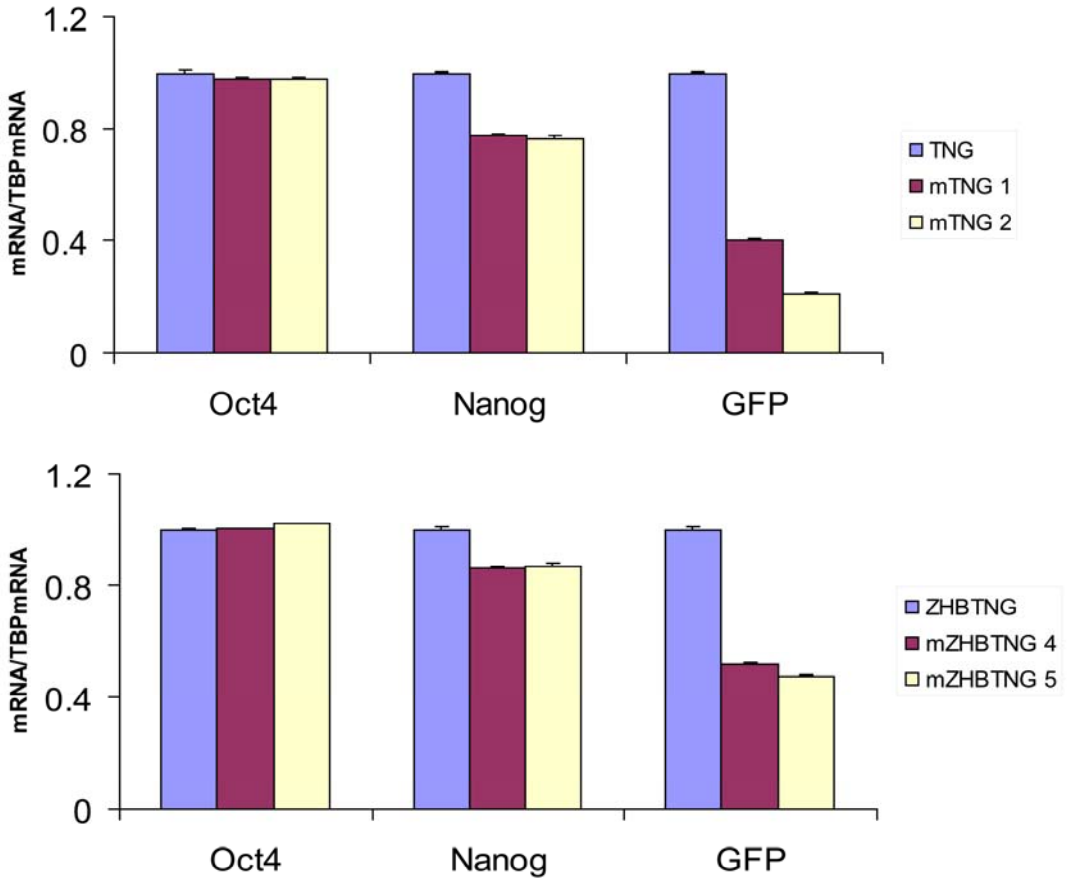

Figure 5.8 Q-PCR analysis in Oct4 mutant cells

Figure shows GFP, Oct4 and Nanog mRNA expression in TNG ($Oct4^{+/+}$; $Nanog^{+/GFP}$) (blue), two mTNG clones (red and yellow) (top panel) and in ZHBTNG ($Oct4^{zeo/BSD}$; $Nanog^{+/GFP}$; Oct4 transgene on) (blue) and two mZHBTNG clones (red and yellow) (bottom panel). mRNA expression, normalised to TBP mRNA expression, is represented relative to either TNG cells (top panel) or ZHTNG cells (bottom panel), which are set as 1. Errors bars represent the standard deviation of the mean (n=3).

Clones carrying the mutation could be obtained from both cell lines (Figure 5.2), indicating immediately that the Oct4 binding site was not essential for *Nanog* expression as suggested by transient reporter assays (Kuroda, 2005; Rodda et al., 2005) and suggesting that Oct4 is not the only positive activator of Nanog. The targeting efficiency for both lines was 100% (E14Tg2a, n=10; ZHBTc4.1, n=9), similar to the targeting efficiency obtained previously using non-mutant vector. In addition, all ZHBTc4.1 derived clones had incorporated the mutation. However, only 3/10 targeted E14Tg2a derivatives had incorporated the mutation. The distance between the 5'end of the 3620 bp 5' homology arm and the mutated Oct4 binding site is 3250 bp whereas the distance from the mutated Oct4 site to the 3'end of the 5' homology arm is 370 bp. One might therefore expect resolution of the Holliday junction in the 5' homology arm to incorporate the mutated Oct4 site at a frequency of $3250/3620$ x 100% (i.e. 90%). However, only 30% of the targeted clones contained the Oct4 mutant site (Figure 5.1). This suggests that E14Tg2a derived clones carrying the mutated Oct4 mutant site are at a strong disadvantage. In this situation the introduced mutation may have reduced expression towards a critical boundary for expression of drug resistance, thereby reducing cell survivability. This outcome was probably not seen in ZHBTc4.1 cells because *Nanog* expression in ZHBTc4.1 cells is upregulated relative to Oct4 wild type ES cells. These observations suggest that clones containing the Oct4 mutation express *Nanog* at lower levels. The cell response to increasing levels of Puromycin, the selection drug for the targeting event was consistent with this interpretation. As shown in Figure 5.3 and 5.4, mutated cells have decreased *Nanog:GFP* expression in both cell lines. This also showed that mTNG cells exhibited reduced survival at Puromycin concentrations of

1 µg/ml or higher. To directly study the heterogeneity of Nanog in the mutated clones, the cells had to be relieved from the Puromycin selection and observed over a longer period of time. This resulted in an increase of Nanog heterogeneity and a shift of the GFP peak towards the GFP low compartment in both Oct4 mutant cell lines (Figure 5.6 and 5.7). This reduction of GFP was confirmed by Q-PCR analysis (Figure 5.8). In summary the results represented in this chapter proved that deletion of the proximal Oct4 binding site results in a decrease in Nanog promoter activity and an increase in Nanog heterogeneity. However, as binding sites are described by ChIP for Oct4 at both the *Nanog* promoter and the *Nanog* enhancer region (Levasseur et al., 2008) it would in future be of interest to examine, whether deletion of the enhancer binding site would effect *Nanog* expression.

As shown elsewhere in this thesis, ZHTNG are homogenous for Nanog and overexpression of Oct4 in ZHTNG cells reinduces heterogenous Nanog expression. One approach to further examine the role of Oct4 in *Nanog* expression is to introduce the Oct4 mutant Nanog:GFP reporter construct into ZHTc6 cells to make mZHTNG cells. If an increase in GFP heterogeneity was observed this would suggest that Oct4 acts either as an indirect suppressor of *Nanog* or acts directly via another binding site. Conversely, if Oct4 acts via the Oct4 binding site in the proximal promoter to reinduce Nanog heterogeneity, such heterogeneous Nanog:GFP expression should not be induced in these cells. It would also be interesting to determine whether a regulatable form of Nanog could rescue heterogeneity, particular in the latter situation. A complementary approach would be to introduce an additive transgene into ZHTc6 cells in which

Nanog:GFP was expressed from the proximal promoter without the *Nanog* -5kb enhancer region. If an increase in heterogeneity could not be induced from this Nanog:GFP construct by upregulating of Oct4 in ZHTc6 cells this would indicate an important role for the enhancer region in inducing Nanog heterogeneity.

Chapter 6

Solexa gene expression analysis

6.1 Nanog is expressed heterogeneously in undifferentiated mouse ES cells

To investigate Nanog expression at the single cell level, the genetically unmodified ES cell line E14Tg2a was plated at clonal density. After four days, colonies had formed that morphologically contained small tightly packed cells at their centre and more elongated or flatter cells at their periphery. Staining for Oct4 showed the centrally located population to contain a higher proportion of strongly Oct4 positive cells then the peripheral population (Figure 6.1). In comparison to Oct4, expression of Nanog varies widely in ES cell colonies. Again the centrally located population contained a higher proportion of strongly expressing cells then the peripheral population. However, there does not appear to be a simple relationship between levels of Oct4 and Nanog since not all nuclei strongly expressing Oct4 had the highest Nanog levels. It is also noteworthy that on a closer observation single cells were found that expressed reasonable Nanog levels but in which Oct4 was weakly detectable (Figure 6.1).

6.2 Gene expression analysis between Nanog^{high} and Nanog^{low} states

To investigate how the different expression states of Nanog are regulated and what might be involved in switching between Nanog^{high} and Nanog^{low} states, I took advantage

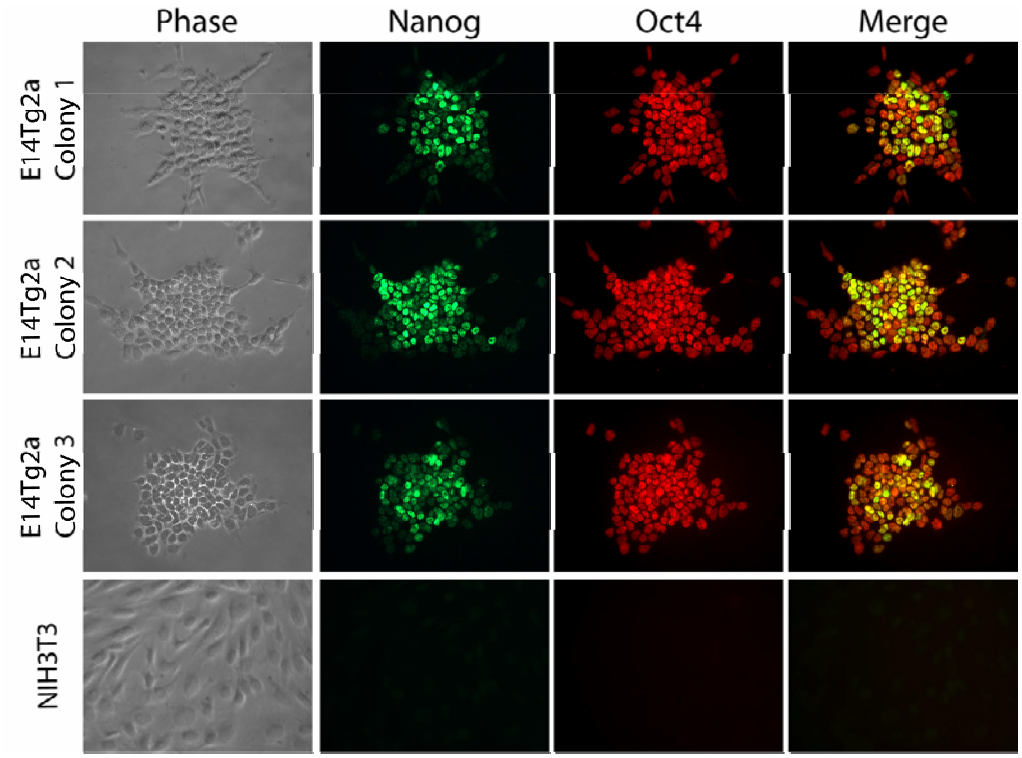

Figure 6.1 Nanog and Oct4 expression in mouse ES cells

Immunofluorescence analysis of three representative colonies from the genetically unmodified ES cell line E14Tg2a and NIH3T3 cells, which do not express Nanog or Oct4. Analysis shows that Nanog expression vary widely in comparison to Oct4 expression. Nanog is even undetectable in some morphologically undifferentiated Oct4 positive cells. However it appears that Oct4 as well shows differences in expression between single cells.

of a cell line in which eGFP was expressed from the AUG codon of endogenous *Nanog* in the mouse ES cell line E14Tg2a (Chambers et al., 2007). The resulting cells (TNG for E14Tg2a, Nanog and GFP (Figure 6.2A)) express GFP in a heterogenous pattern and can be sorted into different populations according to the expression of GFP (Figure 6.2B). To define genes that distinguish between Nanog positive and Nanog negative ES cells and to potentially identify genes that might influence the transition from the $Nanog^{high}$ to the $Nanog^{low}$ state, the TNG cells were sorted into GFP^{high} and GFP^{low} populations (Figure 6.3A). This sort was performed by simultaneous staining for SSEA1, a cell surface marker considered to identify undifferentiated ES cells (Solter and Knowles, 1978). The purity of the sort was 97.7% in the GFP^{low} population and 98.5% in the GFP^{high} population (Figure 6.3A). To determine whether these sorted populations had segregated Nanog expression, the GFP^{high} and GFP^{low} cells were assessed by immunoblotting (Figure 6.3B). Analysis using an anti-GFP antibody, confirmed the efficiency of the FACS protocol (Figure 6.3B). Importantly, an antibody against Nanog showed Nanog to be strongly present in the GFP^{high} population but barely detectable in the GFP^{low} population (Figure 6.3B). Furthermore, Q-PCR analysis showed that the population with low GFP levels expressed ~37% the level of Nanog mRNA present in the GFP^{high} population (Figure 6.4A).

The aim of this sort was to identify genes that distinguish between $Nanog^{high}$ and $Nanog^{low}$ states. In the first instance however, the pluripotency genes Oct4, Sox2, Klf4, Rex1, and Esrrb were investigated by Q-PCR. Interestingly, Klf4, Rex1 and Esrrb show a positive correlation with Nanog. However, the degree of variation was different for

A

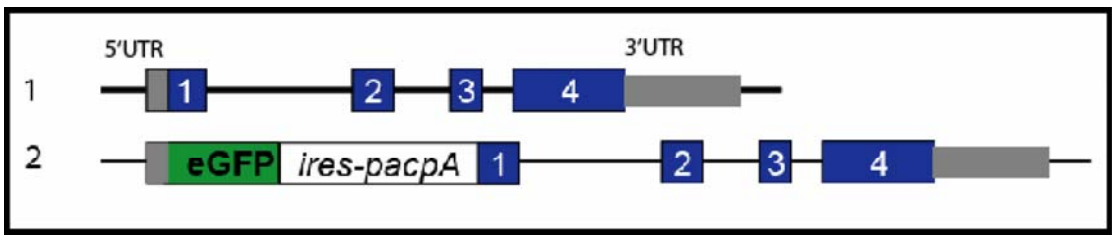

Figure 6.2A Structure of the Nanog alleles in TNG cells

Panel A shows the two endogenous Nanog alleles in the Nanog:GFP reporter cell line TNG. The TNG targeting construct contains an eGFP-ires-pac-polyA-cassette fused to the Nanog AUG codon of Nanog. (Adapted from Chambers et al., 2007)

B

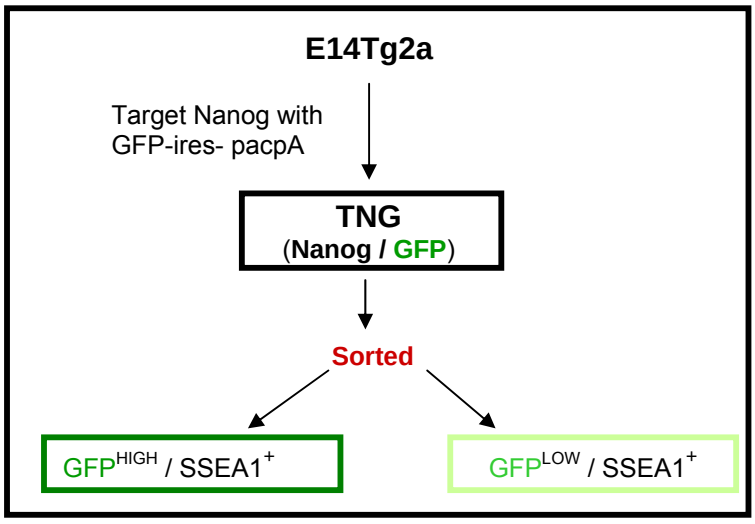

Figure 6.2B Schematic representation of the derivation of TNG cells and the sorted Nanog:GFP populations

E14Tg2a wild type ES cells were targeted with a Nanog eGFP-ires-pacPa vector. As Nanog expression is reported by GFP, these cells can be sorted according to GFP expression. In this analysis, GFP^{high} and GFP^{low} cells were sorted in the SSEA1 positive compartment. (Adapted from Chambers et al., 2007)

A

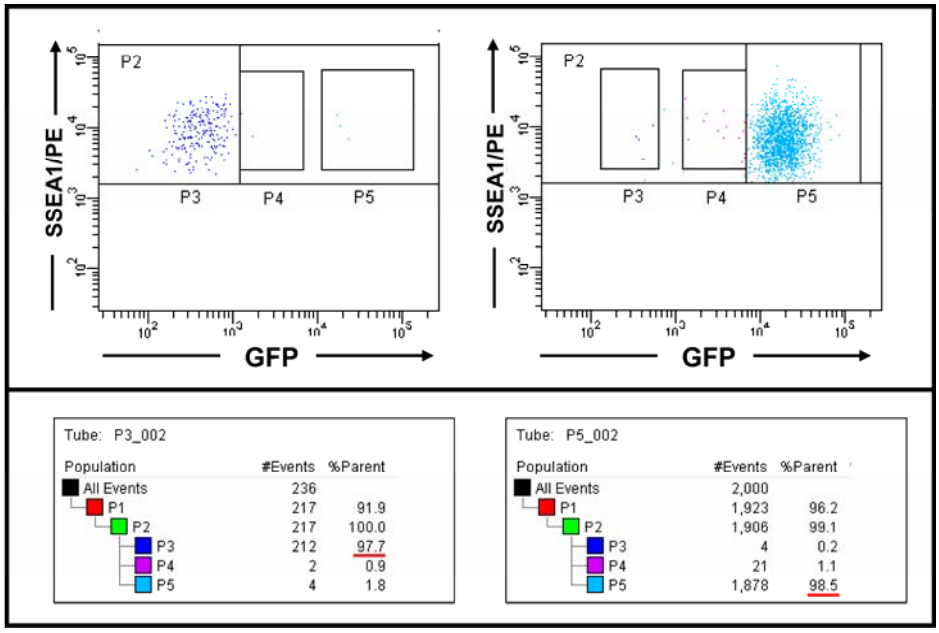

B

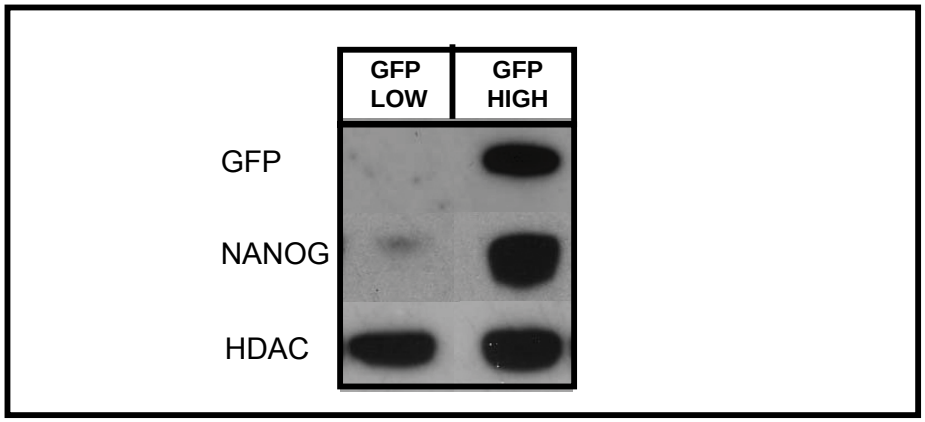

Figure 6.3 FACS purity and protein analysis in sorted populations

A: Purity analysis directly after TNG cells were sorted into GFP^{high}/ $SSEA1^{+}$ and GFP^{low}/$SSEA1^{+}$ cells.
B: Immunoblot analysis of the GFP^{high} and GFP^{low} fractions from sorted TNG cells probed with an anti-GFP and anti-Nanog antibody reveals that Nanog is only weakly detectable in the GFP^{low} fraction. HDAC acts as a loading control.

each gene. The smallest differences were observed for Oct4 and Sox2, which were decreased by < 10% in the Nanog low population (Figure 6.4A). In contrast, Klf4 and Esrrb were reduced in expression by > 50% in the Nanog low cells, with Klf4 in particular being reduced by 75% (Figure 6.4A). To determine, if the expression of these genes is dependent on Nanog levels, three cell lines in which the levels of Nanog were genetically manipulated were investigated by Q-PCR for the expression of Nanog, Oct4, Sox2, Essrb and Klf4. In this analysis the following cell lines were investigated: RCN (Nanog overexpressers), E14Tg2a (Nanog wild type) and RCNβH(t) (Nanog null cells). Interestingly all genes correlated positively with Nanog (Figure 6.4 B).

Genes that are expressed in differentiated cells and whose expression may be expected on the basis of lineage priming (Hu et al., 1997), were also monitored in the sorted GFP^{high} and GFP^{low} populations. Fgf5, Brachyury and Gata4, early differentiation markers of ectoderm, mesoderm and endoderm, all showed a negative correlation with Nanog, although the degree of alteration was again different for each gene (Figure 6.4 C).

6.3 Cell lines investigated by Solexa analysis

As the above sorted populations provided a good opportunity to investigate further potential genes involved in the switch between $Nanog^{high}$ and $Nanog^{low}$ states, RNA was analysed by Solexa sequencing. In addition cell lines in which the levels of Nanog were genetically manipulated were analysed by Solexa sequencing. Three cell lines were

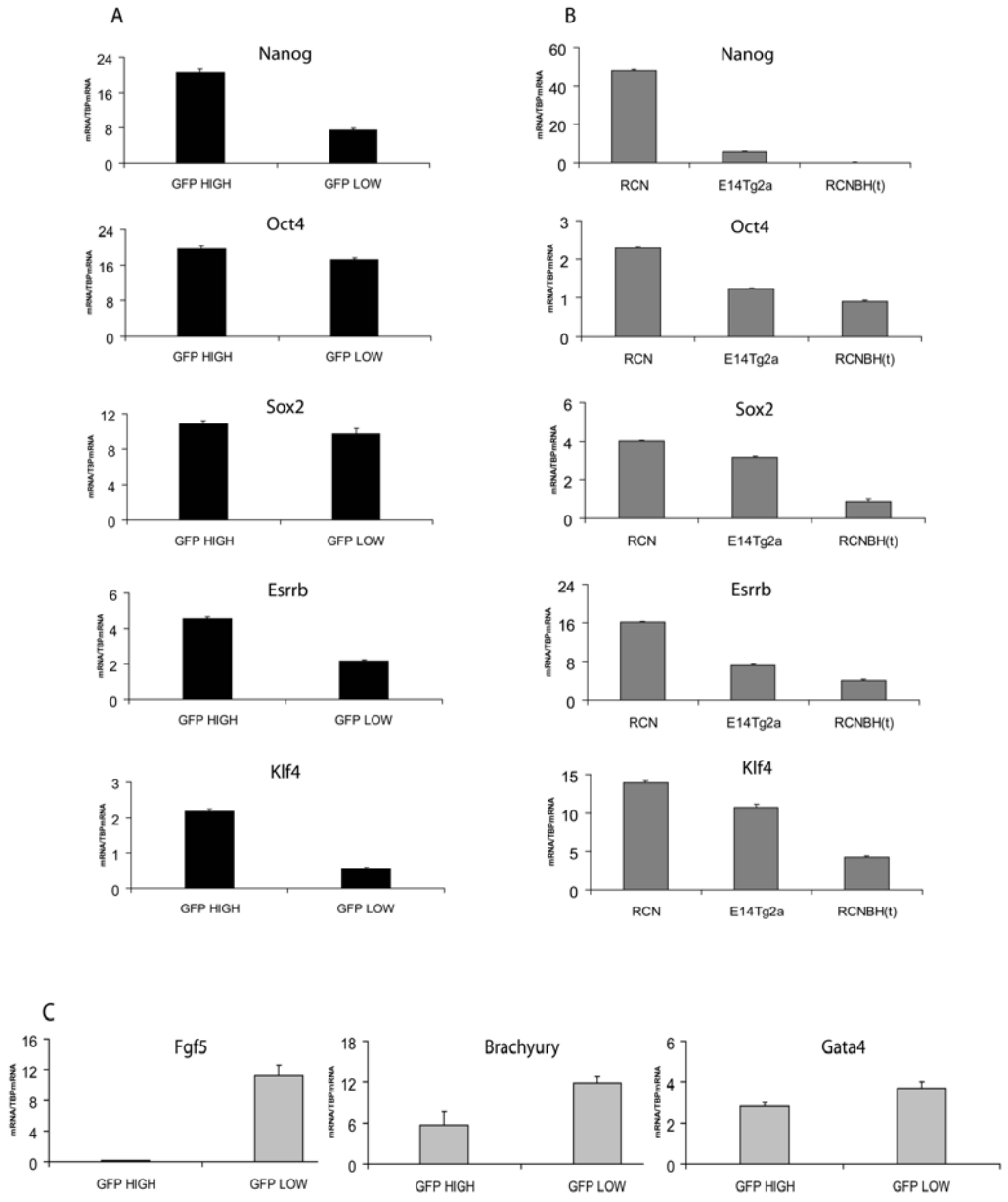

Figure 6.4 Q-PCR analysis

Shown is Q-PCR analysis for Nanog, Oct4, Sox2, Esrrb and Klf4 in sorted $GFP^{high}/SSEA1^{+}$ and $GFP^{low}/SSEA1^{+}$ TNG populations (A) and in cell lines with diverse Nanog levels RCN, E14Tg2a and RCNβH(t) (B). Analysis for Brachyury, Gata4 and FGF5 in sorted $GFP^{high}/SSEA1^{+}$ and $GFP^{low}/SSEA1^{+}$ populations is shown in panel C. mRNA expression was normalised to TBP mRNA expression. Errors bars represent standard deviation of the mean (n=3).

assessed; RCN(t) (Nanog levels comparable to wild type ES cells), EF4 (Nanog overexpressing cells), and RCNβH(t) (Nanog null cells) (Figure 6.5). The origin of the cells and the genetic structure of the Nanog locus is represented in detail in Figure 6.5 and 6.6. In contrast to RCN(t) and RCNβH(t), the Nanog overexpressing cell line EF4 was derived independently, but originated also from the wild type cells E14Tg2a in which a loxP Nanog construct driven by a CAG promoter has been introduced (Figure 6.5 and 6.6).

6.4 Solexa output concept of validation of candidate genes

The Solexa sequencing was performed at the High Throughput Sequencing Facility of the University of Edinburgh and raw data was analysed by Florian Halbritter (Dr. Simon Tomlinson's Group, University of Edinburgh). Subsequently, genes were sorted according to specific criteria. The first lists represent genes which differ in the sorted GFP^{high} and GFP^{low} populations and in which levels correlate with Nanog (Table 6.1 A and B). This pattern of expression suggests that these genes may be targets of Nanog. Yet my interest is in genes that might regulate Nanog rather then being Nanog targets. Therefore two additional lists were created. Genes were selected which were differently expressed in $Nanog^{high}$ and $Nanog^{low}$ sorted cells (cutting point 1.5 fold) and which did not match the same Nanog expression pattern in genetically modified cell lines. Therefore a gene highly expressed in sorted $Nanog^{high}$ cells should not be highly expressed in Nanog overexpressing and Nanog wild type ES cells in comparison to Nanog null cells. This assumption ignores the influence of feedback loops, yet was important to simplify the datasets. Nevertheless genes varying in this way between

A

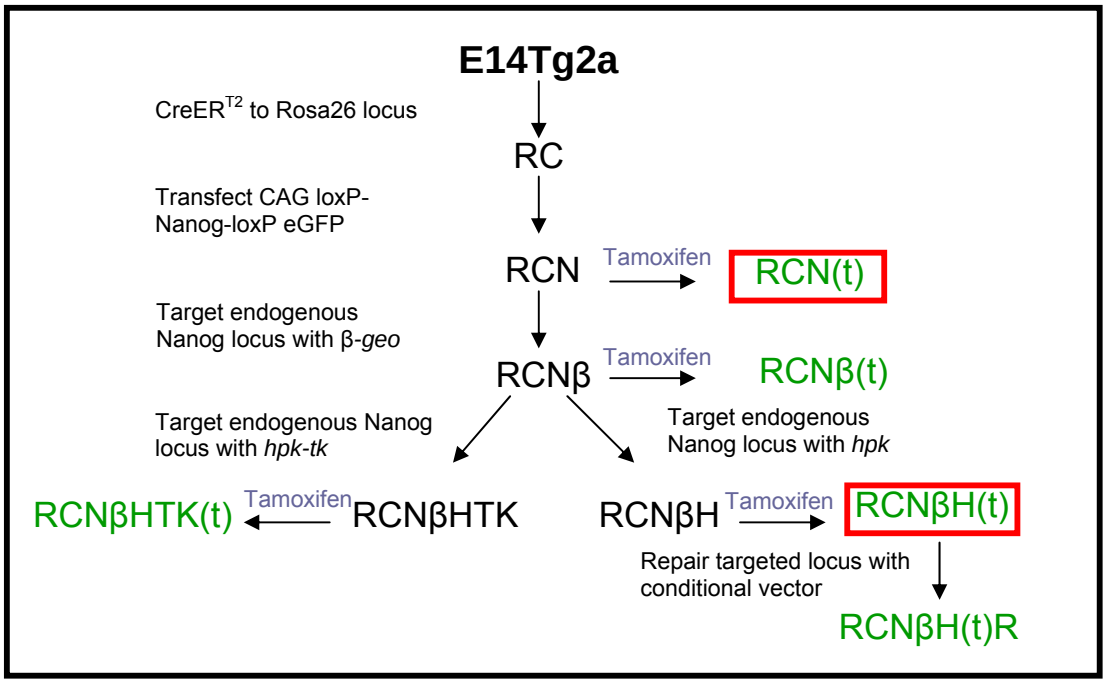

B

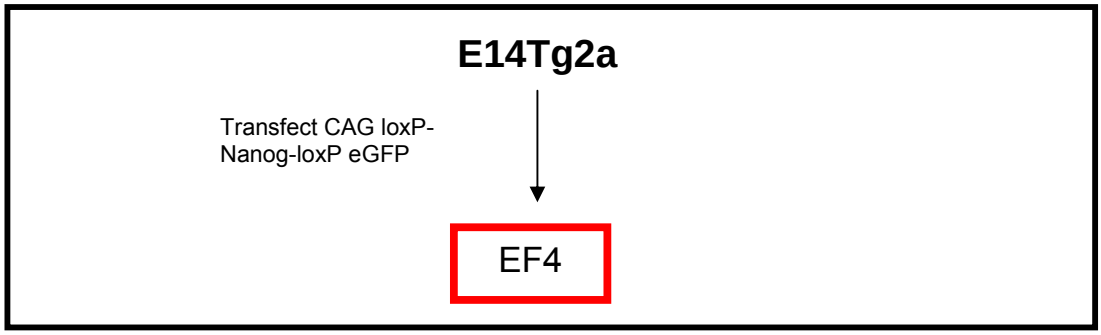

Figure 6.5 Derivation tree of ES cell lines used in the Solexa analysis

A: Derivation tree for RCN(t) and RCNβH(t) cells (red box). (Cre-ER^{T2}) has been initially introduced into E14Tg2a wild type ES cells. RC cells were then transfected with a CAG driven loxP flanked *Nanog* transgene. Activation of Cre recombinase by Tamoxifen led to *Nanog* excision and GFP came under CAG control (shown in green). Two rounds of homologous recombination resulted in cells in which the transgene was the only source of Nanog expression. Tamoxifen treatment led then to a complete deletion of the Nanog sequence.
B: Derivation tree for EF4 cells. A loxP flanked Nanog transgene driven by a CAG promoter was introduced into E14Tg2a cells. (Chambers et al.,2007).

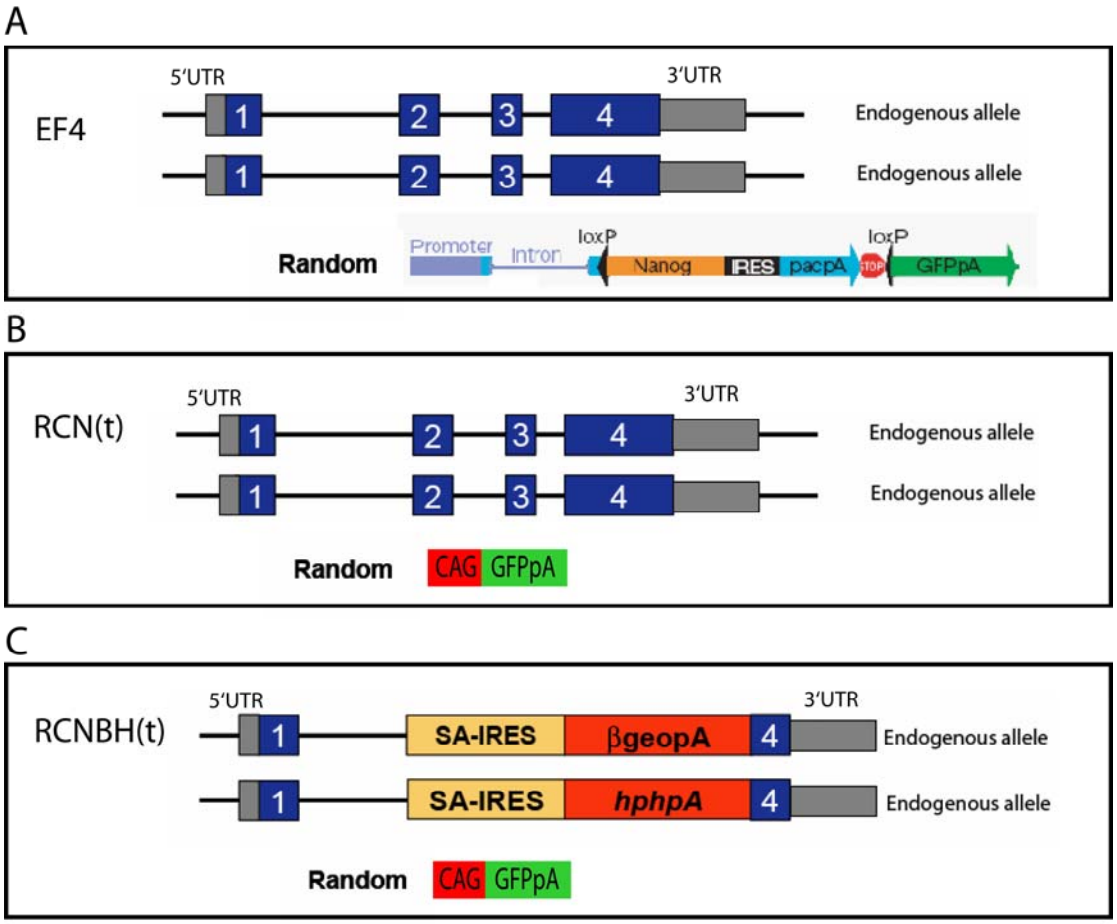

Figure 6.6 Structure of the Nanog locus in genetically modified cell lines

Panel show the two endogenous Nanog alleles. Exons are indicated in blue. The the 5' and 3' UTR regions are indicated in gray.
A: In EF4 (Nanog overexpressing cells) the endogenous Nanog locus is unchanged. These cells however contain a CAG driven loxP-Nanog-loxP-eGFP trangene.
B: In RCN(t) the endogenous Nanog locus is unchanged. RCN cells contained a CAG driven loxP-Nanog-loxP-eGFP transgene. Activation of Cre recombinase by Tamoxifen (t), led to *Nanog* excision and GFP came under CAG control.
C: In RCNβH(t) the two endogenous Nanog alleles have been inactivated with an insertion of a SA-IRES-βgeo-polyA and a SA-IRES-hph-polyA cassette. Treatment with Tamoxifen (t) led to Nanog excision from the CAG driven loxP-Nanog-loxP-eGFP transgene and GFP came under CAG control. (Adopted from Chambers et al., 2007)

A

Name	Stable ID	GFP+	GFP-	EF4	RCN(t)	RCNβH(t)
Spats1	NM_027649	23.26	7.83	74.90	19.76	10.63
Nanog	NM_028016	80.70	15.30	319.61	102.65	25.77
Pgc	NM_025973	93.64	31.39	206.75	80.10	16.80
Inhbb	NM_008381	39.14	9.58	178.03	11.70	1.73
Zc3hav1	NM_028864	162.42	63.10	332.95	76.04	31.07
Gm949	NM_001033446	18.53	6.58	155.91	21.21	5.22
Nmnat3	NM_144533	3.40	0.73	20.53	3.39	1.55
Ampd3	NM_009667	23.84	13.56	90.81	32.57	18.44
Foxn4	NM_148935	43.13	18.10	142.62	10.06	5.42
Ypel2	NM_001005341	11.14	5.85	83.63	24.56	5.45
Ttc9b	NM_028417	19.04	7.11	36.94	6.72	1.55
Mmaa	NM_133823	12.24	7.83	21.55	15.07	7.63
Hormad2	NM_029458	56.19	11.79	85.68	12.54	4.46
Trps1	NM_032000	32.68	10.25	65.32	42.78	24.09
AC154274	ILMN_188518	77.30	23.90	104.29	17.58	8.77
Camk1d	NM_177343	79.34	37.44	103.23	79.29	30.87
Apod	NM_007470	7.05	3.56	31.81	26.11	2.70
Sfrp1	NM_013834	147.33	57.22	321.67	323.32	37.74
Manba	NM_027288	401.35	155.00	519.69	518.48	152.97
Serpinb6c	NM_148942	16.47	1.59	32.33	47.87	4.13
1700016M24Rik	ILMN_220717	3.40	0.73	17.45	25.15	2.85
Krt42	NM_212483	145.89	67.95	73.38	60.12	38.51

B

Name	Stable ID	GFP+	GFP-	EF4	RCN(t)	RCNβH(t)
Tanc2	NM_181071	9.17	16.75	18.47	15.02	67.80
7420416P09Rik	NM_001033776	7.72	80.26	1.51	6.72	15.84
Arl4c	NM_177305	122.91	668.11	27.20	86.00	146.99
Lyrm4	NM_201358	34.03	53.95	9.75	14.42	25.86
Afap1	NM_027373	23.15	59.20	46.69	112.74	321.02
Bdnf	NM_007540	8.48	33.87	0.00	3.37	16.07
Rnf12	NM_011276	101.09	187.21	173.92	443.18	867.13
AC107669.7	ILMN_214306	0.10	0.91	0.37	14.73	29.44
Auts2	NM_177047	22.76	34.55	6.67	7.80	24.19
Ctgf	NM_010217	14.98	120.91	13.35	92.63	198.68
Cyr61	NM_010516	33.37	155.87	19.50	46.73	106.49
Atf3	NM_007498	21.11	59.56	9.24	13.37	24.22
Pkia	NM_008862	5.43	28.80	0.00	1.71	15.89
Dusp6	NM_026268	195.11	599.57	276.52	329.60	615.20
Pdlim4	NM_019417	9.88	15.70	0.62	1.70	26.53
Snai1	NM_011427	5.43	15.67	5.63	6.72	30.06
Camk2d	NM_023813	8.48	29.59	3.62	13.36	25.56
AC102287.16-1	Mm.58847	179.45	273.57	72.34	74.37	166.29
Spsb2	NM_013539	9.82	21.40	0.56	11.70	25.64
Aff3	NM_010678	15.26	63.08	2.06	65.10	148.51
Prex2	NM_029525	22.71	47.35	13.35	19.42	58.82
Dusp4	NM_176933	48.62	230.75	4.11	144.47	241.30

Table 6.1 Genes correlated with Nanog expression

Lists depict genes positively (A) and negatively (B) correlated with Nanog in sorted $GFP^{high}/SSEA1^{+}$ and $GFP^{low}/SSEA1^{+}$ TNG cells and genetically modified cell lines (EF4, RCN(t) and RCNβH(t)). Gene expression is sequence Taq counts quantile normalised

Nanog^{high} and Nanog^{low} cells might affect the switch between these two states. The output of the two designed lists is represented in (Table 6.2 and 6.3). The first list (Table 6.2A) contains genes highly expressed in the Nanog^{high} population of sorted TNG cells. In total 28 genes were identified. Out of this list 8 genes were examined further on the basis of being involved in the pluripotency circuit (Niwa et al., 2009) or showing the lowest correlation with Nanog levels in the genetically modified cells (Table 6.2B). The second list (Table 6.3A) contains genes more highly expressed in the GFP negative compartment of sorted TNG cells. This list shows 24 genes. Eight of those were further investigated on the basis that they showed the lowest correlation to Nanog levels in the genetically modified cell lines (Table 6.3B).

6.5 Candidate genes directly correlated with Nanog in sorted Nanog:GFP populations

To determine whether the genes identified as being positively correlated with Nanog: GFP expression in sorted TNG cells showed a reproducible expression profile, RNAs were analysed by Q-PCR. Sorted GFP^{high} and GFP^{low} TNG cells expressed Nanog appropriately (Figure 6.7), as did EF4, RCN(t) and RCNBH(t) cells (Figure 6.7). Moreover, all the candidate genes showed a similar expression pattern in the sorted Nanog^{high} and Nanog^{low} cells, with the fold changes in individual genes being similar to that observed by Solexa analysis (Figure 6.8). Analysis of the genetically modified cell lines, in general confirmed the Solexa results with the exception of Zfp57. Therefore, all 7 investigated genes were considered as potential effectors of the Nanog switch.

A

Name	Stable ID	GFP+	GFP-	EF4	RCN(t)	RCNβH(t)
Nfatc2ip	NM_010900	430.06	194.35	746.87	181.17	188.43
Id3	NM_008321	190.35	105.22	290.88	11.01	26.31
Tcfcp2l1	NM_023755	365.38	132.32	1002.94	474.75	579.84
Bcl3	NM_033601	404.88	212.22	418.21	116.02	224.73
Aebp2	NM_009556	522.02	338.48	467.36	324.62	449.95
Zfp42	NM_009556	5070.06	1554.75	5023.92	4588.05	5772.52
Ell	NM_007924	127.65	83.06	137.49	66.26	120.77
Brpf3	NM_001081315	148.68	92.29	88.76	71.80	78.30
Mrps31	NM_020560	475.63	297.71	226.26	108.19	187.77
Tbx3	NM_198052	177.24	38.02	473.52	388.30	577.90
Aff1	NM_133919	101.13	45.29	104.14	122.68	154.91
Ncoa3	NM_008679	703.79	390.42	526.87	303.06	561.36
Tcfeb	NM_011549	234.61	150.15	102.60	65.09	101.19
Zfp707	NM_001081065	181.92	119.43	45.15	33.41	43.76
Sirt1	NM_019812	515.89	335.63	451.96	481.42	692.72
Tcfap2c	NM_009335	153.57	71.68	8.74	42.69	44.95
Mlf1ip	NM_027973	115.85	76.67	16.94	44.28	48.58
Mybl2	NM_008652	1673.67	776.48	1300.49	2659.06	3066.73
Zfp553	NM_146201	592.77	342.68	128.78	241.55	317.40
L3mbtl2	NM_145993	270.02	166.52	290.88	421.42	1016.00
Otx2	NM_144841	611.90	407.67	108.76	162.80	302.24
Elf3	NM_007921	247.76	137.15	77.98	139.85	161.14
Zbtb7a	NM_010731	145.40	69.35	41.56	88.18	97.26
Nfkb1	NM_008689	175.89	110.80	103.13	114.71	165.41
Dnajb6	NM_001037941	584.54	299.17	284.74	338.38	664.41
Zfp57	NM_001013745	225.71	100.14	76.45	496.50	510.84
Klf2	NM_008452	1052.56	437.64	326.79	1939.85	3028.73
Trp53	NM_011640	4280.70	2630.45	918.81	2482.32	2925.39

B

Tcfcp2l1	Transcription factor CP2-like protein 1 (CP2-related transcriptional repressor 1)
Zfp42	Zinc finger protein 42 (Zfp-42)(Reduced expression protein 1)(REX-1)(mREX-1)
Tbx3	T-box transcription factor TBX3 (T-box protein 3)
Mybl2	Myb-related protein B (B-Myb)
Dnajb6	DnaJ homolog subfamily B member 6 (Heat shock protein J2)
Zfp57	Zinc finger protein 57 (Zfp-57)
Klf2	Krueppel-like factor 2 (Lung krueppel-like factor)
Trp53	Cellular tumor antigen p53 (Tumor suppressor p53)

Table 6.2 Candidate genes directly correlated with Nanog in sorted Nanog:GFP populations

A: List of genes positively correlated with Nanog in sorted $GFP^{high}/SSEA1^{+}$ and $GFP^{low}/SSEA1^{+}$ TNG cells, but not matching the Nanog expression pattern in genetically modified cell lines. Gene expression is sequence Taq counts quantile normalised. B: List of candidate genes chosen for further validation.

A

Name	Stable ID	GFP+	GFP-	EF4	RCN(t)	RCNβH(t)
Satb1	NM_009122	61.56	160.23	126.72	82.84	28.33
Bbx	NM_027444	62.82	122.30	106.21	99.63	73.60
Trib3	NM_175093	440.29	746.52	331.41	1043.77	273.34
Pou3f1	NM_011141	33.61	460.92	41.04	12.85	12.55
Atf5	NM_030693	638.35	1056.06	42.59	114.87	38.33
Lef1	NM_010703	103.16	180.82	17.45	21.72	13.89
Nsbp1	NM_016710	263.21	481.29	49.77	109.37	71.44
Zfp36	NM_011756	147.08	424.68	113.89	171.92	123.13
Pitx2	NM_011098	5.43	171.37	6.17	46.24	17.08
Notch3	NM_008716	133.02	421.30	29.25	91.46	59.71
Bhlhe40	NM_011498	190.33	344.36	145.19	277.94	189.92
Nfatc4	NM_023699	59.25	130.54	48.74	69.35	44.33
Sox1	NM_009233	20.06	107.71	0.00	33.38	7.02
Hipk1	NM_010432	90.21	147.99	131.85	359.69	339.89
Foxp1	NM_053202	337.46	563.38	25.15	549.84	278.07
Cdkn1c	NM_009876	96.36	291.81	25.15	118.48	78.47
Basp1	NM_027395	420.54	775.11	57.97	246.16	242.11
Ybx2	NM_016875	79.81	121.52	90.82	219.82	214.90
Foxo1	NM_019739	117.47	177.52	60.03	159.39	145.90
Wwtr1	NM_133784	78.55	130.11	36.94	207.96	189.44
Chd9	NM_177224	70.30	182.18	29.25	191.87	148.43
Slc30a9	NM_178651	322.46	594.57	158.01	801.82	682.25
Phf10	NM_024250	175.30	316.34	88.76	369.77	293.51
Pawr	NM_054056	119.84	195.74	29.76	242.00	216.50

B

Satb1	DNA-binding protein SATB1 (Special AT-rich sequence-binding protein 1)
Bbx	HMG box transcription factor BBX (Bobby sox homolog)(HMG box-containing protein 2)
Pou3f1	POU domain, class 3, transcription factor 1 (Octamer-binding transcription factor 6)(Oct-6)
Lef1	Lymphoid enhancer-binding factor 1 (LEF-1)
Zfp36	Tristetraproline (TTP)(Zinc finger protein 36)
Pitx2	Pituitary homeobox 2 (Orthodenticle-like homeobox 2)
Notch3	Neurogenic locus notch homolog protein 3 Precursor (Notch 3)
Nfatc4	nuclear factor of activated T-cells, cytoplasmic, calcineurin-dependent 4

Table 6.3 Candidate genes inversely correlated with Nanog in sorted Nanog:GFP populations

A: List of genes inversely correlated with Nanog in $GFP^{high}/SSEA1^{+}$ and $GFP^{low}/SSEA1^{+}$ TNG cells, but not matching the Nanog expression in genetically modified cell lines. Gene expression is sequence Taq counts quantile normalised. B: List of candidate genes chosen for further validation.

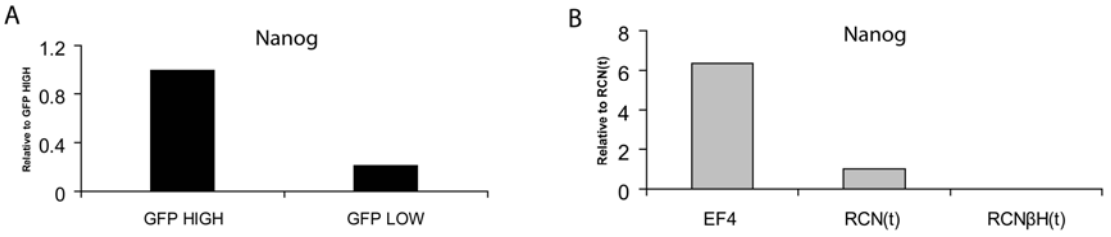

Figure 6.7 Q-PCR analysis for Nanog expression

A: Nanog expression in $GFP^{high}/SSEA1^{+}$ and $GFP^{low}/SSEA1^{+}$ TNG cells. mRNA expression, normalized to TBP mRNA expression, is represented relative to GFP HIGH cells, which are set as 1.
B: Nanog expression in the three genetically modified cell lines EF4 (Nanog overexpressing cells), RCN(t) (express Nanog at wild type levels) and RCNβH(t) cells (Nanog null cells). mRNA expression, normalized to TBP mRNA expression, is represented relative to RCN(t) cells, which are set as 1. Shown is the average of two biological replicates.

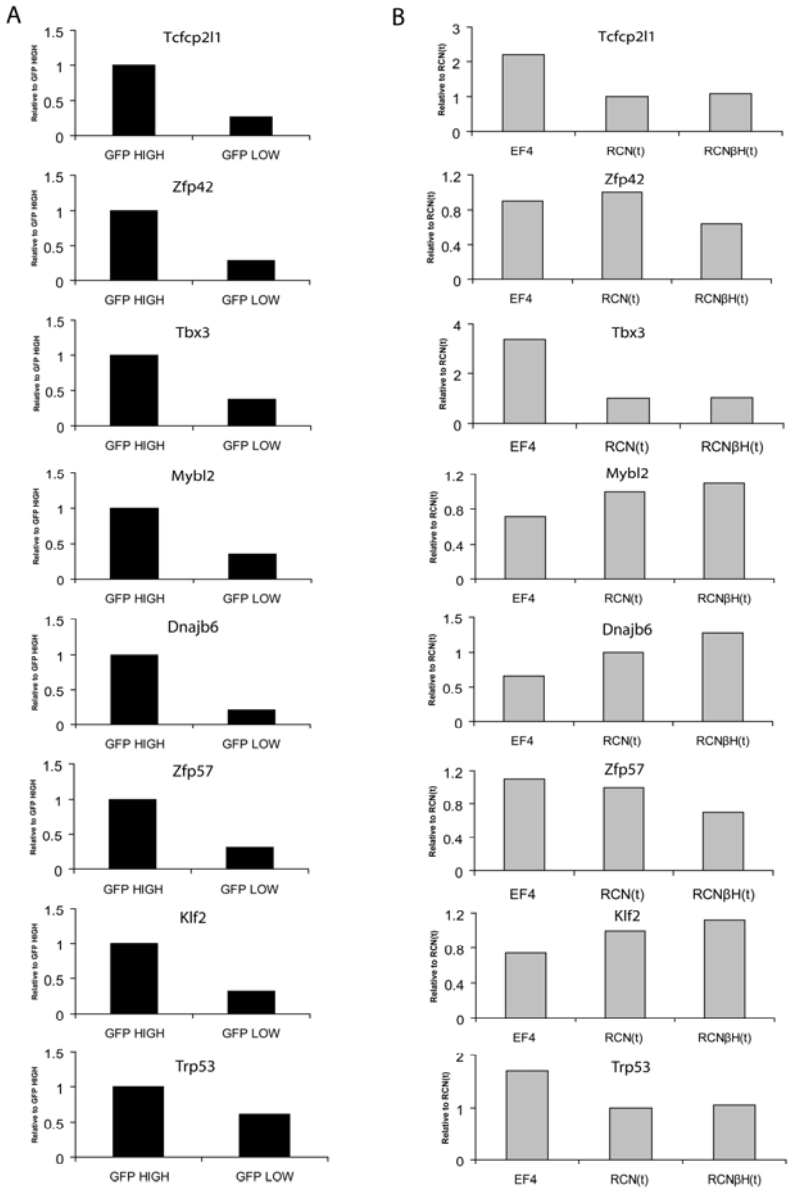

Figure 6.8 Q-PCR analysis for candidate genes directly correlated with Nanog in sorted GFP^{high} and GFP^{low} cells

A: Expression of candidate genes in GFP^{high}/SSEA1^{+} and GFP^{low}/SSEA1^{+} TNG cells. mRNA expression, normalized to TBP mRNA expression, is represented relative to GFP HIGH cells, which are set as 1.
B: Expression of candidate genes in genetically modified cell lines. mRNA expression, normalized to TBP mRNA expression, is represented relative to RCN(t) cells, which are set as 1. Shown is the average of two biological replicates.

6.6 Candidate genes inversely correlated with Nanog in sorted Nanog:GFP populations

Similar analysis were performed on genes that showed an inverted correlation with Nanog in sorted GFP populations (Figure 6.9). The analysis of the sorted populations confirmed the Solexa results and showed differences in magnitude in gene expression between these populations similar to those obtained by Solexa. Expression was subsequently also analysed in the genetically modified cell lines (Figure 6.9). Although the pattern of expression did not match that obtained by Solexa analysis none of the 8 genes showed an expression pattern mining Nanog expression.

6.7 Fluidigm analysis

The above experiments identified genes that could potentially influence fluctuations in Nanog expression. However, these analyses were performed on cell populations. As it would be of future interest to examine gene expression in single cells I decided to investigate the utility of the integrated fluidic circuit chip (IFC) architecture (Fluidigm) for genetic analysis of heterogeneity of Nanog expression. In the first analysis three samples containing each 1000 cells of the $GFP^{high}/SSEA1^{+}$ and GFP^{low} $/SSEA1^{+}$ TNG compartment were sorted and amplified as described in Material and Methods. This analysis confirmed the previously observed differences regarding the gene expression in the sorted populations for Nanog only (Figure 6.10) and for the candidate genes (Figure 6.11 and 6.12). This confirms the utility of the microfluidic system; however, further work will be required to optimise this system, as Satb1 expression could not be detected (Figure 3.12), and to assess the ability to measure gene expression in single cells.

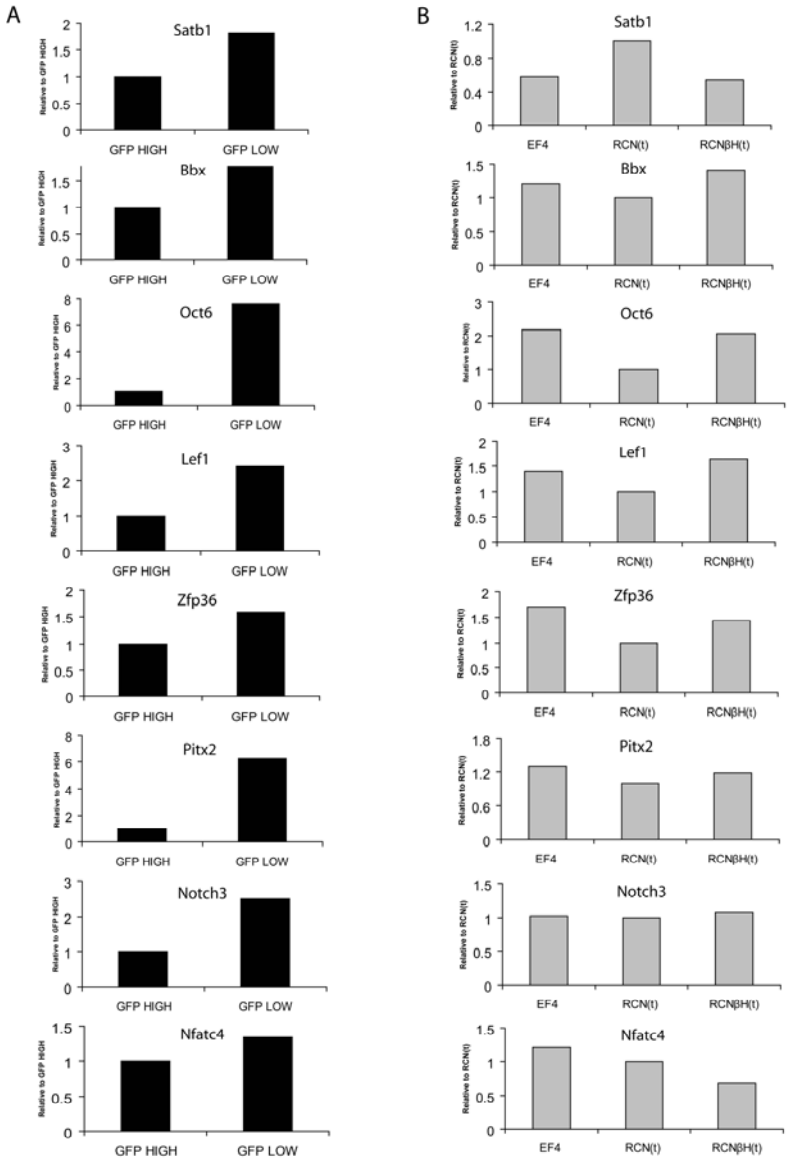

Figure 6.9 Q-PCR analysis for candidate genes inversely correlated with Nanog in sorted GFP^{high} and GFP^{low} cells

A: Expression of candidate genes in GFP^{high}/SSEA1^{+} and GFP^{low}/SSEA1^{+} TNG cells. mRNA expression, normalized to TBP mRNA expression, is represented relative to GFP HIGH cells, which are set as 1.
B: Expression in genetically modified cell lines. mRNA expression, normalized to TBP mRNA expression, is represented relative to RCN(t) cells, which are set as 1. Shown is the average of two biological replicates.

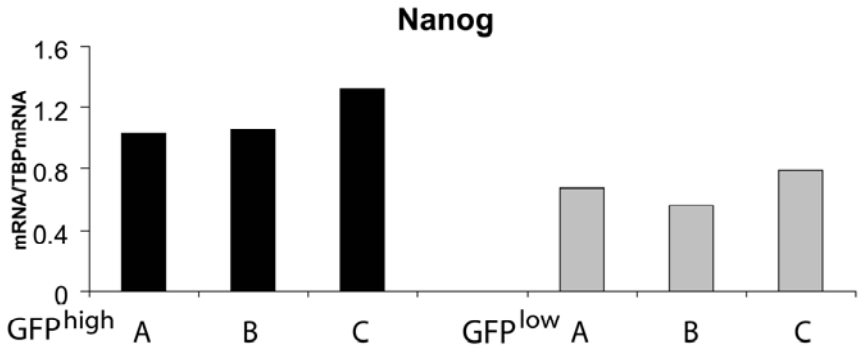

Figure 6.10 Fluidigm analysis for Nanog in 1000 GFP^{high} and GFP^{low} cells

Figure shows Nanog expression in three sets (A,B,C) of each 1000 sorted GFP^{high}/SSEA1^{+} (black) and 1000 sorted GFP^{low}/SSEA1^{+} (grey) cells. mRNA expression was normalized to TBP mRNA expression.

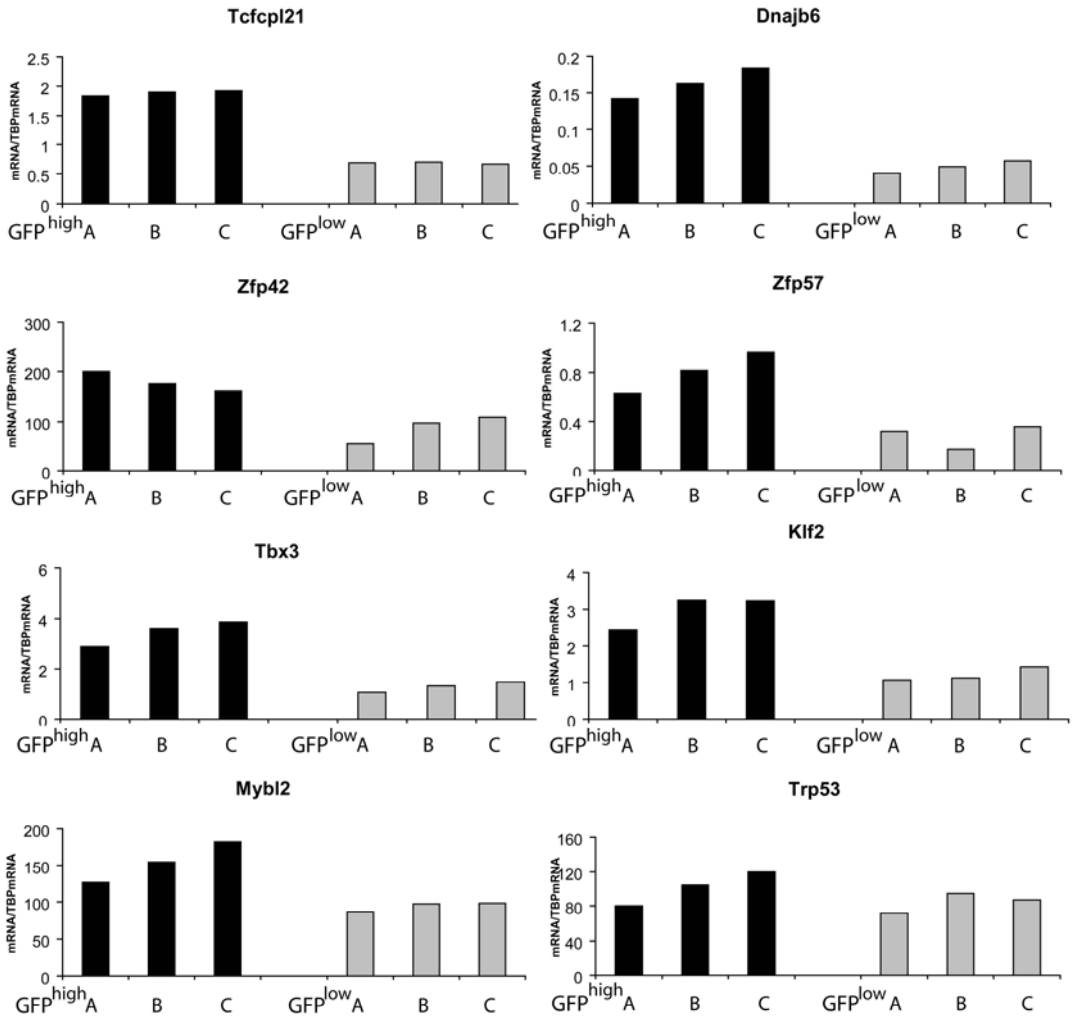

Figure 6.11 Fluidigm analysis for candidate genes directly correlated with Nanog in sorted GFP^{high} and GFP^{low} cells

Figure shows candidate gene expression in three sets (A,B,C) of each 1000 sorted GFP^{high}/SSEA1^{+} (black) and 1000 sorted GFP^{low}/SSEA1^{+} (grey) cells. mRNA expression was normalized to TBP mRNA expression.

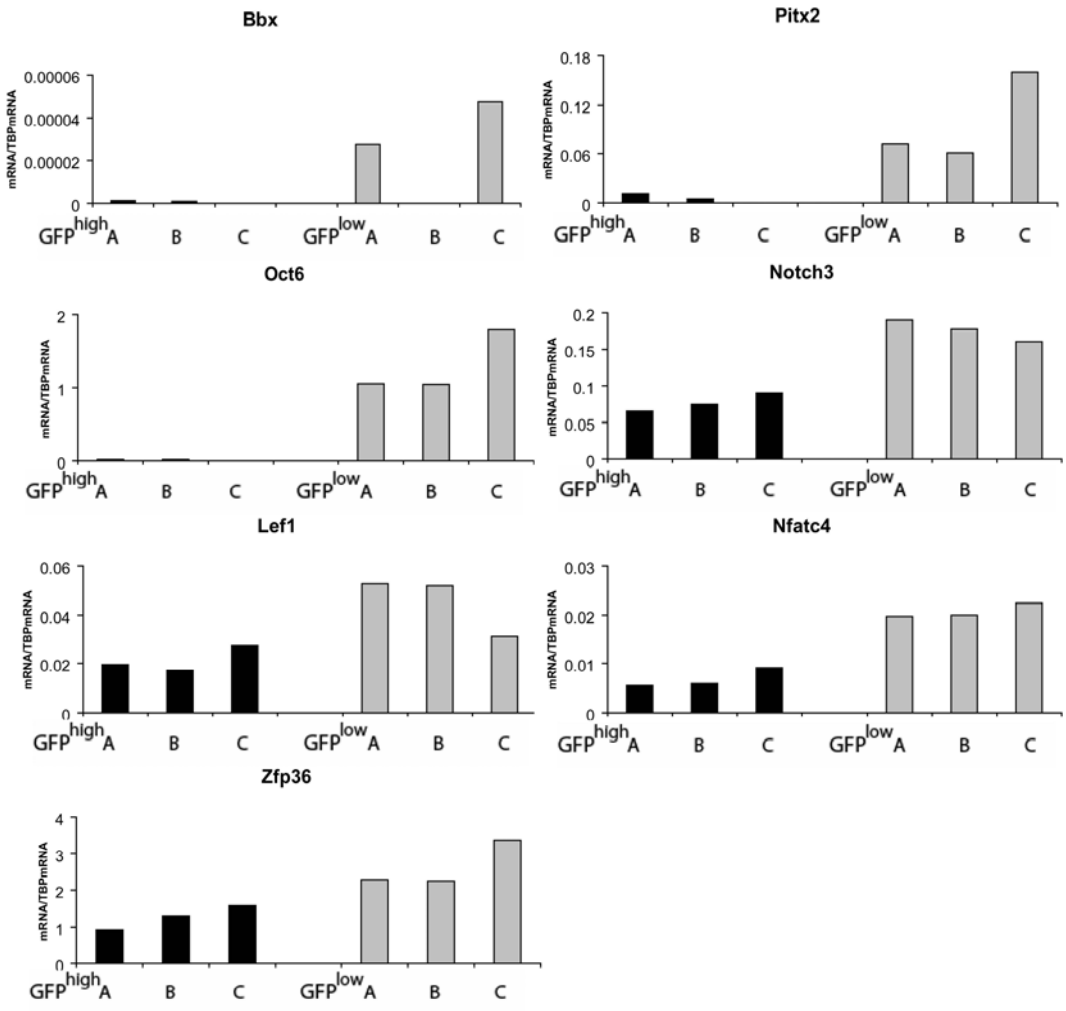

Figure 6.12 Fluidigm analysis for candidate genes inversely correlated with Nanog in sorted GFP^{high} and GFP^{low} cells

Figure shows Nanog expression in three sets (A,B,C) of each 1000 sorted GFP^{high}/SSEA1^{+} (black) and 1000 sorted GFP^{low}/SSEA1^{+} (grey) cells. mRNA expression was normalized to TBP mRNA expression.

6.8 Discussion

In this chapter I have investigated gene expression in sorted Nanog^{high} and Nanog^{low} cells as well as in cells genetically modified for Nanog expression using Solexa Sequencing. The most straight forward output from these analyses was a list of genes showing direct or inverse correlation with Nanog in all cells. Such genes could represent targets of Nanog. In contrast, genes which were either directly or inversely correlated with Nanog in Nanog^{high} and Nanog^{low} cells, but which did not show the same expression pattern in genetically modified cell lines, might represent potential candidate regulators of *Nanog* heterogeneity. This identified 28 genes showing positive correlation and 24 showing a negative correlation. Eight candidate genes from the two lists (Table 6.2 A and B and Table 6.3 A and B) were examined further on the basis of the fact that they were previously hypothesised to be involved in the pluripotency circuit (Niwa et al., 2009) or showing the lowest correlation with Nanog levels in the genetically modified cells. Interestingly, several genes reported to influence Nanog expression, as Klf2 (Hall et al., 2009), p53 (Lin, 2005) or Satb1 (Savarese et al., 2009) appeared on my lists. Out of the 16 candidate genes two genes appear of particular interest.

Satb1 is expressed at higher levels in Nanog:GFP^{low} cells than in Nanog:GFP^{high} cells. Satb1 has been reported to organize chromatin into loops by periodic anchoring to the nuclear matrix. Satb1 also suppresses genes by histone deacetylation and nucleosome remodeling through interaction with chromatin modifiers (Kumar et al., 2006). Furthermore, Satb1$^{-/-}$ ES cultures contain large numbers of Nanog^{high} cells, suggesting

that Satb1 expression in Nanog^{low} cells is not directly responsible for switching the cells back to a Nanog^{high} state. However Satb1$^{-/-}$ ES cells have elevated expression of Satb2 and Satb2 overexpression has been reported to antagonize differentiation-associated silencing of Nanog. As Satb1 and Satb2 both bind *Nanog* a balance between Satb1 and Satb2 may affect *Nanog* expression (Savarese et al., 2009).

The second interesting gene is Oct6. However little is known about the function of Oct6 in ES cells. Interestingly, Oct6 was reported to suppress Rex1 when highly expressed in ES cells (Ben-Shushan et al., 1998). Ben-Shushan et al., reported that Oct6 represses *Rex-1* via the octamer site. My data revealed that Oct6 is almost exclusively expressed in the Nanog^{low} population. It would therefore be important to investigate the role of Oct6 in controlling Nanog levels and in addition, to determine how expression of Oct4 target genes changes upon modulation of Oct6 levels, as Oct6 might antagonise the activity of Oct4 in ES cells.

Further examination of these genes would be of interest. Immonufluorescence would be of use in determing whether levels of proteins reflected the observed differential transcript expression.

Importantly analysis at the single cell level is important to define the precise relationship between Nanog heterogeneity and the timing of increase or downregulation of genes of interest. For example, if a gene is involved in the switch it should be expressed before GFP expression, if sorted Nanog;GFP^{low} cells will begin switching to GFP^{high}.

However, to confirm whether a particular gene has a role in regulating the switch in *Nanog* gene expression would require additional functional analysis. This could be obtained by fusing the protein of interest to a destabilizing domain (DD) that is rapidly and constitutively degraded in the absence of a synthetic ligand (Banaszynski et al., 2006). Alternatively, relocalisation of a protein-of interest-ERT2 fusion to the nucleus in a tamoxifen-dependent manner could also be used to alter the activity level of a protein of interest. Varying such levels would define the directionality of their function.

Chapter 7

Concluding remarks and future directions

Nanog is a critical homeodomain protein responsible for establishing embryonic stem cell pluripotency. Although its heterogenous expression pattern has caught scientific attention (Chambers et al., 2007; Kalmar et al., 2009; Singh et al., 2007), the particular mechanisms responsible for generating this heterogeneity are unknown.

Experiments presented in this thesis demonstrated that a potential origin of Nanog heterogeneity lies within the intrinsic circuitry of the pluripotency gene regulatory network centred around Oct4/Sox2 and Nanog.

7.1 Oct4 influence Nanog heterogeneity

In detail, it was shown that independent Oct4 heterozygote ES cell lines express elevated levels of Nanog mRNA and protein. This general increase in protein and mRNA expression was attributed to a reduction in Nanog heterogeneity resulting in cells mainly expressing Nanog at high levels (Chapter 3). In addition, the functional Oct4 heterozygote ES cells showed a more homogeneous expression pattern for other transcription factors as Rex1 and Esrrb. This was of interest, as these genes were previously described to have a heterogeneous expression pattern in ES cells. Toyooka et al., identified at least two different populations regarding Rex1 expression, a $Rex1^{+}/Oct4^{+}$ and a $Rex1^{-}/Oct4^{+}$ population (Toyooka et al., 2008). They showed that $Rex1^{+}/Oct4^{+}$ and $Rex1^{-}/Oct4^{+}$ cells not only had the ability to convert into each other,

but also had different gene expression patterns and diverse differentiation abilities. In addition, van den Berg et al., showed that Esrrb expression resembles Nanog's mosaic expression pattern in mouse ES cells (van den Berg et al., 2008). They demonstrated that Esrrb binds to the *Nanog* promoter if Oct4 is bound to the Oct4/Sox2 element to activate *Nanog* expression (van den Berg et al., 2008). Yet as Nanog may activate Esrrb (Loh et al., 2006), the relationship between these two genes might have a more complicated conduct. In addition to Esrrb and Rex1, gene heterogeneity was also described for Hex (Canham et al., 2009) and Stella (Hayashi et al., 2008). Interestingly the low appearance in expression of Stella high cells (30%) (Hayashi et al., 2008) in comparison to Nanog high cells (80%) (Chambers et al., 2007) suggests, that the Nanog positive compartment is heterogeneous in itself (Hayashi et al., 2008).

Importantly, as shown in Chapter 3, Nanog mosaicism can be induced by simply restoring the levels of Oct4 in functional Oct4 heterozygote ES cells confirming that the reduction in Nanog heterogeneity is not due to other unrelated genetic modifications. Furthermore, after separation of ZHTNG cells into GFP^{high} and GFP^{low} cells it was demonstrated that high GFP expression is restorable in the GFP^{low} population by addition of Doxycycline. This indicates that the magnitude of Nanog heterogeneity is a consequence of variations in Oct4 levels and can be manipulated in both directions.

In this context and in contradiction to the previously suggested linear relationship between Nanog and Oct4, as indicated in several Luciferase reporter assays (Rodda et al., 2005, Kuroda et al., 2005) and colocalisation studies by ChIP (Boyer et al., 2005; Chen et al., 2008; Kim et al., 2008; Loh et al., 2006), neither the upregulation nor the

downregulation of Oct4 was accompanied by a linear up- or downregulation of Nanog (Chapter 3).

These experiments indicate therefore that Oct4 directly or indirectly suppresses Nanog at high levels and that changes in the expression pattern for other transcription factors as Rex1 and Esrrb might be subject to a similar regulatory mechanism.

In this context the POU family of transcription factors were reported to be capable of acting as transcriptional activators and as suppressors (Liu and Roberts, 1996; Monuki et al., 1993; Welter et al., 1996). In addition Oct4 itself was suggested to have a dual character. Ben-Shushan et al., showed that exogenous Oct4 can repress *Rex1* expression in F9 cells and activates the *Rex1* promoter in P19/RA cells, in which expression of Oct-3/4 is not detectable (Ben-Shushan et al., 1998; Okamoto et al., 1990). These results indicated that the exact levels of Oct4 are critical with respect to whether Oct4 activates or inhibits the *Rex1* promoter (Ben-Shushan et al., 1998).

A second investigation based on Luciferase reporter assays indicated that Oct4 regulates *Nanog* biphasically (Pan, 2006). The authors suggested that Oct4 activates *Nanog* expression at steady-state concentrations and suppresses it above steady state levels. Although these experiments were based exclusively on artificial reporter constructs driven by Luciferase and no further data regarding the action of Oct4 on the endogenous Nanog was provided, these findings are interesting in light of the results represented in this thesis. As shown in Chapter 3, Nanog and Oct4 expression correlated initially positively, when Oct4 was only slightly upregulated. An upregulation at or above wild type levels in ZHTNG cells however induced a strong downregulation of Nanog.

To unravel the direct action of Oct4 on the endogenous *Nanog,* the effects of mutating the Oct4 site in the context of a TNG allele have been investigated in Chapter 5. This was of importance as evidence in support of the action of Oct4 on the endogenous *Nanog* gene is lacking in literature. The experiments performed in Chapter 5 showed however that the deletion of the Oct4 binding site leads to a strong decrease in Nanog expression, similarly to mutagenesis experiments in Luciferase assays (Kuroda, 2005; Pan, 2006; Rodda et al., 2005). Yet, as discussed in section 5.3, it can not be excluded that Oct4 suppressive activity acts directly from a different binding site, especially as a further binding site is described by ChIP for Oct4 at the *Nanog* enhancer region (Levasseur et al., 2008). Additionally the experiments performed in this thesis might be insufficient to exclude a direct suppressive activity of Oct4 from the proximal Oct4 binding site above wild type levels. To investigate this more thoroughly a mutation of this Oct4 binding site should be performed in ZHTc6 cells, in which the expression levels of Oct4 can be upregulated, as discussed in detail in section 5.3.

As it is also possible that the suppressive activity of Oct4 is indirect, further molecules should be examined in future. In particular, as already discussed in section 3.3, the two other members of the regulatory circuit Sox2 and Nanog should be investigated in more detail. This is of particular interest for Nanog, as the mutagenesis experiments presented in Chapter 5 identified Oct4 as a positive activator of Nanog. In addition the kinetic data, (Figure 3.12) and the data featuring the downregulation of Oct4 (Figure 3.13) unraveled a potential suppressive activity from Nanog on *Nanog*.

In addition, it would be important to investigate the role of other signalling pathways associated with Nanog and Oct4. The Wnt signalling pathway for example has been implicated to play a role in self-renewal of mouse ES cells (Doble et al., 2007; Sato et al., 2004). In support of this, Takao et al., reported that β-catenin promotes pluripotency by forming a complex with Oct4 that drives Nanog expression (Takao et al., 2007). Also, some evidence was presented that downregulation of Oct4 increases β-catenin protein levels (Abu-Remaileh et al., 2010). Referring to the data represented here, it would be important to further elucidate the role of Wnt signalling on Nanog heterogeneity by manipulating the Wnt signalling output and to define if levels of β-catenin are increased in functional Oct4 heterozygote ES cells due to a downregulation of Oct4. Furthermore, the secreted frizzled-related protein 1 (SFRP1), a potential Wnt antagonist (Finch et al., 1997; Katoh and Katoh, 2006; Uren et al., 2000) is correlated with Nanog, as presented in Chapter 6 (Table 6.1 A). Hence, it would be important to test the effect of SFRP1 on Nanog heterogeneity and to define if the induction of SFRP1 is caused by Nanog.

Second, Oct4's suppressive activity is possibly mediated via the FGF/Erk signaling pathway. It is reported that a synergistic interaction between Oct4 and Sox2 on the FGF-4 enhancer drives the expression of FGF4 (Ambrosetti et al., 1997). Also, Nanog is upregulated in the presence of inhibitors of the MAP kinase/ERK pathway (Hamazaki et al., 2006; Kunath et al., 2007). Therefore it would be important to define, if an increase in Oct4 is indeed associated with an augmented activity of the ERK signaling pathway.

On the other hand the action of these inhibitors is incompletely understood. Therefore a detailed investigation of the expression levels of Oct4 in cultures treated with inhibitors should be performed. Such an experiment would define if under such culture conditions a reduction of Nanog heterogeneity associates with different expression levels of Oct4. Therefore a connection between the data represented in this thesis to the ground state theory (Silva et al., 2009) will be of importance in future experiments.

In addition to the described interaction between Nanog and Oct4, the analysis of gene expression in cells sorted according to Nanog levels and in genetically modified ES cell lines (Chapter 6), provides a good source for further potential candidate genes involved in the regulatory mechanisms responsible for the switch in Nanog expression. The direct effects of those genes on *Nanog* should be tested in future experiments.

7.2 Changes in Nanog heterogeneity influence cell fate decisions

The levels of Oct4 (Niwa et al., 2000) and Nanog were sufficiently shown to be particularly critical for the cell fate (Chambers et al., 2003; Chambers et al., 2007; Mitsui et al., 2003; Silva et al., 2009; Suzuki et al., 2006; Ying et al., 2003). More importantly in the context of this thesis Chambers et al., showed that sorted $GFP^{low}/SSEA1^{+}$ lost SSEA1 expression faster than the $GFP^{high}/SSEA1^{+}$cells (Chambers et al., 2007). Their investigation was however limited to SSEA1 expression and no direct differentiation protocols were performed on either of these populations.

The results represented in Chapter 4 showed in addition to this data that functional Oct4 heterozygote cells are retarded in their differentiation kinetics compared to wild type ES

cells in LIF withdrawal and neural conditions. These findings are consistent with the model presented by Chambers et al., in which low levels of Nanog constitute a window of opportunity for commitment decisions (Chambers et al., 2007), as the Nanog low compartment is underrepresented in functional Oct4 heterozygote ES cells. Importantly restoring Nanog heterogeneity in functional Oct4 heterozygote ES cells by transiently increasing the levels of Oct4 re-established their differentiation potential (Chapter 4). This observation also de-mystified the previous report by Niwa stating that an increase in Oct4 can cause differentiation (Niwa et al., 2000), as Oct4 acts primary by providing a population of Nanog low cells responsive to differentiation cues. As the functional Oct4 heterozygote ES cells provide a unique opportunity to investigate consequences associated with the dynamic range of Nanog heterogeneity, future experiments could investigate their potential in further differentiation protocols. Also such experiments could help to define more precisely the differences in differentiation timings associated with diverse states of Nanog heterogeneity.

7.3 Theoretical models and heterogeneity

This thesis identified Oct4 as an important player in inducing fluctuations in Nanog expression. The finding that a decrease only about 40-50% of wild type levels of Oct4 can shift the heterogenous pattern of Nanog in an ES cell population will enable more exact modelling of Nanog heterogeneity in the context of the Oct4/Sox2/Nanog regulatory network, something that has so far been limited due to the lack of experimental data. Several attempts in the last years were performed to theoretically

unravel the sources of this heterogenous behaviour. Most recently, Glauche et al., presented a model with two fundamentally different mechanisms to explain Nanog variations (Glauche et al., 2010). This is interesting, as it combines two fundamentally different biological concepts. The oscillation scenario, which describes the transitions between $Nanog^{high}$ and $Nanog^{low}$ cells as a consequence of a deterministic system behaviour (Strohman, 1997) and a noise driven, stochastic model (Elowitz et al., 2002; Kaern et al., 2005; Ozbudak et al., 2002; Swain et al., 2002). Deterministic system behaviour, which has dominated thinking about cellular organization for a long time, describes cell fate as being generally determined by tightly controlled regulatory mechanisms (Huang, 2010). Noise however, which can be further divided into intrinsic and extrinsic noise, is defined as the empirical measure of stochasticity, therefore random events (Elowitz et al., 2002; Shahrezaei and Swain, 2008; Swain et al., 2002). This theoretical data represented by Glauche et al., indicated that the interplay between deterministic transcriptional interactions and noise might be important elements of pluripotency, as both scenarios were able to explain the existing data on Nanog heterogeneity. A similar conclusion can be drawn from the model represented by Kalmar et al., who proposed an excitable system that produces noise-induced transient excursion from a $Nanog^{high}$ state (Kalmar et al., 2009). In addition they proposed, similar to Glauche et al., a negative feedback on Nanog. The authors attributed this finding to high levels of Oct4 based on published luciferase data (Pan, 2006). Considering the data represented in this thesis such could indeed be attributed directly or indirectly to high levels of Oct4. In this context attention should be paid to the fact that Oct4, despite being generally homogenously expressed in ES cells, does show variations in protein

expression on a single cell level (Figure 3.3 and 6.1). Due to the fact that only a slight downregulation of Oct4 in Oct4 functional heterozygote ES cells can influence the magnitude of Nanog heterogeneity, these variations appear to have significant consequences. Therefore it would be further important to determine, if the origin of the variations of Oct4 levels lies within the intrinsic circuitry of the pluripotency gene regulatory network centered around Oct4/Sox2 and Nanog and how intrinsic or extrinsic noise contributes to its development.

Similarly to observations made in the context of stochasticity in gene expression, the reduction of heterogeneity in Oct4 functional heterozygote ES cells however might not necessary be advantageous. In this context studies performed by (Kussell and Leibler, 2005; Thattai and van Oudenaarden, 2004; Wolf et al., 2005), indicate that maintaining stochasticity could be advantagous especially for organisms that need to adapt quickly to sudden changes in environmental conditions. Therefore switching between different phenotypes might be an important factor for persistent bacterial infections after treatment with antibiotics (Balaban et al., 2004). In addition, increased stochasticity in gene expression increases the survival capacity of yeast after sudden stress induction (Blake et al., 2006). In regard to the functional data represented in Chapter 5, the functional Oct4 heterozygote ES cells, which express Nanog more homogenously and which therefore appear to be captured mainly in the $Nanog^{high}$ expressing state, are retarded in their differentiation capacity compared to cells expressing Nanog heterogeneously. A delay in reaction to particular enviromental changes as shown in Chapter 5 in the LIF withdrawal and neural differentiation protocol, could have therefore

significance in the embryo. Such a shift in favour of the self-renewing compartment could be accompanied with the loss of one of the main attributes of an ES cell, the ability to generate effectively tissues of all three germ layers. More generally, the shift in favour of self-renewal due to a reduction in heterogeneity is also interesting in the context that increased stochasticity has been connected to aging (Bahar et al., 2006; Busuttil et al., 2007)

In summary the data represented in this thesis could be helpful in unravelling the relationship between the intrinsic circuit centered around Oct4/Sox2 and Nanog more precisely and to connect this knowledge to the general concept of gene heterogeneity observed in ES cells. However to explore this further, it will be important to visualize the expression of Oct4 and Nanog directly with fluorescence reporters, as only in this way the exact kinetics can be observed dynamically on the single cell level.

References

Abu-Remaileh, M., Gerson, A., Farago, M., Nathan, G., Alkalay, I., Zins Rousso, S., Gur, M., Fainsod, A., and Bergman, Y. (2010). Oct-3/4 regulates stem cell identity and cell fate decisions by modulating Wnt/β-catenin signalling. EMBO J *29*, 3236-3248.

Ambrosetti, D.-C., Basilico, C., and Dailey, L. (1997). Synergistic activation of the fibroblast growth factor 4 enhancer by sox2 and oct-3 depends on protein-protein interactions facilitated by a specific spatial arrangement of factor binding sites. MCB *17*, 6321-6329.

Andrews, P. W. (2002). From teratocarcinomas to embryonic stem cells. Philos Trans R Soc Lond B Biol Sci *357*, 405-417.

Andrews, P. W., Bronson, D. L., Benham, F., Strickland, S., and Knowles, B. B. (1980). A comparative study of eight cell lines derived from human testicular teratocarcinoma. Int J Cancer *26*, 269-280.

Andrews, P. W., Damjanov, I., Simon, D., Banting, G. S., Carlin, C., Dracopoli, N. C., and Fogh, J. (1984). Pluripotent embryonal carcinoma clones derived from the human teratocarcinoma cell line Tera-2. Differentiation in vivo and in vitro. Lab Invest *50*, 147-162.

Andrews, P. W., Goodfellow, P. N., Shevinsky, L. H., Bronson, D. L., and Knowles, B. B. (1982). Cell-surface antigens of a clonal human embryonal carcinoma cell line: morphological and antigenic differentiation in culture. Int J Cancer *29*, 523-531.

Avilion, A. A., Nicolis, S. K., Pevny, L. H., Perez, L., Vivian, N., and Lovell-Badge, R. (2003). Multipotent cell lineages in early mouse development depend on SOX2 function. Genes Dev *17*, 126-140.

Bahar, R., Hartmann, C. H., Rodriguez, K. A., Denny, A. D., Busuttil, R. A., Dolle, M. E., Calder, R. B., Chisholm, G. B., Pollock, B. H., Klein, C. A., and Vijg, J. (2006). Increased cell-to-cell variation in gene expression in ageing mouse heart. Nature *441*, 1011-1014.

Balaban, N. Q., Merrin, J., Chait, R., Kowalik, L., and Leibler, S. (2004). Bacterial persistence as a phenotypic switch. Science *305*, 1622-1625.

Banaszynski, L. A., Chen, L. C., Maynard-Smith, L. A., Ooi, A. G., and Wandless, T. J. (2006). A rapid, reversible, and tunable method to regulate protein function in living cells using synthetic small molecules. Cell *126*, 995-1004.

Beddington, R. S., and Robertson, E.J. (1999). Axis development and early asymmetry in mammals. Cell *96*, 195-209.

Beddington, R. S. P., and Robertson, E. J. (1989). An assessment of the developmental potential of embryonic stem cells in the midgestation mouse embryo. Development *105*, 733-737.

Ben-Shushan, E., Thompson, J. R., Gudas, L. J., and Bergman, Y. (1998). *Rex-1*, a gene encoding a transcription factor expressed in the early embryo, is regulated via Oct-3/4 and Oct-6 binding to an octamer site and a novel protein, Rox-1, binding to an adjacent site. MCB *18*, 1666-1878.

Berstine, E. G., Hooper, M. L., Grandchamp, S., and Ephrussi, B. (1973). Alkaline phosphatase activity in mouse teratoma. Proc Natl Acad Sci U S A *70*, 3899-3903.

Blake, W. J., Balazsi, G., Kohanski, M. A., Isaacs, F. J., Murphy, K. F., Kuang, Y., Cantor, C. R., Walt, D. R., and Collins, J. J. (2006). Phenotypic consequences of promoter-mediated transcriptional noise. Mol Cell *24*, 853-865.

Boyer, L. A., Lee, T. I., Cole, M. F., Johnstone, S. E., Levine, S. S., Zucker, J. P., Guenther, M. G., Kumar, R. M., Murray, H. L., Jenner, R. G., *et al.* (2005). Core transcriptional regulatory circuitry in human embryonic stem cells. Cell *122*, 947-956.

Bradley, A., Evans, M. J., Kaufman, M. H., and Robertson, E. (1984). Formation of germ-line chimaeras from embryo-derived teratocarcinoma cell lines. Nature *309*, 255-256.

Brinster, R. L. (1974). The effect of cells transferred into the mouse blastocyst on subsequent development. J Exp Med *140*, 1049-1056.

Brons, I. G., Smithers, L. E., Trotter, M. W., Rugg-Gunn, P., Sun, B., Chuva de Sousa Lopes, S. M., Howlett, S. K., Clarkson, A., Ahrlund-Richter, L., Pedersen, R. A., and Vallier, L. (2007). Derivation of pluripotent epiblast stem cells from mammalian embryos. Nature *448*, 191-195.

Burdon, T., Stracey, C., Chambers, I., Nichols, J., and Smith, A. (1999). Suppression of SHP-2 and ERK signalling promotes self-renewal of mouse embryonic stem cells. Dev Biol *210*, 30-43.

Busuttil, R., Bahar, R., and Vijg, J. (2007). Genome dynamics and transcriptional deregulation in aging. Neuroscience *145*, 1341-1347.

Canham, M. A., Sharov, A. A., Ko, M. S., and Brickman, J. M. (2010). Functional heterogeneity of embryonic stem cells revealed through translational amplification of an early endodermal transcript. PLoS Biol *8*.

Cartwright, P., McLean, C., Sheppard, A., Rivett, D., Jones, K., and Dalton, S. (2005). LIF/STAT3 controls ES cell self-renewal and pluripotency by a Myc-dependent mechanism. Development *132*, 885-896.

Chambers, I. (2004a). Mechanisms and factors in embryonic stem cell self-renewal. Rend Fis Acc Lincei *s.9, v.16*, 83-97.

Chambers, I. (2004b). The molecular basis of pluripotency in mouse embryonic stem cells. Cloning Stem Cells *6*, 386-391.

Chambers, I., Colby, D., Robertson, M., Nichols, J., Lee, S., Tweedie, S., and Smith, A. (2003). Functional expression cloning of Nanog, a pluripotency sustaining factor in embryonic stem cells. Cell *113*, 643-655.

Chambers, I., Silva, J., Colby, D., Nichols, J., Nijmeijer, B., Robertson, M., Vrana, J., Jones, K., Grotewold, L., and Smith, A. (2007). Nanog safeguards pluripotency and mediates germline development. Nature *450*, 1230-1234.

Chambers, I., and Smith, A. (2004). Self-renewal of teratocarcinoma and embryonic stem cells. Oncogene *23*, 7150-7160.

Chambers, I., and Tomlinson, S. R. (2009). The transcriptional foundation of pluripotency. Development *136*, 2311-2322.

Chazaud, C., Yamanaka, Y., Pawson, T., and Rossant, J. (2006). Early lineage segregation between epiblast and primitive endoderm in mouse blastocysts through the Grb2-MAPK pathway. Dev Cell *10*, 615-624.

Chen, X., Xu, H., Yuan, P., Fang, F., Huss, M., Vega, V. B., Wong, E., Orlov, Y. L., Zhang, W., Jiang, J., *et al.* (2008). Integration of external signaling pathways with the core transcriptional network in embryonic stem cells. Cell *133*, 1106-1117.

Chew, J. L., Loh, Y. H., Zhang, W., Chen, X., Tam, W. L., Yeap, L. S., Li, P., Ang, Y. S., Lim, B., Robson, P., and Ng, H. H. (2005). Reciprocal transcriptional regulation of

Pou5f1 and Sox2 via the Oct4/Sox2 complex in embryonic stem cells. Mol Cell Biol *25*, 6031-6046.

Conti, L., Pollard, S. M., Gorba, T., Reitano, E., Toselli, M., Biella, G., Sun, Y., Sanzone, S., Ying, Q. L., Cattaneo, E., and Smith, A. (2005). Niche-independent symmetrical self-renewal of a mammalian tissue stem cell. PLoS Biol *3*, e283.

Damjanov, I., and Andrews, P. W. (1983). Ultrastructural differentiation of a clonal human embryonal carcinoma cell line in vitro. Cancer Res *43*, 2190-2198.

Damjanov, I., and Andrews, P. W. (2007). The terminology of teratocarcinomas and teratomas. Nat Biotechnol *25*, 1212; discussion 1212.

Dani, C., Chambers, I., Johnstone, S., Robertson, M., Ebrahimi, B., Saito, M., Taga, T., Li, M., Burdon, T., Nichols, J., and Smith, A. (1998). Paracrine induction of stem cell renewal by LIF-deficient cells: a new ES cell regulatory pathway. Dev Biol *203*, 149-162.

Dietrich, J. E., and Hiiragi, T. (2008). Stochastic processes during mouse blastocyst patterning. Cells Tissues Organs *188*, 46-51.

Diwan, S. B., and Stevens, L. C. (1976). Development of teratomas from ectoderm of mouse egg cylinders. J Natl Cancer Inst *57*, 937-942.

Doble, B. W., Patel, S., Wood, G. A., Kockeritz, L. K., and Woodgett, J. R. (2007). Functional redundancy of GSK-3alpha and GSK-3beta in Wnt/beta-catenin signaling shown by using an allelic series of embryonic stem cell lines. Dev Cell *12*, 957-971.

Doetschman, T. C., Eistetter, H., Katz, M., Schmidt, W., and Kemler, R. (1985). The in vitro development of blastocyst-derived embryonic stem cell lines: formation of visceral yolk sac, blood islands and myocardium. J Embryol Exp Morphol *87*, 27-45.

Elowitz, M. B., Levine, A. J., Siggia, E. D., and Swain, P. S. (2002). Stochastic gene expression in a single cell. Science *297*, 1183-1186.

Endoh, M., Endo, T. A., Endoh, T., Fujimura, Y., Ohara, O., Toyoda, T., Otte, A. P., Okano, M., Brockdorff, N., Vidal, M., and Koseki, H. (2008). Polycomb group proteins Ring1A/B are functionally linked to the core transcriptional regulatory circuitry to maintain ES cell identity. Development *135*, 1513-1524.

Evans, M. J., and Kaufman, M. H. (1981). Establishment in culture of pluripotential cells from mouse embryos. Nature *292*, 154-156.

Finch, B. W., and Ephrussi, B (1967). Retention of multiple developmental potentialities by cells of a mouse testicular teratocarcinoma during prolonged culture in vitro and their extinction upon hybridization with cells of permanent lines. Proc NatlAcad Sci USA *57*, 615-621.

Finch, P. W., He, X., Kelley, M. J., Uren, A., Schaudies, R. P., Popescu, N. C., Rudikoff, S., Aaronson, S. A., Varmus, H. E., and Rubin, J. S. (1997). Purification and molecular cloning of a secreted, Frizzled-related antagonist of Wnt action. Proc Natl Acad Sci U S A *94*, 6770-6775.

Gardner, R. L. (1983). Origin and differentiation of extra-embryonic tissues in the mouse. Int Rev Exp Path *24*, 63-133.

Glauche, I., Herberg, M., and Roeder, I. (2010). Nanog variability and pluripotency regulation of embryonic stem cells--insights from a mathematical model analysis. PLoS One *5*.

Hall, J., Guo, G., Wray, J., Eyres, I., Nichols, J., Grotewold, L., Morfopoulou, S., Humphreys, P., Mansfield, W., Walker, R., *et al.* (2009). Oct4 and LIF/Stat3 additively induce Kruppel factors to sustain embryonic stem cell self-renewal. Cell Stem Cell *5*, 597-609.

Hamazaki, T., Kehoe, S. M., Nakano, T., and Terada, N. (2006). The Grb2/Mek pathway represses Nanog in murine embryonic stem cells. Mol Cell Biol.

Hart, A. H., Hartley, L., Ibrahim, M., and Robb, L. (2004). Identification, cloning and expression analysis of the pluripotency promoting Nanog genes in mouse and human. Dev Dyn *230*, 187-198.

Hayashi, K., Lopes, S. M., Tang, F., and Surani, M. A. (2008). Dynamic equilibrium and heterogeneity of mouse pluripotent stem cells with distinct functional and epigenetic states. Cell Stem Cell *3*, 391-401.

Hogan, B., Fellows, M., Avner, P., and Jacob, F. (1977). Isolation of a human teratoma cell line which expresses F9 antigen. Nature *270*, 515-518.

Hu, M., Krause, D., Greaves, M., Sharkis, S., Dexter, M., Heyworth, C., and Enver, T. (1997). Multilineage gene expression precedes commitment in the hemopoietic system. Genes Dev *11*, 774-785.

Huang, S. (2010). Cell lineage determination in state space: a systems view brings flexibility to dogmatic canonical rules. PLoS Biol *8*, e1000380.

Ivanova, N., Dobrin, R., Lu, R., Kotenko, I., Levorse, J., DeCoste, C., Schafer, X., Lun, Y., and Lemischka, I. R. (2006). Dissecting self-renewal in stem cells with RNA interference. Nature *442*, 533-538.

Jacob, F. (1977). Mouse teratocarcinoma and embryonic antigens. Immunol Rev *33*, 3-32.

Kaern, M., Elston, T. C., Blake, W. J., and Collins, J. J. (2005). Stochasticity in gene expression: from theories to phenotypes. Nat Rev Genet *6*, 451-464.

Kalmar, T., Lim, C., Hayward, P., Munoz-Descalzo, S., Nichols, J., Garcia-Ojalvo, J., and Martinez Arias, A. (2009). Regulated fluctuations in nanog expression mediate cell fate decisions in embryonic stem cells. PLoS Biol *7*, e1000149.

Kannagi, R., Cochran, N. A., Ishigami, F., Hakomori, S., Andrews, P. W., Knowles, B. B., and Solter, D. (1983). Stage-specific embryonic antigens (SSEA-3 and -4) are epitopes of a unique globo-series ganglioside isolated from human teratocarcinoma cells. EMBO J *2*, 2355-2361.

Kappen, C., Schughart, K., and Ruddle, F. H. (1993). Early evolutionary origin of major homeodomain sequence classes. Genomics *18*, 54-70.

Katoh, Y., and Katoh, M. (2006). WNT antagonist, SFRP1, is Hedgehog signaling target. Int J Mol Med *17*, 171-175.

Kim, J., Chu, J., Shen, X., Wang, J., and Orkin, S. H. (2008). An extended transcriptional network for pluripotency of embryonic stem cells. Cell *132*, 1049-1061.

Kleinsmith, L. J., and Pierce, G. B. (1964). Multipotentiality of single embryonal carcinoma cells. Cancer Res *24*, 1544-1552.

Kumar, P., Purbey, P. K., Sinha, C. K., Notani, D., Limaye, A., Jayani, R. S., and Galande, S. (2006). Phosphorylation of SATB1, a global gene regulator, acts as a molecular switch regulating its transcriptional activity in vivo. Mol Cell *22*, 231-243.

Kunath, T., Saba-El-Leil, M. K., Almousailleakh, M., Wray, J., Meloche, S., and Smith, A. (2007). FGF stimulation of the Erk1/2 signalling cascade triggers transition of pluripotent embryonic stem cells from self-renewal to lineage commitment. Development *134*, 2895-2902.

Kuroda, T., T, M., Kubota, H., Kimura, H., Hatano, S. Y., Suemori, H., Nakatsuji,N., and Tada,T (2005). Octamer and Sox elements are required for transcriptional cis regulation of Nanog gene expression. Mol Cell Biol *25*, 2475-2485.

Kussell, E., and Leibler, S. (2005). Phenotypic diversity, population growth, and information in fluctuating environments. Science *309*, 2075-2078.

Levasseur, D. N., Wang, J., Dorschner, M. O., Stamatoyannopoulos, J. A., and Orkin, S. H. (2008). Oct4 dependence of chromatin structure within the extended Nanog locus in ES cells. Genes Dev *22*, 575-580.

Li, M., Sendtner, M., and Smith, A. (1995). Essential function of LIF receptor in motor neurons. Nature *378*, 724-727.

Lim, C. Y., Tam, W. L., Zhang, J., Ang, H. S., Jia, H., Lipovich, L., Ng, H. H., Wei, C. L., Sung, W. K., Robson, P., *et al.* (2008). Sall4 regulates distinct transcription circuitries in different blastocyst-derived stem cell lineages. Cell Stem Cell *3*, 543-554.

Lin, T., Chao, C., Saito, S., Mazur, S.J., Murphy, M.E., Appella, E., and Xu, Y. (2005). p53 induces differentiation of mouse embryonic stem cells by suppressing Nanog expression. Nat Cell Biol *7*, 165-171.

Liu, L., and Roberts, R. M. (1996). Silencing of the gene for the β subunit of human chorionic gonadtrophin by the embryonic transcription factor oct-3/4. JBC *271*, 16683-16689.

Loh, Y. H., Wu, Q., Chew, J. L., Vega, V. B., Zhang, W., Chen, X., Bourque, G., George, J., Leong, B., Liu, J., *et al.* (2006). The Oct4 and Nanog transcription network regulates pluripotency in mouse embryonic stem cells. Nat Genet *38*, 431-440.

Martin, G. R. (1981). Isolation of a pluripotent cell line from early mouse embryos cultured in medium conditioned by teratocarcinoma stem cells. Proc Natl Acad Sci USA *78*, 7634-7638.

Martin, G. R., Smith, S., and Epstein, C. J. (1978). Protein synthetic patterns in teratocarcinoma stem cells and mouse embryos at early stages of development. Dev Biol *66*, 8-16.

Matsuda, T., Nakamura, T., Nakao, K., Arai, T., Katsuki, M., Heike, T., and Yokota, T. (1999). STAT3 activation is sufficient to maintain an undifferentiated state of mouse embryonic stem cells. Embo J *18*, 4261-4269.

Matsui, Y., Zsebo, K., and Hogan, B. L. (1992). Derivation of pluripotential embryonic stem cells from murine primordial germ cells in culture. Cell *70*, 841-847.

Mintz, B., and Illmensee, K. (1975). Normal genetically mosaic mice produced from malignant teratocarcinoma cells. Proc Natl Acad Sci U S A *72*, 3585-3589.

Mitsui, K., Tokuzawa, Y., Itoh, H., Segawa, K., Murakami, M., Takahashi, K., Maruyama, M., Maeda, M., and Yamanaka, S. (2003). The homeoprotein Nanog is required for maintenance of pluripotency in mouse epiblast and ES cells. Cell *113*, 631-642.

Monuki, E. S., Kuhn, R., and Lemke, G. (1993). Repression of the myelin P0 gene by the POU transcription factor SCIP. Mech Dev *42*, 15-32.

Morange, M. (2006). What history tells us VII. Twenty-five years ago: the production of mouse embryonic stem cells. J Biosci *31*, 537-541.

Mullin, N. P., Yates, A., Rowe, A. J., Nijmeijer, B., Colby, D., Barlow, P. N., Walkinshaw, M. D., and Chambers, I. (2008). The pluripotency rheostat Nanog functions as a dimer. Biochem J *411*, 227-231.

Nakashima, K., Takizawa, T., Ochiai, W., Yanagisawa, M., Hisatsune, T., Nakafuku, M., Miyazono, K., Kishimoto, T., Kageyama, R., and Taga, T. (2001). BMP2-mediated alteration in the developmental pathway of fetal mouse brain cells from neurogenesis to astrocytogenesis. Proc Natl Acad Sci U S A *98*, 5868-5873.

Nakatake, Y., Fukui, N., Iwamatsu, Y., Masui, S., Takahashi, K., Yagi, R., Yagi, K., Miyazaki, J., Matoba, R., Ko, M. S., and Niwa, H. (2006). Klf4 cooperates with Oct3/4 and Sox2 to activate the Lefty1 core promoter in embryonic stem cells. Mol Cell Biol *26*, 7772-7782.

Navarro, P., Chambers, I., Karwacki-Neisius, V., Chureau, C., Morey, C., Rougeulle, C., and Avner, P. (2008). Molecular coupling of Xist regulation and pluripotency. Science *321*, 1693-1695.

Nichols, J., Chambers, I., Taga, T., and Smith, A. (2001). Physiological rationale for responsiveness of mouse embryonic stem cells to gp130 cytokines. Development *128*, 2333-2339.

Nichols, J., Silva, J., Roode, M., and Smith, A. (2009). Suppression of Erk signalling promotes ground state pluripotency in the mouse embryo. Development *136*, 3215-3222.

Nichols, J., Zevnik, B., Anastassiadis, K., Niwa, H., Klewe-Nebenius, D., Chambers, I., Scholer, H., and Smith, A. (1998). Formation of pluripotent stem cells in the mammalian embryo depends on the POU transcription factor Oct4. Cell *95*, 379-391.

Nishimoto, M., Fukushima, A., Okuda, A., and Muramatsu, M. (1999). The gene for the embryonic stem cell coactivator UTF1 carries a regulatory element which selectively interacts with a complex composed of Oct-3/4 and Sox-2. Mol Cell Biol *19*, 5453-5465.

Niwa, H. (2001). Molecular mechanism to maintain stem cell renewal of ES cells. Cell Struct Funct *26*, 137-148.

Niwa, H., Burdon, T., Chambers, I., and Smith, A. (1998). Self-renewal of pluripotent embryonic stem cells is mediated via activation of STAT3. Genes Dev *12*, 2048-2060.

Niwa, H., Miyazaki, J., and Smith, A. G. (2000). Quantitative expression of Oct-3/4 defines differentiation, dedifferentiation or self-renewal of ES cells. Nat Genet *24*, 372-376.

Niwa, H., Ogawa, K., Shimosato, D., and Adachi, K. (2009). A parallel circuit of LIF signalling pathways maintains pluripotency of mouse ES cells. Nature *460*, 118-122.

Oh, J. H., Do, H.J., Yang, H.M., Moon,S.Y.,Cha,K.Y., Chung,H.M., and Kim, J.H. (2005). Identification of a putative transactivation domain in human Nanog. Exp Mol Med *37*, 250-254.

Okamoto, K., Okazawa, H., Okuda, A., Sakai, M., Muramatsu, M., and Hamada, H. (1990). A novel octamer binding transcription factor is differentially expressed in mouse embryonic cells. Cell *60*, 461-472.

Okita, C., Sato, M., and Schroeder, T. (2004). Generation of optimized yellow and red fluorescent proteins with distinct subcellular localization. Biotechniques *36*, 418-422, 424.

Okumura-Nakanishi, S., Saito, M., Niwa, H., Ishikawa, F (2005). Oct-3/4 and Sox2 regulate Oct-3/4 gene in embryonic stem cells. JBC *280*, 5307-5317.

Ozbudak, E. M., Thattai, M., Kurtser, I., Grossman, A. D., and van Oudenaarden, A. (2002). Regulation of noise in the expression of a single gene. Nat Genet *31*, 69-73.

Palmieri, S. L., Peter, W., Hess, H., and Scholer, H. R. (1994). Oct-4 transcription factor is differentially expressed in the mouse embryo during establishment of the first two extraembryonic cell lineages involved in implantation. Dev Biol *166*, 259-267.

Pan, G., Li,J., Zhou, Y., Zheng, H., and Pei, D. (2006). A negative feedback loop of transcriptional factors that control stem cell pluripotency and self-renewal. Faseb *20*, 1730-1732.

Pan, G., and Pei, D. (2005). The stem cell pluripotency factor NANOG activates transcription with two unusually potent subdomains at its C terminus. J Biol Chem *280*, 1401-1407.

Pan, G. J., and Pei, D. Q. (2003). Identification of two distinct transactivation domains in the pluripotency sustaining factor nanog. Cell Res *13*, 499-502.

Papaioannou, V. E., McBurney, M. W., Gardner, R. L., and Evans, M. J. (1975). Fate of teratocarcinoma cells injected into early mouse embryos. Nature *258*, 70-73.

Pera, M. F., Cooper, S., Mills, J., and Parrington, J. M. (1989). Isolation and characterization of a multipotent clone of human embryonal carcinoma cells. Differentiation *42*, 10-23.

Pereira, L., Yi, F., and Merrill, B. J. (2006). Repression of Nanog Gene Transcription by Tcf3 Limits Embryonic Stem Cell Self-Renewal. Mol Cell Biol.

Resnick, J. L., Bixler, L. S., Cheng, L., and Donovan, P. J. (1992). Long-term proliferation of mouse primordial germ cells in culture. Nature *359*, 550-551.

Rodda, D. J., Chew, J. L., Lim, L. H., Loh, Y. H., Wang, B., Ng, H. H., and Robson, P. (2005). Transcriptional regulation of nanog by OCT4 and SOX2. J Biol Chem *280*, 24731-24737.

Rosner, M. H., Vigano, M. A., Ozato, K., Timmons, P. M., Poirier, F., Rigby, P., and Staudt, L. M. (1990). A POU-domain transcription factor in early stem cells and germ cells of the mammalian embryo. Nature *345*, 686-692.

Ruzinova, M. B., and Benezra, R. (2003). Id proteins in development, cell cycle and cancer. Trends Cell Biol *13*, 410-418.

Sato, N., Meijer, L., Skaltsounis, L., Greengard, P., and Brivanlou, A. H. (2004). Maintenance of pluripotency in human and mouse embryonic stem cells through activation of Wnt signaling by a pharmacological GSK-3-specific inhibitor. Nat Med *10*, 55-63.

Savarese, F., Davila, A., Nechanitzky, R., De La Rosa-Velazquez, I., Pereira, S. F., Engelke, R., Takahashi, K., Jenuwein, T., Kohwi-Shigematsu, T., Fischer, A. G., and Grosschedl, R. (2009). Satb1 and Satb2 regulate embryonic stem cell differentiation and Nanog expression. Genes Dev *23*, 2625-2638.

Scholer, H. R., Dressler, G. R., Balling, R., Rohdewohld, H., and Gruss, P. (1990). Oct-4: a germline-specific transcription factor mapping to the mouse t-complex. EMBO J *9*, 2185-2195.

Schroeder, T. (2008). Imaging stem-cell-driven regeneration in mammals. Nature *453*, 345-351.

Shahrezaei, V., and Swain, P. S. (2008). The stochastic nature of biochemical networks. Curr Opin Biotechnol *19*, 369-374.

Shamblott, M. J., Axelman, J., Wang, S., Bugg, E. M., Littlefield, J. W., Donovan, P. J., Blumenthal, P. D., Huggins, G. R., and Gearhart, J. D. (1998). Derivation of pluripotent stem cells from cultured human primordial germ cells. Proc Natl Acad Sci U S A *95*, 13726-13731.

Shevinsky, L. H., Knowles, B. B., Damjanov, I., and Solter, D. (1982). Monoclonal antibody to murine embryos defines a stage-specific embryonic antigen expressed on mouse embryos and human teratocarcinoma cells. Cell *30*, 697-705.

Shimozaki, K., Nakashima, K., Niwa, H., and Taga, T. (2003). Involvement of Oct3/4 in the enhancement of neuronal differentiation of ES cells in neurogenesis-inducing cultures. Development *130*, 2505-2512.

Silva, J., Nichols, J., Theunissen, T. W., Guo, G., van Oosten, A. L., Barrandon, O., Wray, J., Yamanaka, S., Chambers, I., and Smith, A. (2009). Nanog is the gateway to the pluripotent ground state. Cell *138*, 722-737.

Sinclair, A. H., Berta, P., Palmer, M. S., Hawkins, J. R., Griffiths, B. L., Smith, M. J., Foster, J. W., Frischauf, A. M., Lovell-Badge, R., and Goodfellow, P. N. (1990). A gene

from the human sex-determining region encodes a protein with homology to a conserved DNA-binding motif. Nature *346*, 240-244.

Singh, A. M., Hamazaki, T., Hankowski, K. E., and Terada, N. (2007). A heterogeneous expression pattern for Nanog in embryonic stem cells. Stem Cells *25*, 2534-2542.

Smith, A. G. (2001). Embryo-derived stem cells: of mice and men. Ann Rev Cell Dev Biol *17*, 435-462.

Smith, A. G., Heath, J. K., Donaldson, D. D., Wong, G. G., Moreau, J., Stahl, M., and Rogers, D. (1988). Inhibition of pluripotential embryonic stem cell differentiation by purified polypeptides. Nature *336*, 688-690.

Smith, A. G., and Hooper, M. L. (1987). Buffalo rat liver cells produce a diffusible activity which inhibits the differentiation of murine embryonal carcinoma and embryonic stem cells. Dev Biol *121*, 1-9.

Solter, D. (2006). From teratocarcinomas to embryonic stem cells and beyond: a history of embryonic stem cell research. Nat Rev Genet *7*, 319-327.

Solter, D., and Knowles, B. B. (1978). Monoclonal antibody defining a stage-specific mouse embryonic antigen (SSEA-1). PNAS *75*, 5565-5569.

Solter, D., Skreb, N., and Damjanov, I. (1970). Extrauterine growth of mouse egg cylinders results in malignant teratoma. Nature *227*, 503-504.

Stevens, L. C. (1958). Studies on transplantable testicular teratomas of strain 129 mice. J Natl Cancer Inst *20*, 1257-1275.

Stevens, L. C. (1967a). The biology of teratomas. Adv Morphog *6*, 1-31.

Stevens, L. C. (1967b). Origin of testicular teratomas from primordial germ cells in mice. J Natl Cancer Inst *38*, 549-552.

Stevens, L. C. (1970a). The development of transplantable teratocarcinomas from intratesticular grafts of pre- and postimplantation mouse embryos. Dev Biol *21*, 364-382.

Stevens, L. C. (1970b). Experimental production of testicular teratomas in mice of strains 129, A/He, and their F1 hybrids. J Natl Cancer Inst *44*, 929–932.

Stevens, L. C., and Little, C.c. (1954). Spontaneous testicular teratomas in an inbred strain of mice. PNAS *40*, 1080-1087.

Stewart, C. L., Kaspar, P., Brunet, L. J., Bhatt, H., Gadi, I., Kontgen, F., and Abbondanzo, S. J. (1992). Blastocyst implantation depends on maternal expression of leukaemia inhibitory factor. Nature *359*, 76-79.

Strohman, R. C. (1997). The coming Kuhnian revolution in biology. Nat Biotechnol *15*, 194-200.

Suwinska, A., Czolowska, R., Ozdzenski, W., and Tarkowski, A. K. (2008). Blastomeres of the mouse embryo lose totipotency after the fifth cleavage division: expression of Cdx2 and Oct4 and developmental potential of inner and outer blastomeres of 16- and 32-cell embryos. Dev Biol *322*, 133-144.

Suzuki, A., Raya, A., Kawakami, Y., Morita, M., Matsui, T., Nakashima, K., Gage, F. H., Rodriguez-Esteban, C., and Belmonte, J. C. (2006). Maintenance of embryonic stem cell pluripotency by Nanog-mediated reversal of mesoderm specification. Nat Clin Pract Cardiovasc Med *3 Suppl 1*, S114-122.

Swain, P. S., Elowitz, M. B., and Siggia, E. D. (2002). Intrinsic and extrinsic contributions to stochasticity in gene expression. Proc Natl Acad Sci U S A *99*, 12795-12800.

Tada, T., Tada, M., Hilton, K., Barton, S. C., Sado, T., Takagi, N., and Surani, M. A. (1998). Epigenotype switching of imprintable loci in embryonic germ cells. Dev Genes Evol *207*, 551-561.

Takahashi, K., Tanabe, K., Ohnuki, M., Narita, M., Ichisaka, T., Tomoda, K., and Yamanaka, S. (2007). Induction of pluripotent stem cells from adult human fibroblasts by defined factors. Cell *131*, 861-872.

Takahashi, K., and Yamanaka, S. (2006). Induction of pluripotent stem cells from mouse embryonic and adult fibroblast cultures by defined factors. Cell *126*, 663-676.

Takao, Y., Yokota, T., and Koide, H. (2007). Beta-catenin up-regulates Nanog expression through interaction with Oct-3/4 in embryonic stem cells. Biochem Biophys Res Commun *16*, 699-705.

Takeda, K., Noguchi, K., Shi, W., Tanaka, T., Matsumoto, M., Yoshida, N., Kishimoto, T., and Akira, S. (1997). Targeted disruption of the mouse *Stat3* gene leads to early embryonic lethality. Proc Natl Acad Sci U S A *94*, 3801-3804.

Tam, P. P., and Behringer, R.R. (1997). Mouse gastrulation: the formation of a mammalian body plan. Mech Dev *68*, 3-25.

Tarkowski, A. K., and Wroblewska, J. (1967). Development of blastomeres of mouse eggs isolated at the four- and eight-cell stages. JEEM *18*, 155-180.

Tesar, P. J., Chenoweth, J. G., Brook, F. A., Davies, T. J., Evans, E. P., Mack, D. L., Gardner, R. L., and McKay, R. D. (2007). New cell lines from mouse epiblast share defining features with human embryonic stem cells. Nature *448*, 196-199.

Thattai, M., and van Oudenaarden, A. (2004). Stochastic gene expression in fluctuating environments. Genetics *167*, 523-530.

Thomas, K. R., and Capecchi, M. R. (1987). Site directed mutagenesis by gene targeting in mouse embryo-derived stem cells. Cell *51*, 503-512.

Thompson, S., Clarke, A. R., Pow, A. M., Hooper, M. L., and Melton, D. W. (1989). Germ line transmission and expression of a corrected gene produced by gene targetting in embryonic stem cells. Cell *56*, 313-321.

Thomson, J. A., Itskovitz-Eldor, J., Shapiro, S. S., Waknitz, M. A., Swiergiel, J. J., Marshall, V. S., and Jones, J. M. (1998). Embryonic stem cell lines derived from human blastocysts. Science *282*, 1145-1147.

Tokuzawa, Y., Kaiho, E., Maruyama, M., Takahashi, K., Mitsui, K., Maeda, M., Niwa, H., and Yamanaka, S. (2003). Fbx15 is a novel target of Oct3/4 but is dispensable for embryonic stem cell self-renewal and mouse development. Mol Cell Biol *23*, 2699-2708.

Tomioka, M., Nishimoto, M., Miyagi, S., Katayanagi, T., Fukui, N., Niwa, H., Muramatsu, M., and Okuda, A. (2002). Identification of Sox-2 regulatory region which is under the control of Oct-3/4-Sox-2 complex. Nucleic Acids Res *30*, 3202-3213.

Toyooka, Y., Shimosato, D., Murakami, K., Takahashi, K., and Niwa, H. (2008). Identification and characterization of subpopulations in undifferentiated ES cell culture. Development *135*, 909-918.

Tsien, R. Y. Nobel lecture: constructing and exploiting the fluorescent protein paintbox. Integr Biol (Camb) *2*, 77-93.

Uren, A., Reichsman, F., Anest, V., Taylor, W. G., Muraiso, K., Bottaro, D. P., Cumberledge, S., and Rubin, J. S. (2000). Secreted frizzled-related protein-1 binds directly to Wingless and is a biphasic modulator of Wnt signaling. J Biol Chem *275*, 4374-4382.

van den Berg, D. L., Zhang, W., Yates, A., Engelen, E., Takacs, K., Bezstarosti, K., Demmers, J., Chambers, I., and Poot, R. A. (2008). Estrogen-related receptor beta interacts with Oct4 to positively regulate Nanog gene expression. Mol Cell Biol *28*, 5986-5995.

Wang, J., Levasseur, D. N., and Orkin, S. H. (2008). Requirement of Nanog dimerization for stem cell self-renewal and pluripotency. Proc Natl Acad Sci U S A *105*, 6326-6331.

Welter, J. F., Gali, H., Crish, J. F., and Eckert, R. L. (1996). Regulation of human involucrin promoter activity by POU domain proteins. J Biol Chem *271*, 14727-14733.

Williams, D. C., Jr., Cai, M., and Clore, G. M. (2004). Molecular basis for synergistic transcriptional activation by Oct1 and Sox2 revealed from the solution structure of the 42-kDa Oct1.Sox2.Hoxb1-DNA ternary transcription factor complex. J Biol Chem *279*, 1449-1457.

Wolf, D. M., Vazirani, V. V., and Arkin, A. P. (2005). Diversity in times of adversity: probabilistic strategies in microbial survival games. J Theor Biol *234*, 227-253.

Yamaguchi, S., Kimura, H., Tada, M., Nakatsuji, N., and Tada, T. (2005). Nanog expression in mouse germ cell development. Gene Expr Patterns *5*, 639-646.

Yamanaka, S. (2007). Strategies and new developments in the generation of patient-specific pluripotent stem cells. Cell Stem Cell *1*, 39-49.

Ying, Q. L., Nichols, J., Chambers, I., and Smith, A. (2003). BMP induction of Id proteins suppresses differentiation and sustains embryonic stem cell self-renewal in collaboration with STAT3. Cell *115*, 281-292.

Ying, Q. L., Wray, J., Nichols, J., Batlle-Morera, L., Doble, B., Woodgett, J., Cohen, P., and Smith, A. (2008). The ground state of embryonic stem cell self-renewal. Nature *453*, 519-523.

Yoshida, K., Chambers, I., Nichols, J., Smith, A., Saito, M., Yasukawa, K., Shoyab, M., Taga, T., and Kishimoto, T. (1994). Maintenance of the pluripotential phenotype of embryonic stem cells through direct activation of gp130 signalling pathways. Mech Dev *45*, 163-171.

Yoshida, K., Taga, T., Saito, M., Suematsu, S., Kumanogoh, A., Tanaka, T., Fujiwara, H., Hirata, M., Yamagami, T., Nakahata, T.*, et al.* (1996). Targeted disruption of gp130, a common signal transducer for the interleukin 6 family of cytokines, leads to myocardial and hematological disorders. PNAS *93*, 407-411.

Yu, J., Vodyanik, M. A., Smuga-Otto, K., Antosiewicz-Bourget, J., Frane, J. L., Tian, S., Nie, J., Jonsdottir, G. A., Ruotti, V., Stewart, R.*, et al.* (2007). Induced pluripotent stem cell lines derived from human somatic cells. Science *318*, 1917-1920.

Yuan, H., Corbi, N., Basilico, C., and Dailey, L. (1996). Developmental-specific activity of the FGF-4 enhancer requires the synergistic action of Sox2 and Oct-3. GD *9*, 2635-2645.

Zhang, J., Tam, W. L., Tong, G. Q., Wu, Q., Chan, H. Y., Soh, B. S., Lou, Y., Yang, J., Ma, Y., Chai, L.*, et al.* (2006). Sall4 modulates embryonic stem cell pluripotency and early embryonic development by the transcriptional regulation of Pou5f1. Nat Cell Biol *8*, 1114-1123.

Zhang, J. G., Owczarek, C. M., Ward, L. D., Howlett, G. J., Fabri, L. J., Roberts, B. A., and Nicola, N. A. (1997). Evidence for the formation of a heterotrimeric complex of leukaemia inhibitory factor with its receptor subunits in solution. Biochem J *325 (Pt 3)*, 693-700.

Appendix

Cell line Appendix

CELL LINES	DERIVED FROM	GENETIC MODIFICATIONS
E14TG2a	129/ Ola mouse strain	Deficient in HPRT
CGR8	129/ Ola mouse strain	No modifications
ZIN40	129/ Ola mouse strain	Express a randomly integrated lacZ-ires-neo transgene
OKO8	E14Tg2a	An IRES-βgeopA cassette has been introduced into one Oct4 allele by homologous recombination
OKO160	CGR8	An IRES-βgeopA cassette has been introduced into one Oct4 allele by homologous recombination
ZHTc6	CGR8	Contains a Dox-suppressible Oct4 transgene. One allele has been inactivated by targeted intergration of an IRESzeopA cassette.
ZHBTc4.1	CGR8	As ZHTc6 cells but the second Oct4 allele has been inactivated by targeted integration of an IRESBSDpA cassette.
D7A3 PE	E14Tg2a	*Lif*$^{-/-}$ cells

CELL LINE	DERIVED FROM	GENETIC MODIFICATIONS
TNG	E14Tg2a	An eGFP IRESpacpA cassette has been inserted at the AUG codon of Nanog into one allele of the Nanog gene by homologous recombination
OKOTNG	OKO160	An IRES-βgeopA cassette has been introduced into *one* allele of the Oct4 gene by homologous recombinations. In addition, an eGFP IRESpacpA cassette has been inserted at the AUG codon of Nanog into one allele of the Nanog gene by homologous recombination.
ZHTNG	ZHTc6	Contains a Dox-suppressible Oct4 transgene in an $Oct4^{+/-}$ background. ES cells maintained with 1000ng/ml Doxycycline. In addition, an eGFP IRESpacpA cassette has been inserted at the AUG codon of Nanog into one allele of the Nanog gene by homologoues recombination.
ZHBTNG	ZHBTc4.1	Contains a Dox-suppressible Oct4 transgene, in an $Oct4^{-/-}$ background. ES cells maintained in the absence of Doxycycline. In addition, an eGFP IRESpacpA cassette has been inserted at the AUG codon of Nanog into one allele of the Nanog gene by homologoues recombination.